uOttawa

L'Université canadienne
Canada's university

FACULTÉ DES ÉTUDES SUPÉRIEURES ET POSTOCTORALES

uOttawa

L'Université canadienne
Canada's university

FACULTY OF GRADUATE AND POSDOCTORAL STUDIES

Tia Corinne Moffat

AUTEUR DE LA THÈSE / AUTHOR OF THESIS

Ph.D. (Biochemistry)

GRADE / DEGREE

Department of Biochemistry, Microbiology and Immunology

FACULTÉ, ÉCOLE, DÉPARTEMENT / FACULTY, SCHOOL, DEPARTMENT

Targeting the Signalling Cascades Responsible for Human Neuronal Apoptosis Elicited by the Lipid Neuromodulator Platelet Activating Factor

TITRE DE LA THÈSE / TITLE OF THESIS

Steffany Bennett

DIRECTEUR (DIRECTRICE) DE LA THÈSE / THESIS SUPERVISOR

CO-DIRECTEUR (CO-DIRECTRICE) DE LA THÈSE / THESIS CO-SUPERVISOR

EXAMINATEURS (EXAMINATRICES) DE LA THÈSE / THESIS EXAMINERS

Nicolas Bazan (videoconference)

Fraser Scott

Sheng Hou

Majambu Mbikay

Gary W. Slater

Le Doyen de la Faculté des études supérieures et postdoctorales / Dean of the Faculty of Graduate and Postdoctoral Studies

# TARGETING THE SIGNALLING CASCADES RESPONSIBLE FOR HUMAN NEURONAL APOPTOSIS ELICITED BY THE LIPID NEUROMODULATOR PLATELET ACTIVATING FACTOR

**Tia Corinne Moffat**

A thesis submitted to
The Faculty of Graduate and Postdoctoral Studies
In partial fulfillment of the requirements for the degree of
Doctor of Philosophy

Department of Biochemistry, Microbiology, and Immunology
University of Ottawa
Ottawa, ON, Canada

*Your file Votre référence*
*ISBN: 978-0-494-41609-9*
*Our file Notre référence*
*ISBN: 978-0-494-41609-9*

**Abstract**

Apoptosis is known to underlie neuronal loss in many human neurodegenerative disorders, such as Alzheimer disease (AD), HIV-dementia and ischemic stroke. Phospholipid signalling is involved in each of these conditions; changes in phospholipid membrane composition and phospholipid synthesis enzyme activity occurs in AD, while in HIV-dementia and ischemia there is an increased production and accumulation of inflammatory bioactive phospholipid mediators. Pathophysiological exposure to the phospholipid neuromodulator platelet activating factor (PAF) can initiate apoptotic pathways, and has been hypothesized to be a key mediator of neuronal death in these neurodegenerative disorders. It has been assumed that PAF signals exclusively through its G-protein coupled receptor (PAFR). However, our laboratory has shown that PAF can also induce apoptosis independently of PAFR and that ectopic expression of PAFR renders cells resistant to PAF-induced toxicity. This is relevant to neurodegenerative disease since PAFR expression in the human brain is found predominantly in non-neuronal cells suggesting that PAFR-independent signalling is also involved in neurodegeneration. This thesis focused on elucidating the PAF-induced, PAFR-independent apoptotic pathways in human neurons with the overarching goal of identifying new therapeutic targets capable of inhibiting neuronal loss in neurodegenerative disease. Here, PAF is shown to induce endoplasmic reticulum (ER) stress resulting in caspase-2 activation, leading to the activation of caspase-7, and culminating in DNA fragmentation in human neurons (hNTs) lacking PAFR. Mitochondrial effects,

specifically release of cytochrome *c* from the mitochondria, caspase-9 activation, reactive oxygen species (ROS) production, and mitochondrial uncoupling protein-2 (UCP2) upregulation were initiated downstream of this primary ER cascade. To target this pathway, a panel of natural and synthetic compounds was screened for their ability to protect hNTs from neurotoxicity initiated by PAF and by the AD-related neurotoxic peptide amyloid-$\beta_{1-42}$ (Aβ). Several compounds were identified as PAF/Aβ inhibitors. One of these compounds, nelfinavir (NFV), was tested for *in vivo* efficiency using the middle cerebral artery occlusion (MCAO) model of focal ischemia. NFV reduced infarct size, prevented neuronal apoptotic-like death, and improved behavioural recovery, solidifying the relation between PAF, AD, HIV-dementia, and ischemia-induced neuronal apoptosis. Together, these studies demonstrate that PAF can trigger neuronal apoptosis independently of PAFR, that inhibiting PAF-mediated pathways of neurotoxicity can protect human neurons *in vitro* from PAF and Aβ, and that targeting secondary apoptotic pathways elicited by PAF can reduce neuronal death *in vivo* in mouse models of human disease. The identification of compounds capable of inhibiting the primary and secondary PAFR-independent apoptotic events triggered by PAF represents a new means of targeting phospholipid signalling in neurodegenerative disease.

**Acknowledgements**

I would like to thank Dr. Steffany A. L. Bennett for inviting me to pursue a graduate career in her lab. Her ambition, determination and passion for discovery are unsurpassed and are certainly an inspiration. I would also like to thank Dr. Mary-Ellen Harper for her patience and optimism both as a co-supervisor and later as a thesis advisory committee member. I wish to thank the other members of my dynamic thesis advisory committee, Drs. Heidi McBride, John MacManus, Ilona Skerjanc, and Martin Holcik for their constructive criticisms and encouragements. In addition, I would like to thank Susan Jiang for her guidance during *in vivo* experiments. Thank you to all the members of the Bennett lab, both past and present, for their constant support, both professionally and socially. A special thanks to Lysanne and Ashleigh for their revisions and formatting advice regarding this thesis. Last, but certainly not least, I would like to thank my devoted family (both 2-legged and 4-legged) for their patience, understanding, and support throughout this arduous task that is the PhD. You are my strength and I would not have made it through without you. This thesis is dedicated to the loving memory of Ivy Gibson and her battle against Alzheimer disease.

**Table of Contents**

## List of Figures

**List of Appendices**

## List of Abbreviations

| | |
|---|---|
| $\alpha_1$ | $\alpha_1$ subunit of PAFAH |
| $\alpha_2$ | $\alpha_2$ subunit of PAFAH |
| $\Delta\Psi_m$ | mitochondrial membrane potential |
| Aβ | amyloid-$\beta_{1-42}$ |
| AD | Alzheimer disease |
| AIF | apoptosis inducing factor |
| ANOVA | analysis of variance |
| ANT | adenine nucleotide transporter |
| APP | amyloid precursor protein |
| AraC | cytosine β-D-arabinofuranoside |
| Bcl-2 | B-cell lymphoma-2 |
| BiP | binding protein |
| B-PAF | bodipy platelet activating factor |
| bp | base pair |
| BSA | bovine serum albumin |
| C-terminus | carboxy-terminus |
| $Ca^{2+}$ | calcium |
| cDNA | complementary deoxyribonucleic acid |
| CGN | cerebellar granule neuron |
| CMC | critical micelle concentration |
| CNS | central nervous system |
| COX IV | cytochrome oxidase IV |
| cPAF | methyl carbamyl platelet activating factor |
| DMEM | Dulbecco's modified eagle medium |
| DMSO | dimethyl sulfoxide |
| DNA | deoxyribonucleic acid |
| dNTP | deoxynucleotide triphosphate |
| DTT | dithiothreitol |
| EndoG | endonuclease G |
| ER | endoplasmic reticulum |
| EthD-1 | ethidium homodimer-1 |
| EtOH | ethanol |
| Etop | etoposide |
| FAM-peptide-FMK | carboxyfluorescein analog of Z-peptide-FMK |
| FBS | fetal bovine serum |
| FudR | 5-fluoro-2'-deoxyuridine |
| GAP43 | growth-associated protein 43 |
| GAPDH | glyceraldehyde-3'-phosphate dehydrogenase |
| GFAP | glial fibrillary acidic protein |
| GPCR | G-protein coupled receptor |
| GRP | glucose-related protein |
| $H_2O_2$ | hydrogen peroxide |
| HIV | human immunodeficiency virus |

| | |
|---|---|
| hNT | terminally differentiated human neurons derived from the NT2 teratocarcinoma-derived neural precursor cell line |
| HRP | horseradish peroxidase |
| JC-1 | 5,5',6,6'-tetrachloro-1,1',3,3'-tetraethylbenzimidazolocarbocyanine iodide |
| KO | knock-out |
| LTP | long-term potentiation |
| MCAO | middle cerebral artery occlusion |
| mtDNA | mitochondrial DNA |
| MTR | MitoTracker Red CMXRos |
| mRNA | messenger ribonucleic acid |
| Myelin PLP | myelin proteolipid protein |
| N-terminus | amino-terminus |
| Neu N | neuronal nuclei |
| NF-68 | neurofilament-68 |
| NF-$H_2O$ | nuclease free double-distilled water |
| NFV | nelfinavir |
| NSE | neuron-specific enolase |
| NT2 | NT2/D1 subclone of the NT2 human teratocarcinoma-derived neural precursor cell line |
| PAF | platelet activating factor |
| PAFAH | platelet activating factor acetylhydrolase |
| PAFR | platelet activating factor receptor |
| PBS | phosphate buffered saline |
| PCNA | proliferating cell nuclear antigen |
| PI | protease inhibitor |
| $PLA_2$ | phospholipase $A_2$ |
| PTPC | permeability transition pore complex |
| RA | retinoic acid |
| RIT | ritonavir |
| RNA | ribonucleic acid |
| ROS | reactive oxygen species |
| RT-PCR | reverse transcriptase polymerase chain reaction |
| SDS | sodium dodecyl sulfate |
| SEM | standard error of the mean |
| STS | staurosporine |
| TdT | terminal deoxynucleotidyl transferase |
| TMRM | tetramethylrhodamine methyl ester |
| TTC | 2,3,5-triphenyltetrazolium chloride |
| Tubulin | β-tubulin III |
| TUNEL | TdT deoxyuridine triphosphate nick end labeling |
| UCP | uncoupling protein |
| Urd | uridine |
| UV | ultraviolet |
| WT | wild-type |
| Z-peptide-FMK | benzyloxycarbonyl-peptide-fluoromethyl ketone |

# Chapter 1: Introduction to platelet activating factor in neuronal apoptosis and neurodegenerative disease

## 1.1 Neurodegenerative disease

Loss of brain function can occur due to a variety of pathologies, including neurotrauma and neurodegenerative disease. Examples of neurodegenerative disorders include Alzheimer disease (AD), Parkinson's disease, Huntington disease, human immunodeficiency virus (HIV)-dementia, and in some cases, stroke. Each of these disorders is associated with a progressive, irreversible loss of central nervous system (CNS) function resulting from the degeneration and death of neurons. Patients present with symptoms and disease characteristics that are dependent, in part, upon the region of the CNS in which neuronal death is maximal or most rapid. Despite diverse etiologies, many of the underlying mechanisms of neuronal death share common pathways each of which represent potential therapeutic targets. Yet, to date, no single target or pathway has proven effective at inhibiting progressive neuronal loss following stroke, AD, or HIV-dementia. It has become increasingly apparent that a broader therapeutic approach is required. To this end, the focus of this thesis is to explore the role of lipid signalling, specifically the platelet activating factor (PAF) family of glycerophospholipids (1-alkyl-2-acetyl-*sn*-3-glycerophosphocholine), in modulating multiple cell death pathways common to AD, HIV-dementia and stroke (reviewed below).

## 1.2 AD

AD is a progressive neurodegenerative disease that represents the most common form of dementia in the elderly, affecting 12 million patients worldwide and approximately 1 in 20 Canadians over the age of 65[1] . The financial cost of caring for AD patients is overwhelming with over $5.5 billion/year spent on home and palliative care for Canadians with AD[2]. AD is characterized by loss of cognitive function due to neuronal dysfunction followed by neuronal death in memory-related brain regions such as the hippocampus. In AD patients, regions of the brain involved in learning and memory not only exhibit decreased cellular energy metabolism, but are also smaller due to progressive atrophy (Mattson 2004). While the molecular mechanisms underlying the cause of AD remain elusive, AD pathology has been associated with impairments of multiple systems including mitochondrial and oxidative functions, cytoskeletal proteins, neurotransmitters, phospholipids, and atypical processing of tau and amyloid precursor protein (APP) resulting in the formation of the two main pathological hallmarks of AD; neurofibrillary tangles and amyloid plaques (Hardy and Selkoe, 2002; Kanfer et al., 1998; Mattson, 2004; Selkoe, 2002).

### *1.2.1 Tau protein and neurofibrillary tangles*

The elongated shape of neurons demands an efficient transport system to carry proteins, lipids and other cell components along the length of the cell. This

---

[1] (2006) Alzheimer Society of Canada. Alzheimer Disease: Statistics, People Affected with Alzheimer's disease and Related Dementias. http://www.alzheimer.ca/english/disease/stats-people.htm.

[2] (2005) Alzheimer Society of Canada. Alzheimer Disease: Statistics, Economic Costs of Dementia. http://www.alzheimer.ca/english/disease/stats-costs.htm.

system depends on microtubules, filamentous intracellular organelles along which proteins can be transported, for example, from the cell soma through the axon. Tau, one of the predominant microtubule-associated proteins in neuronal axons, is known to stabilize these microtubules (Mandelkow et al., 2003). During neurodegenerative disease states such as AD, excessive phosphorylation and/or aberrant oxidative modifications of tau detach the modified tau protein from neuronal microtubules, resulting in the aggregation of tau into intracellular fibrils known as neurofibrillary tangles. The net result is an interruption in axonal transport and a general congestion of cytosolic space along the axon, inhibiting axonal protein transport (Mandelkow et al., 2003; Mattson, 2004).

### *1.2.2 Amyloid-β peptide and amyloid plaques*

The abberant proteolytic cleavage of APP that results in the production, accumulation, secretion and aggregation of neurotoxic forms of amyloid-β peptide is central to the neuropathology of AD. The most damaging species of the amyloid-β peptide fragments is amyloid-$\beta_{1-42}$ (Aβ)[3].

Although APP is expressed in many cell types, including neurons, its role in normal cellular functions remains unclear. APP is a receptor-like integral membrane protein found at the cell surface embedded in the plasma membrane, or intracellularly in the Golgi or endoplasmic reticulum (ER) membranes. APP can be cleaved at various sites by a group of enzymes known as secretases via two pathways (Figure 1.1). Under normal physiological conditions, secretase processing through the "non-amyloidogenic" pathway does not result in the production of Aβ

[3] In this thesis, the term Aβ is used to refer specifically to amyloid-$\beta_{1-42}$ unless otherwise specified.

**Figure 1.1 Proteolytic processing of APP.** APP can be cleaved by α and β-secretases to produce sAPPα through the non-amyloidogenic pathway, or by β and γ-secretases to produce the toxic Aβ peptide through the amyloidogenic pathway (adapted from (Mattson, 2004)).

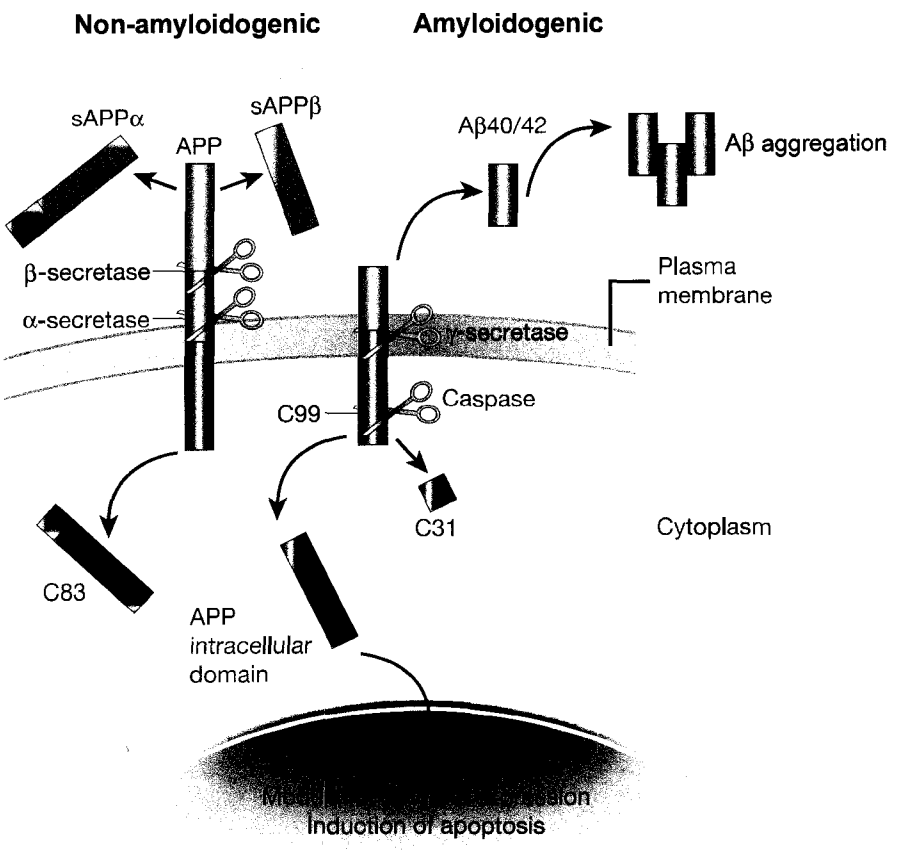


Figure 1.1

(Buxbaum et al., 1993). α-secretase cleaves APP within the fragment defining the toxic Aβ region, releasing a secreted APP fragment (sAPPα) and leaving an intracellular membrane-bound carboxy-terminal APP fragment of 83 amino acids in length (C83). Production of sAPPα has been shown to promote neuronal survival by increasing the resistance of neurons to metabolic and oxidative stress (Mattson, 1997; Mattson, 2004). Subsequent C83 cleavage by γ-secretase yields an APP intracellular domain, also known as the C-terminal fragment (CTFγ), that can translocate to the nucleus and regulate gene expression (Kimberly et al., 2001). Under pathological conditions, APP processing through the "amyloidogenic" pathway results in the production of neurotoxic Aβ. This pathway involves the cleavage of APP by β-secretases into a secreted APP fragment (sAPPβ) and a carboxy-terminal APP fragment of 99 amino acids in length (C99). Cleavage of C99 by γ-secretase yields 1) an APP intracellular domain or CTFγ that, as in the "non-amyloidogenic" pathway, can translocate to the nucleus and regulate gene expression and 2) either $A\beta_{1-40}$ or $A\beta_{1-42}$, depending on the cleavage site.

Neurons are more susceptible than other cell types to the toxicity involved in Aβ production. Not only do neurons produce the highest amount of APP, they also display the highest β-secretase activity (Hartmann, 1999). Furthermore, since neurons are postmitotic, they are not capable of diluting the concentration of intracellular Aβ through mitosis as mitotic cells can. Together, these factors put neurons at the highest risk of Aβ toxicity, which is purported by the "amyloid cascade hypothesis" to underly AD neuronal dysfunction and death (Figure 1.2) (Hardy and Selkoe, 2002). Moreover, since APP can be localized to the plasma membrane or the Golgi/ER membranes, APP cleavage can lead to an increase in either secreted

**Figure 1.2: The role of lipid signalling in the amyloid cascade hypothesis.** The amyloid cascade hypothesis (red) describes a series of events whereby Aβ production and accumulation leads to AD pathology (adapted from (Hardy and Selkoe, 2002; Selkoe, 2002)). Lipid signaling (green) exacerbates the progression of this cascade through the Aβ-induced production of bioactive glycerophospholipids that can reciprocally enhance Aβ aggregation, and through the Aβ-induced activation of microglia resulting in the production of proinflammatory bioactive lipids, such as PAF.

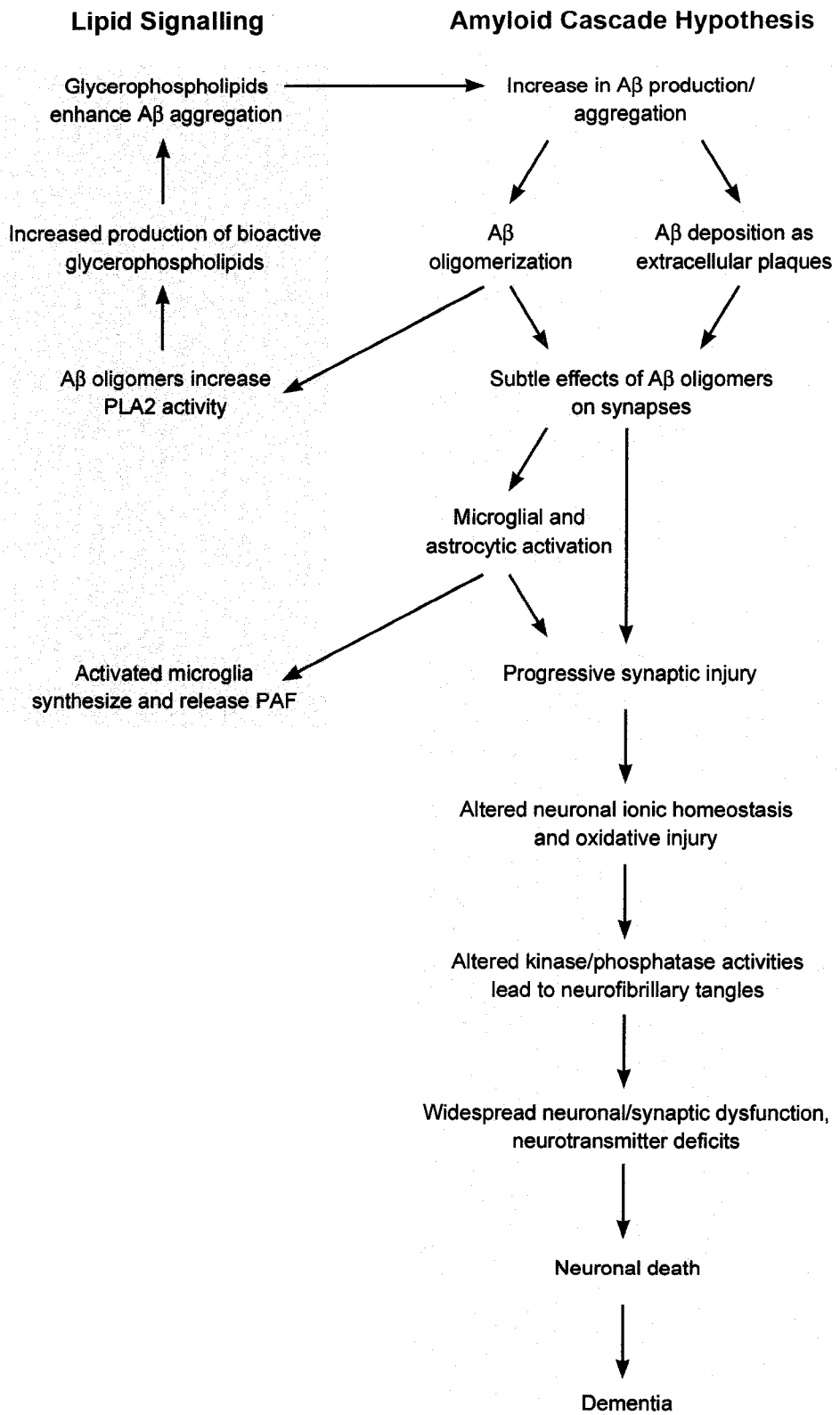


Figure 1.2

or intracellular concentration of Aβ thereby influencing neuronal function directly or contributing indirectly to neuronal death through plaque formation and subsequent activation of microglia to release inflammatory toxins (Mattson, 2004). The gradual accumulation of secreted Aβ can lead to its aggregation into soluble oligomers and insoluble fibrils that "seed" into the neurodegenerative plaques characteristic of AD (Selkoe, 2005).

Intracellular Aβ production can be modeled *in vitro*. Aberrant proteolytic processing of APP to yield intracellular Aβ was initially described in the human teratocarcinoma-derived neural precursor cell line, NT2, and was shown to increase during the differentiation of NT2 cells to hNT postmitotic neurons (Wertkin et al., 1993). It has been suggested that intracellular accumulation of Aβ in AD brain precedes the formation of extracellular amyloid plaques, and has been observed in areas of the brain known to be affected early in the progression of AD, such as the hippocampus (Zhang et al., 2002). This early appearance of intraneuronal Aβ indicates that intracellular accumulation of Aβ, and not amyloid plaques, represents the initiating step in Aβ-mediated neuronal dysfunction in AD (Gouras et al., 2000).

While early studies in AD attributed neurotoxicity to insoluble, fibrillar forms of Aβ in culture and *in vivo* (Lorenzo and Yankner, 1994; Pike et al., 1991), the number of Aβ plaques in AD brain does not form a strong correlation with the degree of cognitive impairment (Hardy and Selkoe, 2002). More recently, soluble oligomers of Aβ have been shown to directly cause cognitive deficits in rodents (Cleary et al., 2005). Due to the subtlety of cognitive impairment early in the progression of AD in the absence of other clinical signs of brain injury, it has been suggested that discrete alterations in hippocampal synaptic efficacy occurs prior to neuronal death (Selkoe,

2002). Recent evidence has shown that soluble oligomers of Aβ mediate synaptic toxicity, a process hypothesized to trigger the neurodegenerative process in AD (Cleary et al., 2005; Selkoe, 2002).

While there is growing evidence that Aβ is toxic to neurons, controversy surrounds whether neuronal loss is a consequence of exposure to extracellular amyloid plaque-associated Aβ, extracellular pre-plaque Aβ, or intracellular accumulation of Aβ (Cleary et al., 2005; Hartmann, 1999; Zhang et al., 2002). Despite these controversies, there is general consensus that neurodegeneration is exacerbated by Aβ through the "amyloid cascade hypothesis", which states that Aβ accumulation in the brain is the foundation of AD pathogenesis (Figure 1.2) (Hardy and Selkoe, 2002). Following the Aβ-induced injury to synapses, a series of detrimental cellular and biochemical alterations can occur, including changes in ionic homeostasis, oxidative injury, and synaptic and neuronal dysfunction, leading to neuronal death (Figure 1.2). The neurotoxicity mediated by Aβ has been shown *in vitro* and *in vivo* to involve the activation of apoptotic cell death pathways in neurons yet no therapeutic strategy has proven effective in inhibiting these pathways in face of ongoing Aβ production (Mattson, 2000; Mattson, 2004; Takuma et al., 2005). Here, since altered glycerophospholipid synthesis, catabolism and membrane composition have been linked with AD, a potential role is hypothesized for bioactive glycerophospholipid signalling in the Aβ neurotoxicity cascade that has yet to be thoroughly explored (Figure 1.2) (Kanfer et al., 1998).

## 1.3 Cell death in neurodegenerative disease

Neuronal cell death is most frequently described as either apoptosis or necrosis. For the purposes of this thesis, necrosis will be defined as cell death accompanied by membrane disruption. Apoptosis is also referred to as cell suicide or programmed cell death, and is essential for development and homeostasis of tissue. However, apoptosis is known to underlie neuronal death in many human neurodegenerative disorders, such as AD, Parkinson's disease, Huntington disease, HIV-dementia, stroke, epilepsy, and brain trauma (Mattson, 2000; Mattson et al., 2005). There are numerous signalling pathways that culminate in apoptotic death. These pathways can be divided into different categories according to either the dependency on enzymatic activation (eg. caspases), or to the organelle involved (eg. mitochondria, plasma membrane, and ER).

### *1.3.1 Caspase-dependent apoptosis*

Caspases are a family of cysteine proteases that cleave proteins with specific consensus sequences following a conserved aspartic acid residue (Earnshaw et al., 1999). Caspases are critical apoptotic mediators. Each family member is synthesized as a proenzyme, which upon activation initiates a cascade of catalytic events often beginning with initiator caspases, and ending with executioner caspases that orchestrate the regulated disassembly of the targeted cell. Executioner caspase activation can be achieved either through cleavage by an upstream initiator caspase or, in the case of these initiator caspases, by autocatalytic activity or catalytic complex formation (i.e., the apoptosome). To date, 14 caspase family members have been identified. Executioner caspases, including

caspase-3, -6, and -7, are responsible for the majority of morphological changes associated with apoptosis such as DNA degradation, chromatin condensation and membrane blebbing. Initiator caspases including caspase-2, -8, -9, and -12, respond to apoptotic signals and initiate the caspase cascade.

Caspase-dependent apoptosis can be divided into intrinsic and extrinsic pathways depending on the nature of the apoptotic signal. The extrinsic apoptotic pathway (see (Degterev et al., 2003) for a review) is activated through death domain (DD) containing death receptors at the plasma membrane, the most studied of which are CD95/Fas and tumor necrosis factor $\alpha$ (TNF$\alpha$) receptor (TNFR). Ligand-induced receptor multimerization forms the death inducing signalling complex (DISC) that includes adaptor molecules such as Fas associated DD (FADD) recruited to the DISC through its DD. FADD also contains a death effector domain (DED) that interacts with the DED within the prodomain of caspase-8. The recruitment of caspase-8 to the DISC results in its oligomerization and autocatalytic activation. Caspase-8 can cleave other caspases containing its LETD consensus sequence such as executioner caspase-3 and -7. The intrinsic apoptotic pathway is mitochondrial-dependent. Upon loss of mitochondrial membrane potential ($\Delta\Psi_m$) and the opening of the permeability transition pore complex (PTPC), the release of cytochrome *c* from the mitochondrial intermembrane space into the cytosol triggers the formation of the apoptosome complex defined by the cytosolic apoptotic protease activating factor-1 (Apaf-1), cytochrome *c*, ATP, and procaspase-9. Apoptosome formation enhances the basal catalytic activity of caspase-9 that then

cleaves executioner caspases, including caspase-3 and -7, at its consensus sequence LEHD.

While the extrinsic and intrinsic apoptotic pathways are initiated by different mechanisms, they have the potential to converge at the mitochondria via the B-cell lymphoma-2 (Bcl-2) family of proteins. The Bcl-2 protein family consists of both pro-apoptotic members including Bax, Bad, Bak, Bid and Bim, and anti-apoptotic members such as Bcl-2 and Bcl-$x_L$, that collaboratively regulate the continuation of the apoptotic cascade at the level of mitochondrial membrane permeabilization (Leist and Jaattela, 2001; Mattson, 2004). During extrinsic apoptosis, caspase-8 can cause truncation/activation of the pro-apoptotic Bid to tBid, which translocates to the mitochondria and can trigger release of pro-apoptotic mitochondrial proteins such as cytochrome *c* (Li et al., 1998). As described above, cytoplasmic cytochrome *c* triggers the activation of intrinsic apoptosis, including the formation of the apoptosome and downstream cleavage of executioner caspases.

### *1.3.2 Apoptotic cross-talk between the mitochondrion and the ER*

The cooperative nature of the mitochondria and the ER has been studied in the regulation of metabolism, $Ca^{2+}$ signalling, and more recently in apoptotic signalling (Walter and Hajnoczky, 2005). Mitochondria are often found in close contact with ER, enabling efficient cross-talk (Mannella et al., 1998). Molecules known to participate in ER-mitochondrial cross-talk include caspases and $Ca^{2+}$. While the ER is the organelle known as the major site of protein translation, post-translational protein modification, and intracellular $Ca^{2+}$ storage, recent studies have shown that the ER is also involved in cell death in neurodegenerative diseases

including AD, HIV-dementia and stroke (Walter and Hajnoczky, 2005). Cellular stresses such as disruption of $Ca^{2+}$ homeostasis can cause ER stress as a result of an accumulation of misfolded proteins in the ER (Takuma et al., 2005). This triggers the activation of the unfolded protein response in an attempt to alleviate the ER stress through the induction of ER chaperones such as the glucose-regulated protein (GRP) family, of which GRP78 or binding protein (BiP) is one of the best-characterized (Kaufman, 1999). If the ER stress is prolonged, caspase activation and subsequent apoptosis can ensue (Takuma et al., 2005).

In rodents, caspase-12 activation is associated with ER apoptotic induction. Rodent caspase-12 primarily localizes to the ER and is cleaved during ER stress (Hitomi et al., 2004). Caspase-12 cleaves and activates caspase-9 at its consensus site ATAD precipitating the executioner caspase cascade (Morishima et al., 2002). Because the human homologue of caspase-12 is non-functional, debate is ongoing regarding which caspase assumes its role in ER apoptosis in human cells (Fischer et al., 2002). Some have suggested either caspase-4 or caspase-2 as the candidate human ER caspase despite distinct consensus sequences (LEVD and VDVAD) since both have been shown to be localized to the ER and become activated upon ER stress in human cell lines (Dahmer, 2005; Hitomi et al., 2004; Katayama et al., 2004). However, since caspase-4 was not found to be expressed in human brain (Lin et al., 2000), caspase-2 is likely the human neuronal ER caspase.

ER caspases are activated by ER stress, which affects $Ca^{2+}$ homeostasis. Since $Ca^{2+}$ controls many vital cell functions, it is required to be under tight regulation. $Ca^{2+}$ has been dubbed the "principal language of the ER-mitochondrial communication" since both organelles are equipped with $Ca^{2+}$ transport mechanisms

(Walter and Hajnoczky, 2005). A $Ca^{2+}$-induced apoptotic pathway can involve a release of $Ca^{2+}$ from the ER, a substantial or prolonged increase in cytosolic $Ca^{2+}$, and an increase in $Ca^{2+}$ in the mitochondrial matrix (Walter and Hajnoczky, 2005). Mitochondrial permeability is known to be triggered by an increase in $Ca^{2+}$ in the mitochondrial matrix (Orrenius et al., 2003). Certain pro- and anti-apoptotic Bcl-2 family members can be localized to either the mitochondria or the ER where they play a role in the maintenance of $Ca^{2+}$ homeostasis (Breckenridge et al., 2003; Scorrano et al., 2003). Calpains are $Ca^{2+}$-activated cysteine proteases that can cleave and activate caspase-12, cleave Bid to form tBid, and cleave anti-apoptotic Bcl-2 family members rendering them pro-apoptotic (Orrenius et al., 2003). Despite a growing body of research into ER stress signalling, the mechanisms through which human caspase-2 or -4 are cleaved (and thus activated) by ER stress have not been fully defined.

### *1.3.3 Caspase-independent apoptosis*

In addition to caspase-mediated apoptosis, caspase-independent pathways can also contribute to apoptotic-like cell death through the activities of apoptosis-inducing factor (AIF), endonuclease G (endoG), and reactive oxygen species (ROS). AIF is a flavoprotein that normally resides in the mitochondria, but upon apoptotic stimulation is released into the cytosol. A nuclear localization signal allows AIF to translocate to the nucleus where it induces DNA damage (Susin et al., 1999). AIF induces apoptotic-like death as demonstrated by chromatin condensation, DNA fragmentation, mitochondrial membrane potential collapse, mitochondrial cytochrome *c* release, and exposure of phosphatidylserine on the plasma

membrane (Susin et al., 1999). However, none of these characteristics of apoptosis were prevented with the general caspase inhibitor benzyloxycarbonyl-VAD-fluoromethyl ketone (Z-VAD-FMK), indicating that AIF-induced apoptosis was caspase-independent (Susin et al., 1999). Similar mechanisms of DNA damage occur under the control of endoG. Under normal conditions, endoG is localized to the mitochondria and is involved in the replication of mitochondrial DNA (mtDNA) (Li et al., 2001). However, similar to AIF, endoG released from the mitochondria upon apoptotic stimuli and due to a nuclear localization signal is translocated to the nucleus (Li et al., 2001). Once in the nucleus, the endonuclease activity of endoG can precipitate DNA degradation. Finally, the majority of ROS is generated by the mitochondrial electron transport chain (Boss et al., 2000). It has been shown that apoptotic signalling involving ROS second messengers leads to the opening of the PTPC (Zamzami et al., 1996).

Each of the apoptotic pathways briefly described above have been associated with progressive neurodegeneration (reviewed in (Mattson, 2004; Vila and Przedborski, 2003)) and, in this thesis, will be assessed in the context of how lipid imbalances associated with neurodegenerative disease may play a role in this signalling.

### *1.3.4 Apoptosis in ischemia, HIV-dementia, and AD: a brief overview*

The overarching goal of this thesis is to establish whether intervention in phospholipid signalling, specifically in the apoptotic signal transduction pathways described above, represents a potential therapeutic target for neurodegenerative disease. A brief overview of the diseases in which bioactive glycerophospholipids,

in particular PAF family members, have been implicated in disease pathology follows.

Stroke, or cerebral ischemia, results from a transient or permanent impairment of oxygen-rich blood flow in a major brain artery. Global ischemia describes the reduction in blood flow to the entire brain, whereas focal ischemia occurs when a portion of the brain experiences reduced blood flow. The brain damage resulting from focal ischemic stroke is characterized by an ischemic infarct area, where neurons die rapidly by necrosis due to the abolition of blood flow, and a surrounding peri-infarct area or penumbra in which neurons die over days or weeks, primarily by apoptosis (Dirnagl et al., 1999; Graham and Chen, 2001; Mattson, 2000). In rodent models of stroke, neurons in the ischemic penumbra show morphological changes consistent with apoptosis, as well as DNA damage, caspase activation, and cytochrome *c* release (Dirnagl et al., 1999). ER stress is known to play an important role in ischemia/reperfusion-induced neuronal damage. Neuronal caspase-12 activation and Bip expression have been detected in a mouse model of focal ischemia known as middle cerebral artery occlusion (MCAO) (Shibata et al., 2003).

HIV-dementia describes a range of cognitive and motor dysfunctions following the infection of the CNS with HIV. Symptoms can include short-term memory deficiency, behavioural abnormalities, and Parkinson's disease-like motor impairment due to neuronal death in areas such as the hippocampus, cortex, and basal ganglia (Gonzalez-Scarano and Martin-Garcia, 2005; Mattson et al., 2005). Although neurons themselves are not infected, HIV-infected monocytes in the bloodstream are able to migrate across the blood-brain barrier and differentiate into

HIV-infected perivascular macrophages, which in turn can infect microglia. These cell types can cause neuronal damage by producing neurotoxic compounds such as viral proteins, cytokines, and inflammatory bioactive phospholipid mediators, including PAF (Gelbard et al., 1994; Gonzalez-Scarano and Martin-Garcia, 2005; Mattson et al., 2005; Perry et al., 2005). The neuronal apoptotic pathways associated with HIV-dementia include disrupted $Ca^{2+}$ homeostasis, ROS production, and caspase activation (Mattson et al., 2005).

Aβ-mediated neurotoxicity in AD involves the activation of apoptotic cell death pathways in neurons as a result of caspase activation, dissipation of $\Delta\Psi_m$, ROS production, alteration of $Ca^{2+}$ homeostasis, chromatin condensation, nuclear damage and DNA fragmentation (Eckert et al., 2003; Mattson, 2000; Mattson, 2004; Takuma et al., 2005). It has been recently suggested that pathways involving both mitochondrial dysfunction and ER stress are fundamental to neuronal apoptosis in AD (Takuma et al., 2005). In addition, bioactive phospholipids have been hypothesized to play a role in AD. Soluble Aβ oligomers are known to increase cytosolic phospholipase $A_2$ ($cPLA_2$) activity (Kriem et al., 2005). This can lead to an enhanced production of bioactive glycerophospholipids, and reciprocally, glycerophospholipids can enhance Aβ aggregation (Mandal et al., 2004). Together, these data implicate glycerophospholipids as potential mediators of cell loss in neurodegenerative disease although individual species have yet to be systematically assessed.

## 1.4 The PAF family of biologically active glycerophospholipids and neuromodulators

Although the majority of known signal transduction pathways in cellular function is attributed to proteins, it is becoming increasingly apparent that lipids have important bioactive activities and can play an integral role in pathways such as cell death (Bazan, 2005). Phospholipids are the main constituents of cellular membranes and are characterized by a hydrophilic head group and a hydrophobic tail. Phospholipids with a glycerol backbone are known as glycerophospholipids made up of multiple families.

1-*O*-alkyl-2-acetyl-*sn*-glycero-3-phosphocholine (PAF) is a glycerophospholipid that was first discovered in 1972 (Figure 1.3) (Benveniste et al., 1972). Although originally named for its ability to stimulate platelet aggregation, PAF has been found to have a variety of biological effects in numerous cell types. Currently, the term PAF represents a family of structurally similar endogenous phospholipids. The alkyl group at the *sn*-2 position is essential for the function of PAF since removing this group to form *lyso*-PAF diminishes PAF's biological activity. The predominant and most potent PAF species have either $C_{16}H_{33}$ or $C_{18}H_{37}$ as the R group at the *sn*-1 position, and a phosphocholine group at the *sn*-3 position[4].

### *1.4.1 PAF metabolism*

The biological activity of PAF can be regulated by controlling its concentration through synthetic and degradative pathways. PAF can be synthesized through two

[4] In this thesis, the term PAF will be used to refer specifically to the $C_{16}H_{33}$ species unless otherwise stated.

**Figure 1.3: PAF synthesis pathways.** PAF can be synthesized through the *de novo* or the remodeling pathway. PAFAH is responsible for the hydrolysis of PAF into *lyso*-PAF.

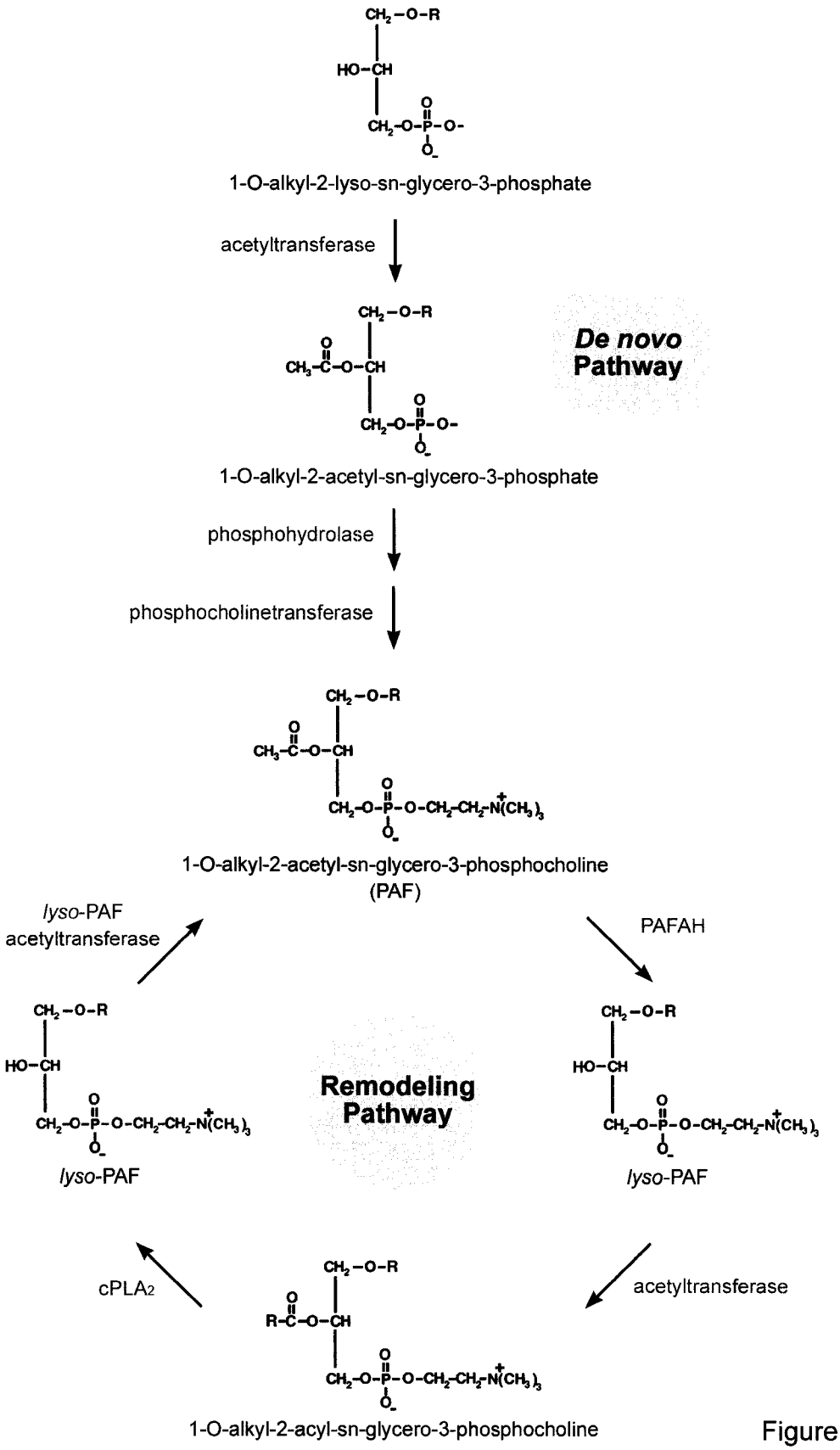


Figure 1.3

main pathways: the *de novo* pathway and the remodeling pathway (Figure 1.3) (Venable et al., 1993). In the *de novo* pathway, alkylglycerophosphates are converted to PAF through a stepwise sequence of reactions catalyzed by acetyltransferase, phosphohydrolase, and phosphocholinetransferase. This $Ca^{2+}$-independent *de novo* pathway is much slower than the remodeling pathway and is responsible for maintaining basal PAF levels under normal physiological conditions. The remodeling pathway is a cyclical pathway wherein PAF is synthesized from its immediate precursor, *lyso*-PAF, and then degraded back into *lyso*-PAF. $cPLA_2$ cleaves existing alkylacylglycerophosphocholines in membranes into *lyso*-PAF, the immediate precursor of PAF, which is then converted to PAF by *lyso*-PAF acetyltransferase. PAF can then be hydrolyzed to *lyso*-PAF by one of three different PAF acetylhydrolases (PAFAH) (see Section 1.4.2). *Lyso*-PAF undergoes an acyltransferase-catalyzed reaction to yield the same parental alkylacylglycerophosphocholines that began the remodeling pathway. The synthetic half of the cyclic remodeling pathway produced PAF more rapidly than the synthetic *de novo* pathway and is dependent on $Ca^{2+}$ release from the ER. Through the remodeling pathway, PAF can be both synthesized and hydrolyzed very quickly. In addition to these two metabolic/catalytic pathways, PAF-like family members can also be generated by oxidation of membrane glycerophospholipids producing PAF-like lipids with longer *sn*-2 fatty acids (Prescott et al., 2000).

### *1.4.2 PAF catabolism*

PAFAH acts to abolish the biological activity of PAF by removing the acetyl group from the *sn*-2 position of the PAF molecule's glycerol backbone to form *lyso*-

PAF. There are three isoforms of PAFAH: the intracellular PAFAH I and PAFAH II, and the plasma PAFAH. PAFAH I, also known as PAFAH Ib or the brain PAFAH I isoform, is composed of two catalytic subunits named $\alpha_1$ and $\alpha_2$, and a regulatory subunit known as β or LIS1.

### *1.4.3 PAF signalling*

PAF is known to bind a single G-protein coupled receptor (PAFR) that was first cloned from guinea pig lung, closely followed by the cloning of human PAFR from leukocytes (Honda et al., 1991; Nakamura et al., 1991). PAFR is expressed in most tissues, including brain, and has been assumed to be responsible for the majority of PAF effects (Ishii and Shimizu, 2000). However, ectopic expression of PAFR can be either pro- and anti-apoptotic depending on death ligand and cell type suggesting that a closer examination of PAF-mediated cell death is required (Brewer et al., 2002; Li et al., 2003; Southall et al., 2001).

PAF can both elicit neuronal death and promote neuronal function. This paradoxical nature of PAF is concentration-dependent, as demonstrated by its ability at high concentrations or with prolonged exposure to trigger neurotoxicity, and at low concentrations following transient exposure to strengthen synaptic signalling. At low physiological concentrations (pM-nM range), PAF can act as a neuronal retrograde messenger influencing learning and memory by mediating long-term potentiation, the process through which activation of a post-synaptic neuron is strengthened to a pre-synaptic signal by the pre- and post-synaptic release of glutamate (Chen et al., 2001; Francescangeli et al., 2002; Kato, 1999; Teather et al., 1998). At high physiological concentrations (nM-uM range), PAF becomes neurotoxic and initiates

apoptotic-like death (Bonin et al., 2004; Brewer et al., 2002; DeCoster et al., 1998; Tong et al., 2001). At concentrations higher than its critical micelle concentration of 3 μM, PAF has non-specific lytic detergent effects on plasma membranes resulting in necrotic-like death (Brewer et al., 2002).

The Bennett laboratory and others have demonstrated that in rat brain, PAFR is predominantly expressed in microglia and is also expressed at lower levels in neurons (Bennett et al., 1998; Mori et al., 1996). Recent data indicate that the expression pattern of PAFR in the hippocampus is species-dependent. While neurons in the CA3 region of the mouse hippocampus express PAFR, CA3 neurons in the human hippocampus do not express PAFR (Appendix 1). In the human brain, neurons that innervate CA3 pyramidal neurons die during AD (Maki et al., 2002; Menschik and Finkel, 1998). However, in transgenic mouse models of AD, neurons that innervate the CA3 region do not die to the same extent (Gau et al., 2002). It is of interest that the failure of experimental models to recapitulate all of the phenotypes of human disease correlates with PAFR expression. Colleagues in the Bennett laboratory have shown that in the PC12-AC cell line, a clonal derivative of the well-established rat pheochromocytoma PC12 cells, physiological concentration of PAF induced apoptosis in the absence of PAFR (Bonin et al., 2004; Brewer et al., 2002). Ectopic expression of human PAFR protects PC12-AC cells from PAF-induced apoptosis (Brewer et al., 2002). These results have led to the focus of this thesis, namely to pursue the underlying mechanisms of cell death triggered in human neurons in the absence of PAFR, in order to test the hypothesis that the lack of PAFR expression is key to human neuronal susceptibility common to multiple progressive neurodegenerative disorders.

### *1.4.4 PAF in neurodegenerative disease*

Pathophysiological exposure to PAF has been hypothesized to be a key mediator of neuronal death in ischemia, HIV-1 dementia, and AD (Bate et al., 2004c; Bazan, 1998; Birkle et al., 1988; Perry et al., 1998). $cPLA_2$ is activated during ischemia, resulting in the neuronal accumulation of bioactive lipids such as PAF (Bazan, 1998). In support of the causative role of bioactive lipids in neuronal injury, $cPLA_2$ knockout mice exhibited less cerebral injury following transient focal ischemia (Bonventre et al., 1997). In similar fashion, HIV-dementia involves the production of neurotoxic compounds including inflammatory bioactive phospholipid mediators by HIV-infected perivascular macrophages and microglia (Gonzalez-Scarano and Martin-Garcia, 2005). PAF is known to be one of the proinflammatory mediators synthesized by and released from microglia, and has been repeatedly implicated in HIV-induced neuronal death (Gelbard et al., 1994; Perry et al., 1998; Perry et al., 2005) . In addition, the HIV protein Tat can stimulate production of the proinflammatory cytokine tumour TNFα from microglia that can subsequently stimulate further PAF release (Tong et al., 2001). Finally, changes in glycerophospholipid membrane composition and $PLA_2$ activity have been linked with AD (Kanfer et al., 1998). Together, these data form the rationale behind the hypothesis that PAF family members and downstream neurotoxic signalling represent a novel therapeutic target for multiple neurodegenerative disorders.

## 1.5 Rationale, hypothesis and objectives

Sustained exposure to pathophysiological concentrations of PAF has been hypothesized to be a primary mediator of neuronal death in models of

neurodegeneration. The hypothesis that PAF is involved in the neuropathophysiology of AD stems not only from the similarities of PAF- and Aβ-induced apoptotic pathways, but also from the imbalances of substrates and enzymes in the PAF synthesis pathways seen in AD (Kriem et al., 2005; Mandal et al., 2004). While it has been assumed that PAF signals exclusively through PAFR, the Bennett laboratory has explicitly shown that PAFR-independent pathways also contribute to neuronal loss (Bonin et al., 2004; Brewer et al., 2002). In addition, the expression of neuronal PAFR *in vivo* in rodent but not in human hippocampus suggest that key species differences may contribute to discrepancies in rodent models of AD associated with neuronal susceptibility (Appendix 1). **This thesis is driven by the hypothesis that PAF signalling, specifically neurotoxicity triggered independently of PAFR, can be targeted *in vitro* and *in vivo* to protect neurons from apoptosis associated with neurodegenerative disease.** A summary of apoptotic pathways associated with neurodegeneration that PAF could potentially initiate in human neurons are depicted in (Figure 1.4). Using this model as a starting point, the objectives of this thesis are to:

1) Delineate the PAFR-independent neurotoxic pathway induced by PAF *in vitro* in human neurons (Chapters 2,3);
2) Screen a panel of known PAF inhibitors and potential PAF inhibitors for their ability to protect against PAF and Aβ -induced neurotoxicity *in vitro* in human neurons (Chapter 4);
3) Test the ability of a PAF inhibitor to protect from neurotoxicity and behavioural impairment *in vivo* in a mouse model of focal ischemia (Chapter 5).

**Figure 1.4: Potential neurodegenerative cell death pathways initiated by PAF in the absence of PAFR.** In PAFR-negative neurons, PAF could initiate cell death through the extrinsic pathway (death domain receptor-dependent), the intrinsic pathway (mitochondrial-dependent), or the ER stress pathway. All three pathways have been described in neurodegenerative disease, involve the activation of caspases, and culminate in nuclear damage characteristic of apoptosis. In addition, cross-talk can occur between the extrinsic and intrinsic pathways, as well as through ER and mitochondrial signalling.

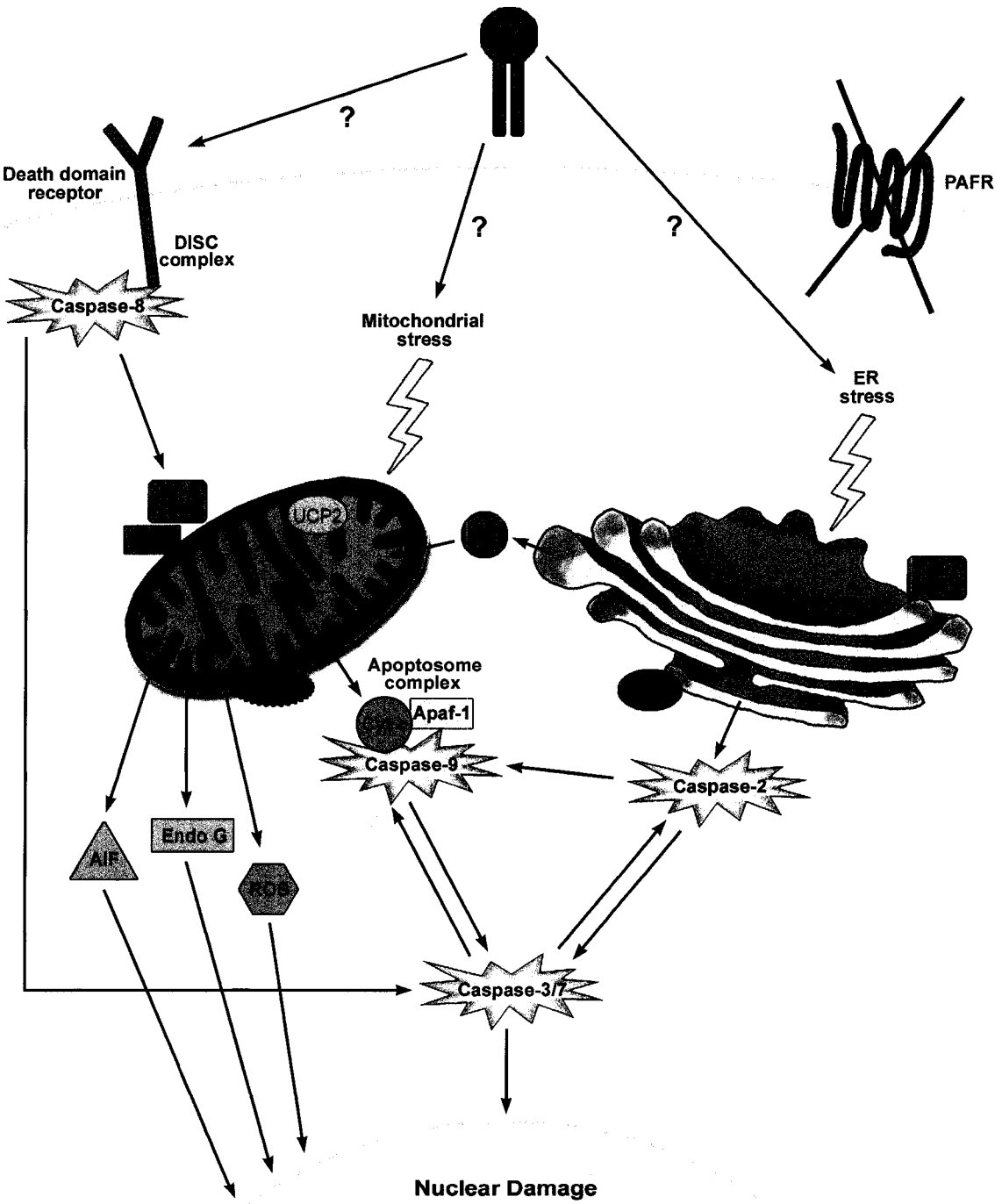


Figure 1.4

# Chapter 2: Platelet activating factor triggers caspase-dependent neuronal apoptosis independently of its receptor

## 2.1 Publications resulting from studies described in this chapter:

Moffat TC, Wong S, Hozturk E, Migahed L, Paliga A, Bennett SAL (2006) Platelet activating factor elicits an endoplasmic reticulum-dependent caspase cascade in human neurons independently of its G-protein coupled receptor, in preparation.

## 2.2 Statement of author contributions

All of the experiments presented in this chapter were either carried out or supervised by Tia C. Moffat. As part of the training in the Bennett laboratory, senior graduate students supervise undergraduate trainees. In this capacity, a portion of the LIVE/DEAD experiments and counts were performed by Aleks Paliga. Serena Wong performed and counted one of the CaspaTag-3/7 experiments and performed the cleaved caspase-3 Western blots. Lamiaa Migahed performed one of the CaspaTag-3/7 experiments and one of the Z-VDVAD-FMK CaspaTag-3/7 experiments. Cell counts were performed by two independent investigators blind to the conditions. Emre Hozturk counted a portion of the CaspaTag and caspase inhibitor LIVE/DEAD experiments. Western blots of PCNA, NF-68, GAP43 and myelin PLP expression in NT2 and hNT cultures were performed by Sherri Boucher as part of her M.Sc. research. All figures and text in this chapter were prepared by Tia C. Moffat with guidance and editorial assistance from Dr. Steffany A.L. Bennett.

## 2.3 Abstract

While it is generally assumed that the majority of PAF effects, including neuronal death, are mediated by activation of the PAFR, the Bennett laboratory has previously shown that PAF can also act independently of PAFR to induce apoptosis in non-neuronal cells (Bonin et al., 2004; Brewer et al., 2002). The signalling pathways underlying PAFR-independent apoptosis have yet to be elucidated. In this study, PAF (1 μM) was shown to trigger caspase-dependent apoptosis in terminally differentiated human neurons that do not express PAFR. Through caspase activity assays and Western blotting, it was found that intrinsic (mitochondrial-mediated) and extrinsic (receptor-mediated) caspase cascades do not initiate PAF-induced apoptosis in the absence of PAFR. Instead, PAF was found to elicit apoptosis in human neurons by triggering ER stress leading to caspase-2 cleavage, followed by caspase-7 activation culminating in apoptotic DNA fragmentation within 24 h of treatment. Cytochrome *c* release from the mitochondria and caspase-9 activation were shown to be later stage events triggered in the minority of neurons surviving a 24 h PAF (1 μM) treatment, and are likely mediated by ER-mitochondrial cross-talk. These data provide new insight into the pathophysiological actions of PAF in a human neuronal system.

## 2.4 Introduction

As described in Chapter 1, PAF is recognized as a principal mediator of neuronal death *in vitro* and *in vivo* in a variety of neurodegenerative conditions (Bate et al., 2004a; Bate et al., 2004c; Bazan, 1998; Bazan, 2005; Birkle et al., 1988; Darst et al., 2004; Gelbard et al., 1994; Perry et al., 1998; Tong et al., 2001; Yue and Feuerstein, 1994). The biological activity of PAF is attributed generally to activation of PAFR (for a review, see (Ishii and Shimizu, 2000)), yet PAF has been shown to trigger cell death *in vitro* through PAFR-dependent and PAFR-independent pathways (Bonin et al., 2004; Brewer et al., 2002; Darst et al., 2004; Li et al., 2003; Ma and Bazan, 2001; Perry et al., 1998; Southall et al., 2001). The neuronal death pathways elicited by PAF have not been systematically evaluated, nor is it clear whether PAF is toxic to subsets of neurons expressing PAFR, or whether PAF can trigger apoptosis in neurons lacking PAFR as has been shown in non-neuronal cell types (Bonin et al., 2004; Brewer et al., 2002). This distinction is important given that PAFR expression is restricted to discrete neuronal subpopulations (Bennett et al., 1998; Mori et al., 1996) yet PAF is purported to underlie significant neuronal loss in human conditions as reviewed in Chapter 1. Here, the NT2/hNT human CNS neuronal differentiation model was used to elucidate whether, and if so, how PAF triggers cell death in human neurons that do not express PAFR.

## 2.5 Methods

### *2.5.1 Reagents*

Unless otherwise specified, all cell culture reagents were obtained from Invitrogen, and all chemical reagents were obtained from Sigma.

### 2.5.2 *Cell culture*

Cells were cultured at 37°C in a 5% $CO_2$/95% air atmosphere. NT2/D1 (NT2)[5] cells, originally obtained from Stratagene, were cultured in 10 cm tissue culture plates using Dulbecco's Modified Eagle Medium:Nutrient Mixture F-12 (DMEM/F12) supplemented with 10% fetal bovine serum (FBS), 1% penicillin/streptomycin, 2 mM L-glutamine (complete media). Cells were passaged every 2-3 days. Differentiation of NT2/D1 cells into hNTs was performed as described in (Boucher and Bennett, 2003). Briefly, 2 X $10^6$ NT2 cells were plated into 75-$cm^2$ flasks and fed three times a week with complete media supplemented with 10 µM retinoic acid (RA) for 4-5 weeks. Cells were then trypsinized and split 1:3 into new 75-$cm^2$ flasks without RA (replate 1). After 48 h, the phase-bright hNT neurons were separated from more adherent non-neuronal cells by mechanical force and trypsinization (replate 2). Prior to trypsinization, media were collected from the cells (conditioned media) and a 1:1 mixture of complete media and conditioned media was used to plate cells on tissue culture dishes coated with laminin (20 µg/mL) and poly-D-lysine (100 µg/ml) at a density of 1.25 x $10^5$ cells/ $cm^2$. Cells were treated 24 h following replate 2 with the mitotic inhibitors cytosine β-D-arabinofuranoside (ara-C, 1 µM, Sigma) and 5-fluoro-deoxyuridine (FUdR, 10 µM, Sigma). Cells were fed 4 days later with complete media supplemented with ara-C and FUdR, and subsequently every 4 days with complete media

[5] Throughout this thesis, the term NT2 is used specifically to refer to the NT2/D1 subclone of the NT2 teratocarcinoma cell line.

supplemented with ara-C, FUdR and uridine (Urd, 10 μM, Sigma). Terminally differentiated hNT cultures were obtained following 3 weeks of mitotic inhibition.

### *2.5.3 Cell treatments*

Prior to treatment, cells were washed with 10 mM phosphate-buffered saline (PBS; 2.5 mM monobasic sodium phosphate, 7.5 mM dibasic sodium phosphate, 154 mM NaCl, pH 7.2). Cells were treated with either EtOH (0.1%; vehicle), PAF (0.001 – 1 μM, BioMol)[6], methyl carbamyl PAF (cPAF, 0.1 – 10 μM), etoposide (42 μM), staurosporine (STS, 1 μM), Aβ (25 μM), or tunicamycin (1 μg/mL). These agents were diluted in serum-free treatment media consisting of DMEM/F12 supplemented with 1% penicillin/streptomycin, 2 mM L-glutamine, and 0.025% bovine serum albumin (BSA, BioShop).

### *2.5.4 Immunocytochemistry*

Cells were replated either in 4-well LabTek slides or in tissue culture dishes containing glass coverslips coated with either gelatin (0.1%, NT2s) or laminin/poly-D-lysine (hNTs) as described in *2.5.2*. Cells were washed in 10 mM phosphate-buffered saline (PBS) and fixed for 20 min in 3.7% paraformaldehyde diluted in PBS. Immunofluorescence was performed as described in (Boucher and Bennett, 2003). Primary antibodies used were rabbit polyclonal anti-nestin (1:400, Chemicon), rabbit polyclonal anti-neuron-specific enolase (NSE, 1:600, Calbiochem), Cy3-conjugated anti-vimentin (1:800, Sigma), Cy3-conjugated anti-glial fibrillary acidic protein

[6] Throughout this thesis, cells were treated with the 1-O-hexadecyl-2-acetyl-sn-glycero-3-phosphocholine PAF species.

(GFAP, 1:800, Sigma), and mouse monoclonal anti-cytochrome *c* (1:5000, BD Pharmingen). Secondary antibodies used were Cy3-conjugated anti-mouse IgG (1:800, Jackson Immunoresearch) and Cy3-conjugated anti-rabbit IgG (1:600, Jackson Immunoresearch). Antibodies were diluted in antibody buffer (PBS, 0.3% Triton X-100, 3% BSA). Where Hoechst staining is indicated, cells were incubated in Hoechst 33258 stain (0.2 µg/mL in PBS) for 20 min and washed 3 times in PBS for 5 min. Cells were mounted in Vectashield (Vector Laboratories) or in an anti-fade mounting media prepared in-house (Bennett et al., 1995) and analyzed with a Leica DMRXA2 epifluorescent microscope equipped with a Hamamatsu ORCA-ER digital camera and OpenLab 3.17 software (Improvision).

### *2.5.5 Reverse transcriptase- polymerase chain reaction (RT-PCR)*

Total RNA was isolated from cells using Trizol reagent according to the manufacturer's protocol. To digest any residual DNA, 10 µg of total RNA was treated with 3 units of RQ1 RNAse-free DNAse (Promega) in transcription-optimized 5x buffer (Promega). RNA template was precipitated and reconstituted in nuclease-free $H_2O$ (Promega). First strand cDNA synthesis with pdN6 random hexamer primers (Promega) was performed with 200 units of the reverse transcriptase Superscript II RT. The cDNA template was amplified in a reaction mixture containing 5 µL 10 X PCR reaction buffer, $MgCl_2$ (0.5 – 2 µM), 4 uL 10 mM deoxynucleotide triphosphates (dNTPs, Promega), 25 pmol each of forward and reverse primers, and 5 units of Taq DNA polymerase in a final volume of 50 µL using a GeneAmp PCR System 2400 (Applied Biosystems). Cycling protocol was 95°C for 5 min, 30 cycles of denaturing at 95°C for 30 sec, annealing at 55°C for 1 min,

and extension at 72°C for 2 min, followed by the final phase of 75°C for 5 min. Primer pairs used were: (i) RPAF5 (sense 5'-CACTTATAACCGCTACCAGGCAG-3' and antisense 5'-AAGACAGTGCAGACCATCCACAG-3') defining a 381 bp amplicon of PAFR, (ii) HPAF1 (sense 5'-GCATCCTACTTCCTCATCCT-3' and antisense 5'-ACTTCAGTGACCGTATCCGT-3') defining a 538 bp amplicon of human PAFR, and (iii) RGAPDH2 (sense 5'-TGGTGCTGAGTATGTCGTGGAGT-3' and antisense 5'-AGTCTTCTGAGTGGCAGTGATGG-3') defining a 292 bp amplicon of GAPDH. PCR amplicons were subjected to electrophoresis through a 1.2% agarose gel. DNA was stained with ethidium bromide and visualized under UV light.

*2.5.6 Cell viability assays (LIVE/DEAD, WST)*

For the LIVE/DEAD Viability/Cytotoxicity assay (Molecular Probes), cells were grown in either 4-well LabTek slides or 96-well black plates with clear bottoms. Survival was determined by the ability of intracellular esterases to cleave calcein-AM, producing a fluorescent wavelength of 515 nm. Necrosis was measured by the ability of ethidium homodimer-1 (EthD-1) to enter cells with damaged membranes and intercalate between DNA strands, emitting a fluorescent wavelength of 635 nm. Cells were washed in warm PBS, and incubated for 5 min in calcein AM (1.25 uM) and EthD-1 (0.75 uM) diluted in warm PBS. Cells were immediately analyzed using a Leica DMIL inverted epifluorescent microscope equipped with a Qimaging QICAM fast 1394 digital camera (Quorum Technologies). Phase contrast and fluorescent photos were taken of 6-15 random fields per well in duplicate or triplicate experiments. For the WST Viability assay (Roche), viability was determined by the ability of mitochondrial dehydrogenases to cleave the WST tetrazolium salt to a red

formazan dye. Cells were grown in five replicate 10 cm dishes. Following treatments, cells were incubated for 30 min at 37°C and 5% $CO_2$ in serum-free treatment media containing a 1 in 30 dilution of WST reagent. Media were collected and viability was spectrophotometrically measured by the absorbance of the formazan dye at 450 nm.

### *2.5.7 Terminal deoxynucleotidyl transferase deoxyuridine triphosphate nick end labeling (TUNEL)*

Cells were replated either in 4-well LabTek slides or in tissue culture dishes containing glass coverslips coated with laminin/poly-D-lysine as described in *2.5.2.* Cells were fixed as described in *2.2.4.* Fixed cells were washed in PBS and permeabilized in ice cold 0.1% sodium citrate / 0.1% Triton-X 100 for 5 min followed by 2 min in 2:1 ethanol:acetic acid on ice. Cultures were rinsed for 2 min in PBS and incubated for 1 hr at 37°C with FITC-labeled dUTP in terminal deoxynucleotidyl transferase (TdT) buffer (30 mM Tris-HCl, pH 7.2, 140 mM sodium cacodylate, and 1 mM cobalt chloride) and TdT according to the protocol provided by the manufacturer (Roche). Negative controls included sections incubated with FITC-labeled dUTP in the absence of TdT. Cells were washed in PBS, mounted in Vectashield (Vector Laboratories) and analyzed with a Leica DMRXA2 epifluorescent microscope equipped with a Hamamatsu ORCA-ER digital camera and OpenLab 3.17 software (Improvision).

### *2.5.8 Caspase activity assay*

Caspase activity in live cells was measured using CaspaTag (caspase-3/7, caspase-8, Chemicon) and FLICA (caspase-2, caspase-9, Intergen) assays. Cells were cultured in 96-well black plates with clear bottoms. Following treatments, media were removed to give a final volume of 50 µL per well. CaspaTag/FLICA assays were performed using a modified protocol from the manufacturer's instructions. Briefly, 1.67 µL of 30x CaspaTag/FLICA reagent (diluted in PBS) was added to each well. Cells were incubated for 1 h at 37°C and 5% $CO_2$. Cells were washed twice in PBS and analyzed with a Leica DMIL inverted epifluorescent microscope equipped with a Qimaging QICAM fast 1394 digital camera. Phase contrast and fluorescent photos were taken of six random fields per well for 5 – 10 replicate wells in duplicate or triplicate experiments. The mean number of cells with active caspases in vehicle-treated cultures at each time point was subtracted from the number of cells with active caspases in PAF-treated cultures, and data were then standardized against untreated controls to determine fold-change in caspase activity attributable to PAF exposure.

### *2.5.9 Protein isolation*

For total cell protein isolation, cells in 10 cm culture dishes were washed with PBS, and lysed with RIPA buffer (PBS, 1% Nonidet P-40, 0.1% sodium dodecyl sulfate (SDS), 0.5% sodium deoxycholate) supplemented with the protease inhibitors aprotinin (50 µg/mL), sodium orthovanadate (1 mM), phenylmethylsulfonyl fluoride (1 mg/mL), and sodium fluoride (1 mM). Lysates were passed through a 26 gauge needle, incubated at 4°C for 30 minutes, and centrifuged at 12000 g for 30

minutes. The supernatant contained total cell protein. For mitochondrial/cytosolic fractionation, cells in 10 cm culture dishes were trypsinized and collected by centrifugation at 1000 g for 5 minutes. The cells were processed using a modified protocol from a mitochondrial protein isolation kit (Pierce). Briefly, cells were lysed using lysis buffer and a tissue homogenizer. Cellular debris and nuclei were pelleted by centrifugation at 700 g for 10 minutes at 4°C. Supernatant was centrifuged at 12000 g for 15 minutes at 4°C. The resulting supernatant was the cytosolic protein fraction. The pellet was washed and centrifuged at 12000 g for 5 minutes at 4°C. The pellet was resuspended in the supplied buffer to give the mitochondrial protein fraction.

*2.5.10 Western blotting*

Protein samples (30 µg for total protein, 7 µg for fractioned protein) were separated by SDS polyacrylamide gel electrophoresis in 7.5%, 12.5%, or 15% acrylamide gels. Separated proteins were transferred to a polyvinylidene difluoride membrane at 100 V for 1 h. Membranes were stained with the protein dye Ponceau Red to ensure proper transfer of proteins. Membranes were blocked in 1% casein (in PBS) for 1 h at room temperature and incubated in primary antibody diluted in 1% casein overnight at 4°C with shaking. Following two 10 minute washes in PBS and two 10 minute washes in 1% casein, membranes were incubated in secondary antibody diluted in 1% casein for 1 h at room temperature with shaking. For anti-cleaved caspase-7 immunoblotting, membranes were washed twice for 10 minutes in PBS and twice for 10 minutes in 1% casein and incubated in tertiary enhancement reagent diluted in 1% casein for 1 h at room temperature with shaking. After

secondary/tertiary antibody incubation, membranes were washed four times for 10 minutes in PBS and incubated for 4 minutes in SuperSignal West Pico chemiluminescent substrate (Pierce). Membranes were exposed to x-ray film to visualize immunoreactivity. Primary antibodies used were anti-proliferating cell nuclear antigen (PCNA, 1:100, Oncogene Research), mouse monoclonal anti-neurofilament-68 (NF-68, 1:400, Sigma), rabbit polyclonal anti-growth associated protein 43 (GAP43, 1:2000, Chemicon), anti-myelin proteolipid protein (myelin PLP, 1:200, Biogenesis), rabbit polyclonal anti-cleaved caspase-3 (1:1000, Cell Signaling Technologies), rabbit polyclonal anti-cleaved caspase-7 (1:1000, Cell Signaling Technologies), mouse monoclonal anti-cytochrome *c* (1:1000, BD Pharmingen), mouse monoclonal anti-cytochrome oxidase IV (COX IV, 1:5000, Molecular Probes), mouse monoclonal anti-β-tubulin III (tubulin, 1:10000, Sigma), and mouse monoclonal anti-binding protein (BiP, 1:1000, Transduction Laboratories). Secondary antibodies used were horseradish peroxidase (HRP)-conjugated anti-mouse IgG (1:2000, Jackson Immuno), HRP-conjugated anti-rabbit IgG (1:5000, Jackson Immuno), biotin-conjugated anti-mouse IgG (1:10000, Sigma). Tertiary enhancement reagent used was extravidin peroxidase (1:1000, Sigma) where indicated.

*2.5.11 Statistical analysis*

Analysis of one condition with respect to another was performed using the Student's *t* test. Analysis of multiple conditions with respect to one control condition was performed using the one-way analysis of variance (ANOVA). In the cases where the ANOVA showed a statistically significant difference throughout the

conditions compared to control, the *post-hoc* Tukey or Dunnett's *t* test was used to determine which condition differed from control in a statistically significant manner and to define the p value measuring the significance of the difference.

## 2.6 Results

### *2.6.1 Characterization of the NT2/hNT human CNS neuronal differentiation model*

NT2 neural precursors (Figure 2.1A, left panel) were terminally differentiated to hNT neurons (Figure 2.1A, right panel) following an eight week differentiation protocol. Cultures contained two primary cell types. Phase-bright hNT neurons (Figure 2.1A, right panel, arrowhead) exhibited a tendency to aggregate into bundles of varying sizes (Figure 2.1A, right panel, arrow) and were found on top of a feeder layer of large adherent flat non-neuronal cells (Figure 2.1A, right panel, asterisk). To confirm terminal differentiation, undifferentiated and differentiated cultures were analyzed with various cell lineage antigenic markers by both immunocytochemistry and Western blotting (Figure 2.1B,C). NT2 cells expressed the intermediate filament protein vimentin not present in terminally differentiated neurons, the intermediate filament protein nestin characteristic of neural precursors, and the cell cycle marker of proliferation PCNA (Figure 2.1B,C). Differentiated hNT cultures expressed the neuronal markers NSE (Figure 2.1B), NF-68 (Figure 2.1C), and GAP43 (Figure 2.1C). PCNA levels were greatly reduced in hNTs (Figure 2.1C) and only observed in the non-neuronal cells when mitotic inhibitors were removed for 24 h (data not shown). The non-neuronal cells in differentiated hNT cultures retained vimentin expression (Figure 2.1B). The oligodendrocyte marker myelin PLP was expressed exclusively in hNT cultures, presumably by the non-neuronal cells (Figure 2.1C).

**Figure 2.1: Characterization of the terminal differentiation of NT2 progenitors into hNT neuronal cultures.** A: NT2 progenitor cells (left panel) can be terminally differentiated to postmitotic hNT neurons (arrow, arrowhead) and non-neuronal cells (*) upon RA treatment and mitotic inhibition (right panel). hNT neurons can aggregate into large bundles (arrow) or are found as single cells (arrowhead). B: Immunocytochemistry of NT2 and hNT cultures shows a loss of the stem cell marker nestin and a gain of NSE upon differentiation. The large non-neuronal cells in the culture retained vimentin expression upon differentiation. (C) Western blot analysis shows a reduction in PCNA and a gain of NF-68, GAP43 and myelin PLP protein expression upon differentiation. Coomassie blue-staining of total protein was used as a loading control since both actin and tubulin protein levels change as NT2 cells terminally commit to an hNT neuronal lineage. Scale bars in A and B, 50 μm.

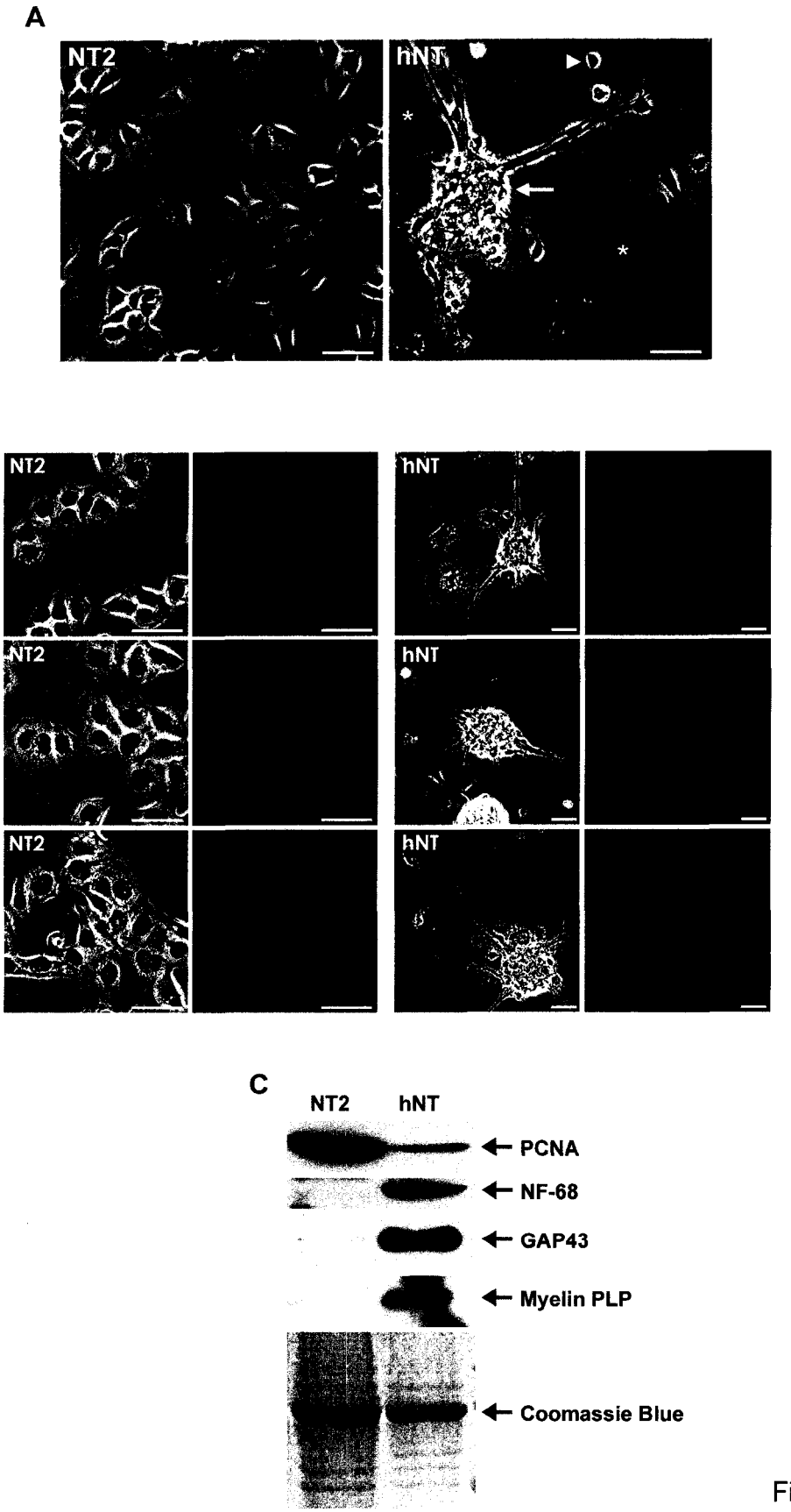


Figure 2.1

The astrocyte marker GFAP was not detected in either NT2s or hNTs (data not shown). Quantitation of cells expressing antigenic lineage markers following immunocytochemistry indicated that hNT cultures were composed of approximately 80% NSE-positive hNT neurons and 20% vimentin-positive non-neuronal cells.

### *2.6.2 NT2 neural precursors and hNT neurons do not express PAFR*

PAFR was not expressed by NT2 and hNT cultures as assessed by RT-PCR using two different PAFR primer pairs (Figure 2.2). Positive controls included NT2 genomic DNA (HPAF1 control, PCR amplified) and PC12-AC cells stably transfected with human PAFR (RPAF1 control, RT-PCR amplified). GAPDH was amplified from each sample to confirm template integrity.

### *2.6.3 PAF triggers apoptotic-like death in hNT neurons but not NT2 neural precursors.*

To establish whether cell death is elicited by PAF in the absence of PAFR, NT2 and hNT cultures were treated with PAF for 24 h. Cell survival was assessed by Trypan Blue exclusion, LIVE/DEAD, TUNEL, and WST assays. PAF did not impact upon the viability of NT2 cells (Figure 2.3A, left panel). To control for possible PAF hydrolysis over time (Bonin et al 2004), cells were treated with cPAF, a PAF analogue resistant to degradation by PAF acetylhydrolases. Treatment with cPAF did not alter NT2 cell viability until cPAF levels exceeded the critical micelle concentration of 3 μM (Figure 2.3A, right panel). At concentrations of 5 μM or higher, cPAF triggered a 75% decrease in cell survival and a significant loss in membrane integrity evident by Trypan Blue exclusion and uptake of the

**Figure 2.2: NT2 progenitors and hNT neuronal cultures do not express PAFR.** RT-PCR analysis using two different PAFR primer pairs demonstrated that NT2 and hNT cultures do not express PAFR. Positive controls (+) were NT2 genomic DNA (HPAF1 control, top panel) or random-primed cDNA from PC12 transfectants stably expressing human PAFR (RPAF5 control, middle panel). cDNA template integrity was confirmed by amplification of GAPDH as an internal standard (bottom panel).

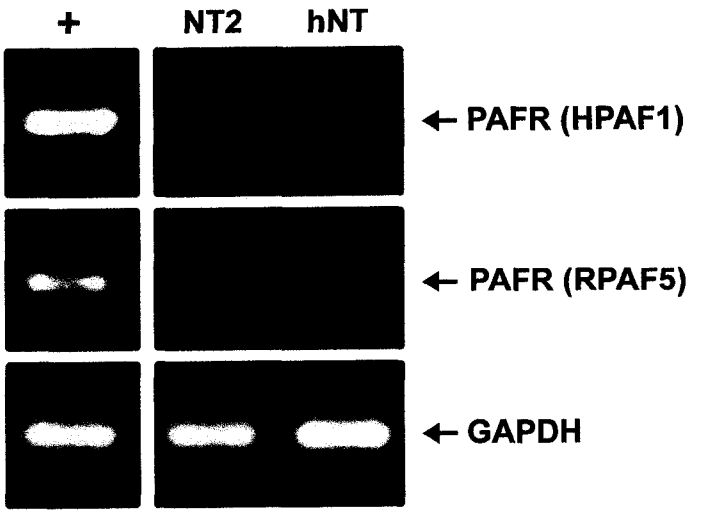


Figure 2.2

**Figure 2.3: Physiological concentrations of PAF trigger cell death in differentiated hNT neuronal cultures but not NT2 progenitors.** (A) Physiological concentrations of PAF (0.1 – 100 nM) did not significantly alter NT2 cell survival following 24 h as measured by Trypan Blue exclusion (left panel). To extend the kinetics of PAF exposure, NT2 cells were treated for 24 h with a PAF analog (cPAF; 0.1 – 10μM) resistant to PAF degradation by PAFAH. Cell death was only observed when cPAF levels exceeded the critical micelle concentration of 3 μM (right panel; ** $p < 0.01$, ANOVA, *post-hoc* Dunnett's *t* test). (B) NT2 cells did not die by necrosis until 24 h cPAF treatments reached 5 μM as evidenced by uptake of EthD-1 (** $p < 0.01$, ANOVA, *post-hoc* Dunnett's *t* test). (C) A dose-dependent reduction in survival of differentiated hNT cultures was observed when cultures were exposed to physiological concentrations of PAF (0.1 nM – 1 μM) for 24 h as measured by calcein AM cleavage (* $p < 0.05$, ** $p<0.01$, ANOVA, *post-hoc* Dunnett's *t* test). (D) PAF-induced loss of hNT cells following 24 h occurred in the absence of significant necrosis as evidenced by a lack of EthD-1 uptake. (A) – (D) Data were expressed as the mean $\pm$ standard error of the mean (SEM; n=12-45 per data point).

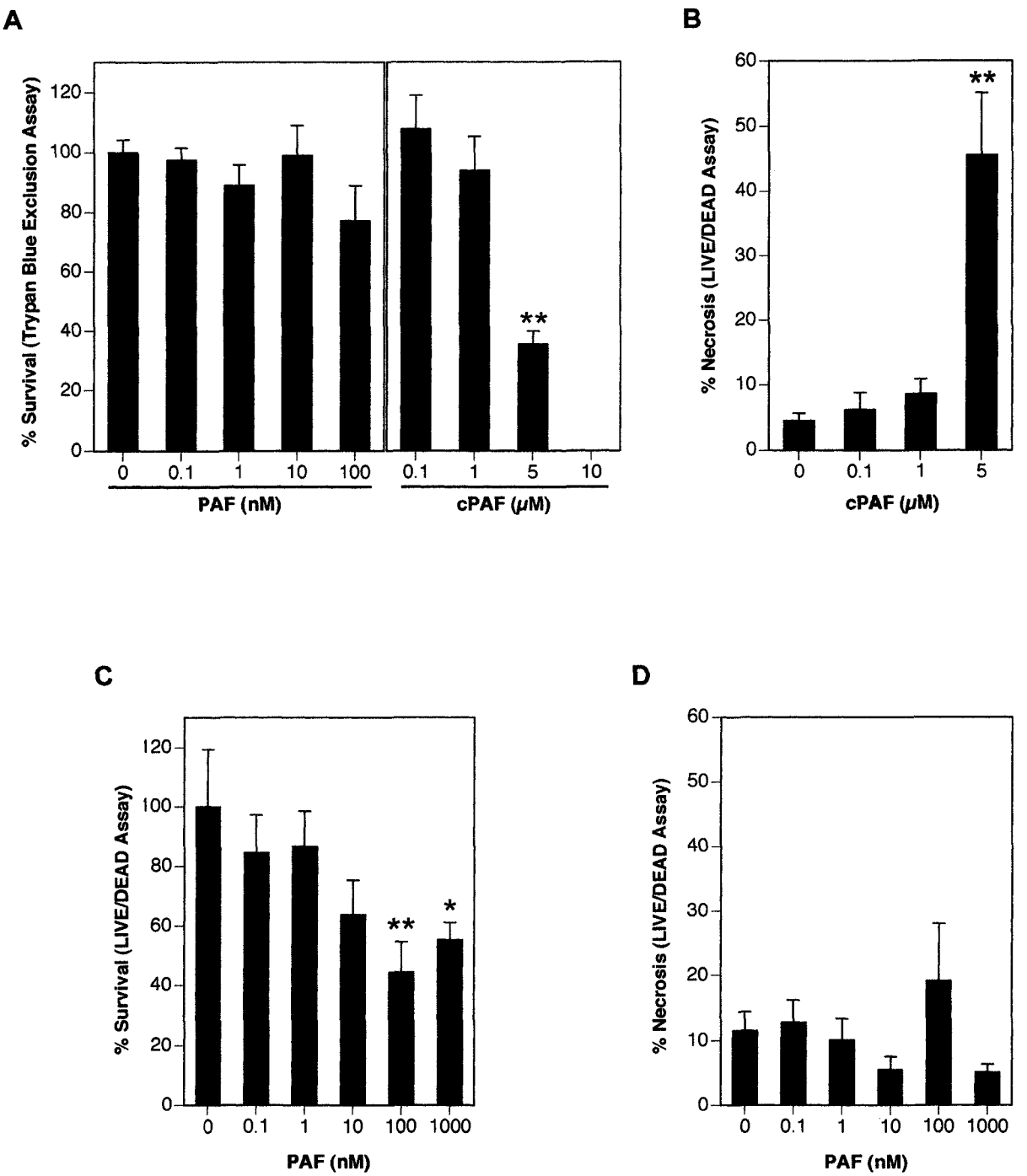


Figure 2.3

membrane-impermeable EthD-1 (Figure 2.3A,B). These observations are consistent with necrotic lysis observed when cells are exposed to artifactually high concentrations of phospholipids.

By contrast, hNTs were sensitive to PAF concentrations below the critical micelle concentration (Figure 2.3C,D, 2.4A-D). A significant reduction in metabolic activity as determined by WST assay was observed when cells were treated with 1 nM - 1 μM PAF (Figure 2.4C). The WST assay measures the cleavage of the WST formazan salt by active mitochondrial dehydrogenases in metabolically active cells. Significant cell death was detected when cells were exposed to 100 nM-1 μM PAF. Cell loss was determined by LIVE/DEAD staining in which viable cells are identified by the enzymatic conversion of calcein AM to fluorescent calcein and by the ability to exclude EthD-1 (Figure 2.3C, 2.4A). Morphological examination of cultures indicated that neurons were preferentially lost following treatment with 1 μM PAF for 24 h (Figure 2.4D). PAF did not compromise membrane integrity (Figure 2.3D) but did elicit a dose-dependent increase in apoptotic-like DNA fragmentation as assessed by TUNEL reactivity (Figure 2.4B).

### *2.6.4 Caspase-7 is the primary executioner caspase involved in the PAF-induced caspase cascade in hNTs.*

To confirm that PAF triggers neuronal apoptosis independently of PAFR, executioner caspase-3 and 7 activation was evaluated by *in vitro* activity assay and Western blotting 0-24 h after PAF exposure. Significant caspase-3/7 activity was detected 1 h after administration of 1 μM PAF as assessed by cleavage of a fluorescent DEVD substrate (Figure 2.5A,B). Caspase-3/7 activity progressively

**Figure 2.4: PAF elicits neuronal death in the absence of PAFR.** PAF (0.1, 1 μM) dose-dependently reduced cell survival (A) and increased DNA fragmentation (B) as measured by the TUNEL assay in hNT neuronal cultures (**p < 0.01, ANOVA, *post-hoc* Tukey). (C) The WST metabolic assay showed a decrease in mitochondrial dehydrogenase activity indicative of compromised cell viability following a 24 h dose response of PAF (**p < 0.01, ANOVA, *post-hoc* Dunnett's *t* test). (A) – (C) Data were expressed as the mean ± SEM (n=5-27 per data point). (D) Representative digital micrographs of hNT cultures following a 24 h treatment of either vehicle (top panel) or 1 μM PAF (bottom panel). Neurons, both single (arrowheads) and in bundles (arrows), were less abundant following PAF treatment, while the number of non-neuronal cells (*) were comparable between treatments. Scale bars, 50 μm.

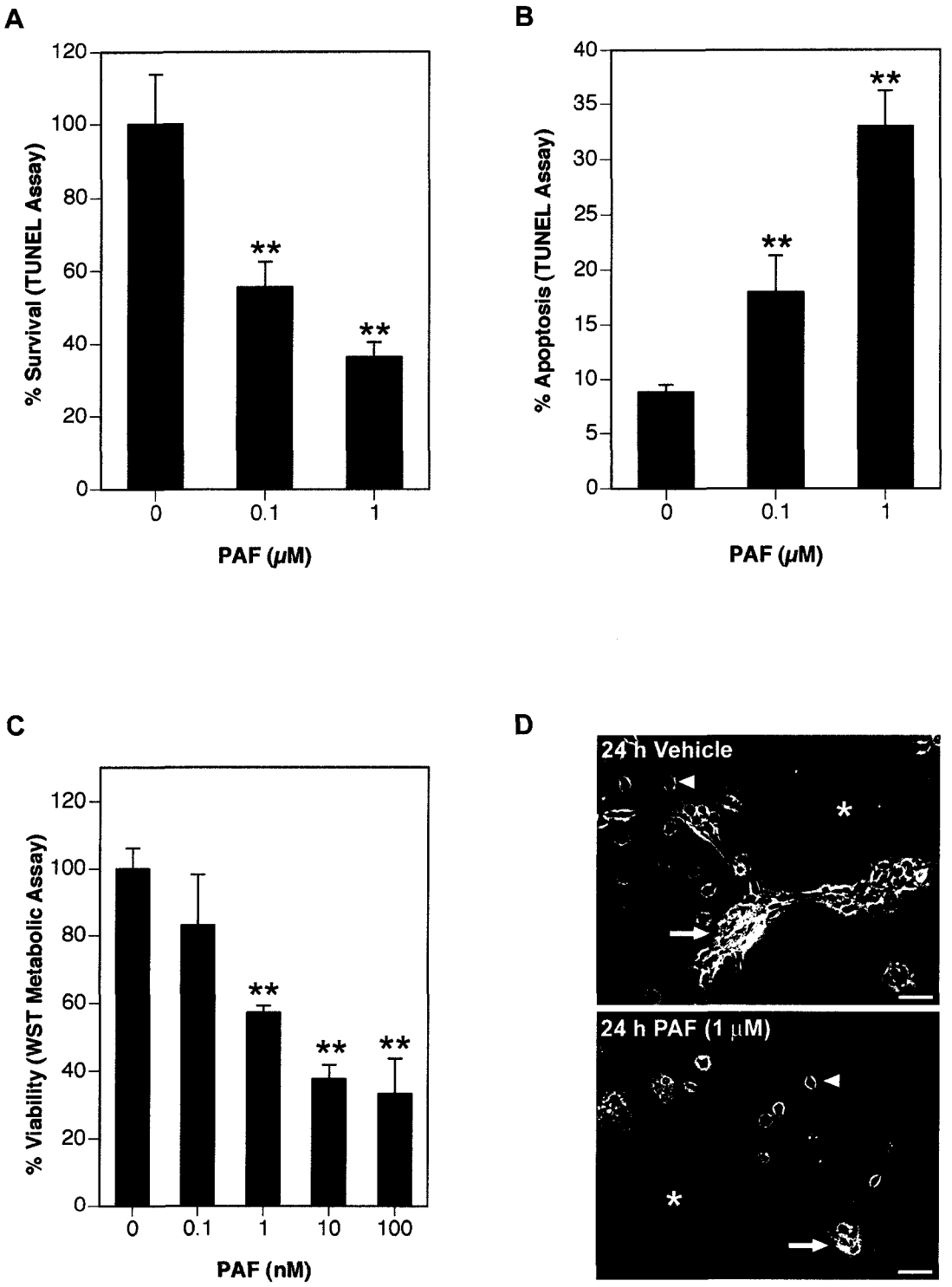


Figure 2.4

**Figure 2.5: PAF elicits neuronal apoptosis through a caspase-3/7-dependent pathway.** Using the CaspaTag assay, cells were labeled with FAM-DEVD-FMK, a fluorescent substrate specific for caspase-3 and -7. (A) Representative digital micrographs of 1 μM PAF-treated hNTs. Arrows point to representative cells in which FAM-DEVD-FMK has been cleaved by caspase-3/7. Scale bars, 50 μm. (B) Caspase-3/7 activation was quantified and data were expressed as the fold change of DEVD cleavage standardized to control (0 h untreated) as described in 2.5.8. Activity was assessed in n=16 PAF-treated cultures and n=16 vehicle-treated cultures conducted in replicate experiments and independently counted by two investigators. The mean number of cells with caspase activity observed over time in vehicle-treated cultures was subtracted from each PAF-treated measure before standardization against control to ensure that caspase activation was PAF-specific and not simply the result of incubation in serum-free media. Caspase-3/7 activation was first observed 1 h after 1 μM PAF administration and increased over time. Data were expressed as the mean $\pm$ SEM (n=96 per data point; $^{**}p<0.01$, ANOVA, *post-hoc* Dunnett's *t* test). Etoposide (Etop; 42 μM) was used as a positive control for caspase-3/7 activation. (C,D) Western blot analysis of cleaved caspase-3 and 7 in hNTs following 24 h of 1 μM PAF treatment. hNTs treated with 24 h Etop (42 μM) or 18 h STS (1 μM) were used as positive controls. Tubulin was used as a loading control.

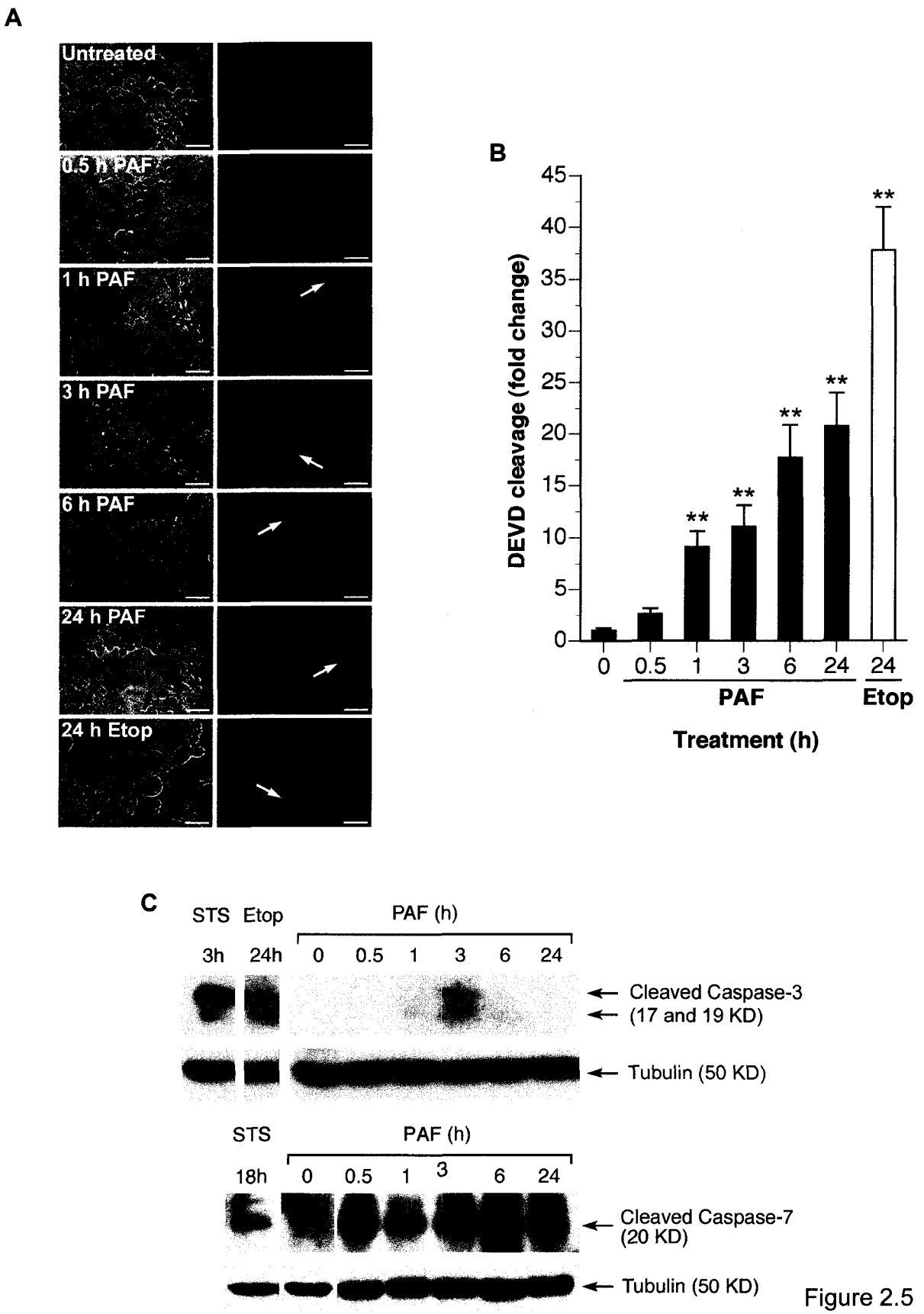


Figure 2.5

increased over a 24 h period (Figure 2.5A,B). Etoposide (42 μM), a chemotherapeutic agent that has been shown to induce apoptosis by activating caspase-3, caspase-7 and caspase-9 (Eischen et al., 1997; Zhuang et al., 1998), was used as a positive control. To distinguish between caspase-3 and caspase-7 activation, Western blots were performed on proteins isolated from PAF-treated hNTs using antibodies specific for the respective caspase fragments cleaved upon activation (Figure 2.5C,D). Cultures were treated with STS, known to induce apoptosis through the activation of caspase-3 and caspase-7 (Marcelli et al., 2000), and etoposide as positive controls. Transient caspase-3 activation was observed 3 h after 1 μM PAF administration. Lasting caspase-7 activation was detected within 1 h of PAF exposure with cleaved protein evident for up to 24 h (Figure 2.5C). To confirm that caspase-7 is required for PAF-induced apoptosis, hNTs were treated with PAF (1 μM) in the presence of the caspase-3/7 inhibitor Z-DEVD-FMK (50 μM). Z-DEVD-FMK partially protected hNTs from both PAF- and etoposide-induced death (Figure 2.6).

### *2.6.5 Caspase-8 is not involved in the PAF-induced caspase cascade in hNTs.*

To delineate the apoptotic cascade induced by PAF, activation of multiple upstream effector/initiator caspases was assessed. Auto-activation of caspase 8 is initiated by recruitment to a receptor with death domains after ligand interaction. PAF did not elicit significant caspase-8 activity as assessed by cleavage of a fluorescent LETD substrate 0-24 h after PAF exposure (Figure 2.7). Since Aβ has been shown to induce caspase-8-mediated neuronal apoptosis (Ivins et al., 1999), Aβ (25 μM) treatment of hNTs was used as a positive control.

**Figure 2.6: PAF-induced neuronal apoptosis is dependent on the activation of caspase-3/7.** hNT's were treated with either PAF (1 μM) or Etop (42 μM; positive control) for 24 h in the presence and absence of the caspase-3/7 inhibitor Z-DEVD-FMK (50 μM). % Survival was measured with the LIVE/DEAD assay and data were expressed standardized to control. Z-DEVD-FMK protected hNTs from both PAF- and Etop-induced death. Asterisks (*) indicate a significant decrease in % survival relative to control. Number signs (#) indicate a significant increase in survival relative to cells treated with death ligand in the absence of caspase inhibitor. Data were expressed as the mean ± SEM (n=72 per data point; ** $p<0.01$, ANOVA, *post-hoc* Dunnett's *t* test; # $p<0.05$, Student's *t* test, PAF vs. PAF + Z-DEVD-FMK; ## $p<0.01$, Student's *t* test, Etop vs. Etop + Z-DEVD-FMK).

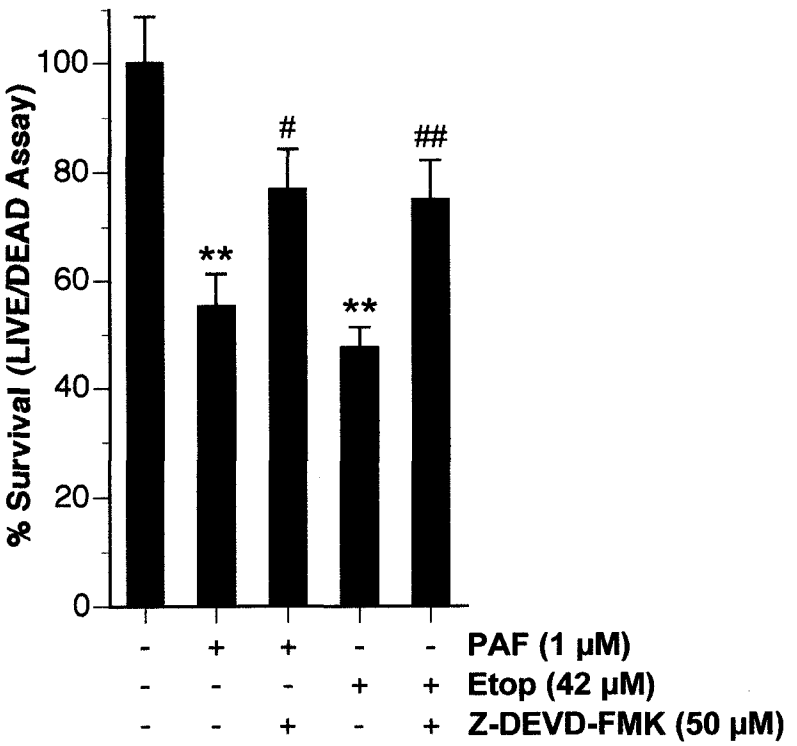


Figure 2.6

**Figure 2.7: PAF does not induce caspase-8 activation.** Using the CaspaTag assay, cells were labelled with FAM-LETD-FMK, a fluorescent substrate specific for caspase-8. Caspase-8 activation was quantified and expressed as the fold change of LETD cleavage above vehicle values as described in 2.5.8 and Figure 2.5. Data were expressed standardized to control. No significant caspase-8 activation was observed following 24 h of 1 μM PAF treatment. Aβ (25 μM) was used as a positive control. Data were expressed as the mean ± SEM (n=72 per data point; **p<0.01, ANOVA, *post-hoc* Dunnett's *t* test).

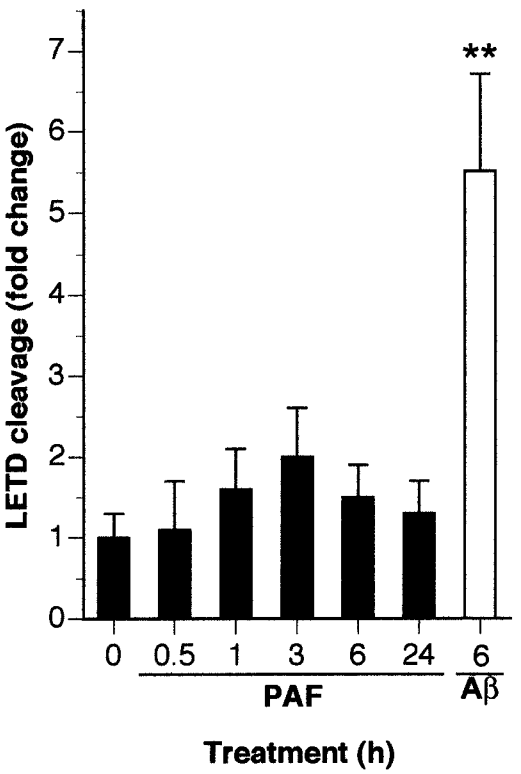


Figure 2.7

*2.6.6 Caspase-9 activation and neuronal mitochondrial cytochrome c release occurs only in later stages of the PAF-induced caspase cascade in hNTs.*

Caspase-9 activation requires formation of the apoptosome; a complex composed of cytochrome *c*, APAF-1, and caspase 9. Formation is dependent upon ATP and cytochrome *c* release from the mitochondria. Activation of caspase-9 was assessed by cleavage of a fluorescent LEHD substrate 0-24 h after PAF exposure. Etoposide (42 μM) was used as a positive control. Significant caspase-9 activity was not detected until 24 h after PAF administration (Figure 2.8A). Since caspase-7 activation was evident within 1 h of PAF exposure, caspase-9 is not likely to activate caspase-7. To support this hypothesis, release of cytochrome *c* from the mitochondria to the cytosol was assessed by Western blotting following treatment with 1 μM PAF. Only a small increase in cytochrome *c* release was detected 24 h after PAF treatment; the majority of cytochrome *c* remained in the mitochondrial fraction (Figure 2.8B). Using immunocytochemistry, cytochrome *c* release was localized to the small subset of neurons still present in cultures 24 h after PAF treatment (Figure 2.8C, arrowheads). No cytochrome *c* translocation from mitochondria to cytosol was detected at earlier time points (data not shown).

*2.6.7 ER stress and caspase-2 activation initiate the PAF-induced caspase cascade in hNTs.*

Cleavage of caspase-2 occurs following ER stress. Caspase-2 activation was assessed by the cleavage of a fluorescent VDVAD substrate 0-24 h after PAF exposure. Since Aβ has been shown to induce caspase-2-mediated neuronal apoptosis (Troy et al., 2000), Aβ (25 μM) was used as a positive control. Significant

**Figure 2.8: PAF induces caspase-9 activation and cytochrome *c* release late in the apoptotic cascade in a discrete population of neurons.** (A) Using the FLICA assay, cells were labelled with FAM-LEHD-FMK, a fluorescent substrate specific for caspase-9. Caspase-9 activation was quantified and expressed as the fold change of LEHD cleavage over vehicle as described in 2.5.8 and Figure 2.5. Data were expressed standardized to control. Caspase-9 activation was not significantly increased until 24 h of 1 μM PAF treatment. Data were expressed as the mean ± SEM (n=72 per data point; **p<0.01, ANOVA, *post-hoc* Dunnett's *t* test). (B) Western blot analysis of mitochondrial (M) and cytosolic (C) fractions revealed a negligible release of cytochrome *c* following 24 h of 1 μM PAF. Cytochrome oxidase IV (COX IV) was used as a loading control for mitochondrial fractions, and tubulin was used as a loading control for cytosolic fractions. (C) Immunocytochemistry revealed that the small amount of cytochrome *c* release induced by 1 μM PAF localized to the few remaining neurons and was not detected in non-neuronal cells. Neuritic extensions in PAF-treated neurons were pyknotic and blebbed compared to the thicker, homogenous neurites in vehicle-treated neurons. Non-neuronal cells in the hNT culture did not exhibit significant cytochrome *c* release in PAF or vehicle treatments. Arrows indicate punctate mitochondrial cytochrome *c* staining. Arrowheads indicate diffuse cytochrome *c* staining indicative of cytochrome *c* release from mitochondria. Small arrows point to neuritic blebbing indicative of damage. Scale bar, 50 μm.

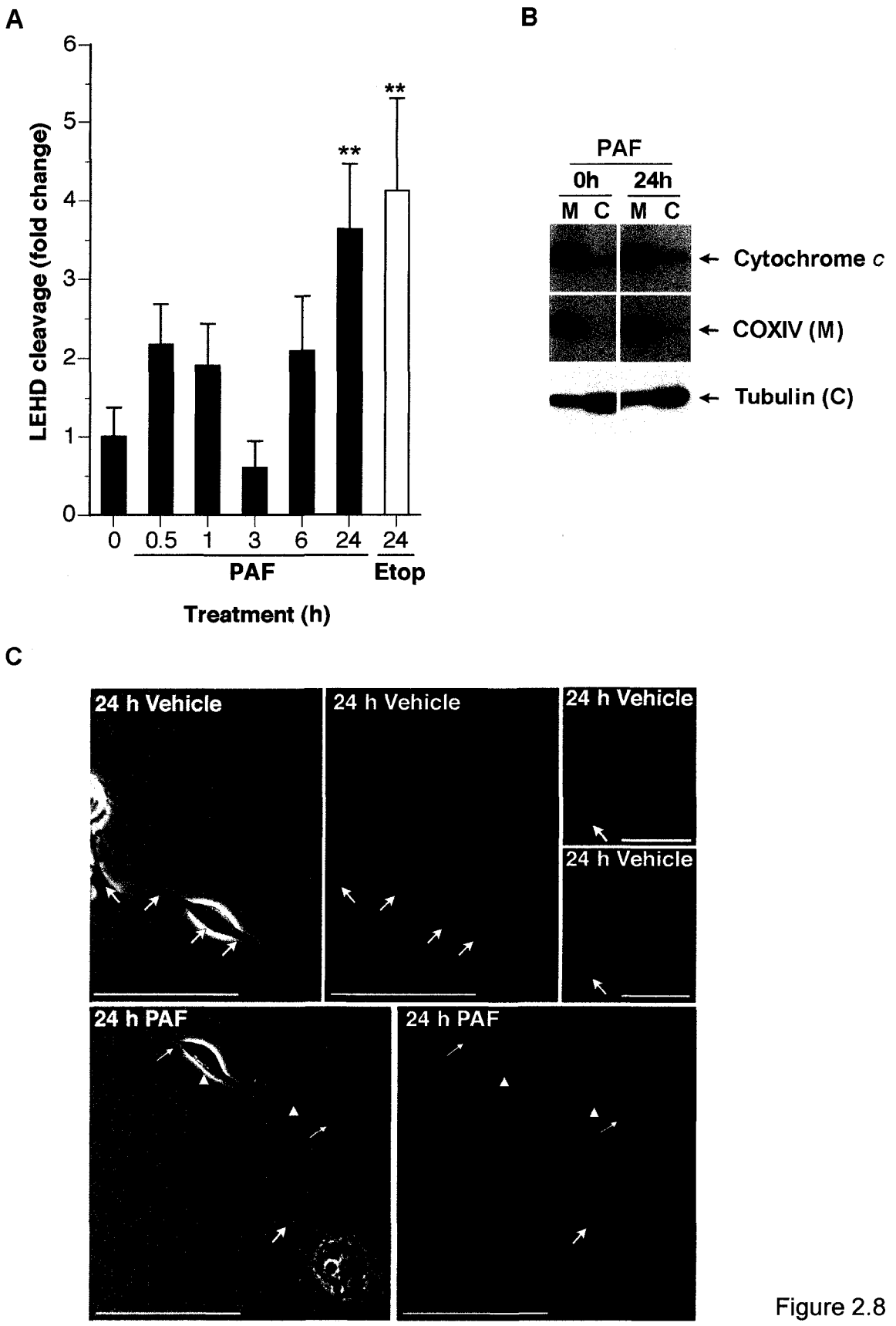


Figure 2.8

caspase-2 activation was detected at 1 and 3 h of PAF treatment (Figure 2.9A). This transient activation occurred early enough following PAF exposure to trigger downstream caspase-7 activation (Figure 2.5). To establish that caspase-2 activation was required for PAF-induced neuronal death, cultures were treated with PAF (1 μM) in the presence of the caspase-2 inhibitor Z-VDVAD-FMK (50 μM). Caspase-2 inhibition completely blocked PAF-induced neuronal death (Figure 2.9B). To confirm that PAF triggers ER stress, BiP expression levels were analyzed through Western blots. An upregulation of BiP, indicative of ER stress, was detected within 30 min of PAF treatment and maintained over 24 h (Figure 2.9C).

### *2.6.8 Caspase-2 activates caspase-7 in the PAF apoptotic cascade*

To establish the sequence of PAF-induced caspase activation, caspase-3/7, caspase-2, and caspase-9 activity was assessed in the presence of the predicted upstream or downstream caspase inhibitors. Z-VDVAD-FMK (50 μM), the caspase-2 inhibitor, completely blocked PAF-induced DEVD cleavage by activated caspase-3/7 (Figure 2.10A). To confirm that caspase-2 activation lies upstream of caspase-7 activation, cultures were treated with PAF in the presence of Z-DEVD-FMK (50 μM), the caspase-3/7 inhibitor. Z-DEVD-FMK had no effect on caspase-2 activation (Figure 2.10B). To determine if caspase-9 activation detected in remaining neurons following 24 h of PAF administration is downstream of caspase-2 and/or caspase-7 activation, hNTs treated for 24 h with PAF in the presence of either Z-VDVAD-FMK or Z-DEVD-FMK were assayed for caspase-9 activity through LEHD cleavage

**Figure 2.9: PAF elicits neuronal apoptosis through an ER-mediated pathway.** (A) Using the FLICA assay, cells were labelled with FAM-VDVAD-FMK, a fluorescent substrate specific for caspase-2. Caspase-2 activation was quantified and expressed as the fold change of VDVAD cleavage over vehicle as described in 2.5.8 and Figure 2.5. Data were expressed standardized to control. Caspase-2 activation was observed 1 and 3 h after 1 μM PAF administration. Aβ (25 μM) was used as a positive control. Data were expressed as the mean ± SEM (n=108 per data point; * $p<0.05$, ** $p<0.01$, ANOVA, *post-hoc* Dunnett's *t* test). (B) Functional dependence of PAF-induced neuronal apoptosis on caspase-2 activation was measured with the LIVE/DEAD assay. hNT's were treated with PAF (1 μM) in the presence and absence of the caspase-2 inhibitor Z-VDVAD-FMK (50 μM). % Survival was expressed standardized to control. Z-VDVAD-FMK protected hNTs from PAF-induced death. Asterisks (*) indicate a significant decrease in survival relative to control. Number signs (#) indicate a significant increase in survival relative to cells treated with death ligand in the absence of caspase inhibitor. Data were expressed as the mean ± SEM (n=72 per data point; ** $p<0.01$, ANOVA, *post-hoc* Dunnett's *t* test; ## $p<0.01$, Student's *t* test, PAF vs. PAF + Z-VDVAD-FMK; ## $p<0.01$). (C) Western blot analysis detected an induction of BiP expression indicative of ER stress within 30 min of 1 μM PAF treatment. A representative Western blot conducted in replicate is presented. Tubulin was used as a loading control.

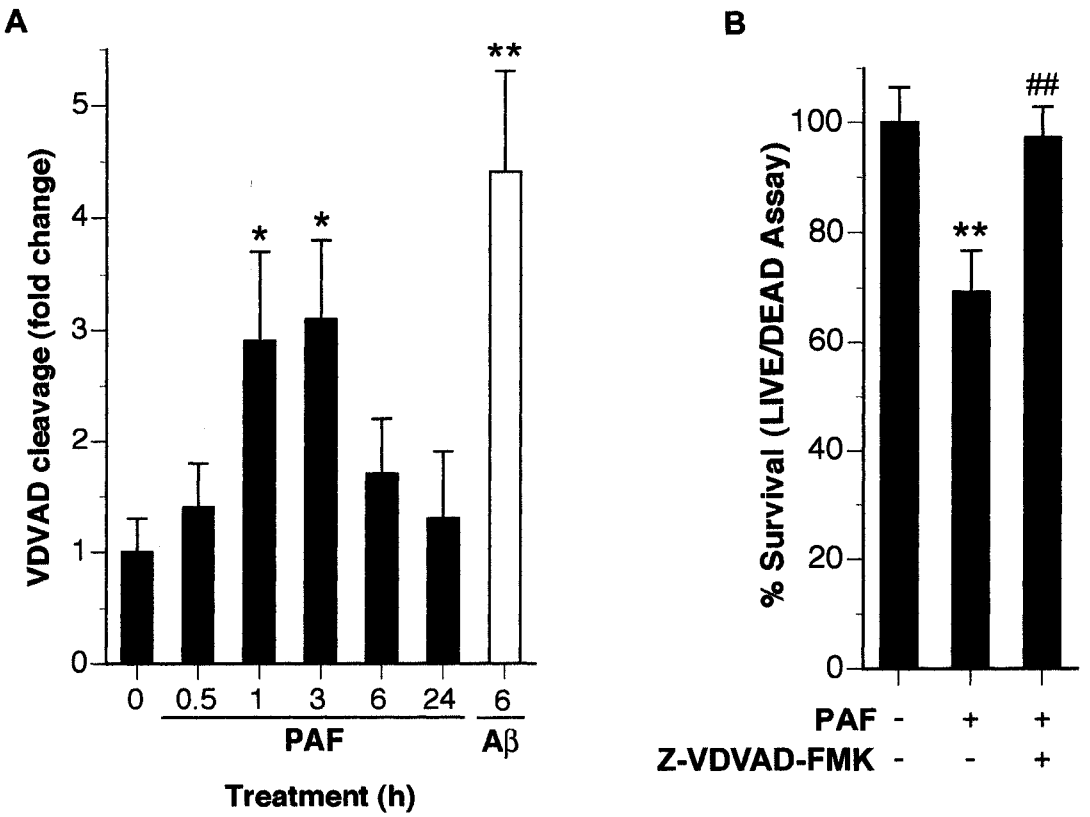


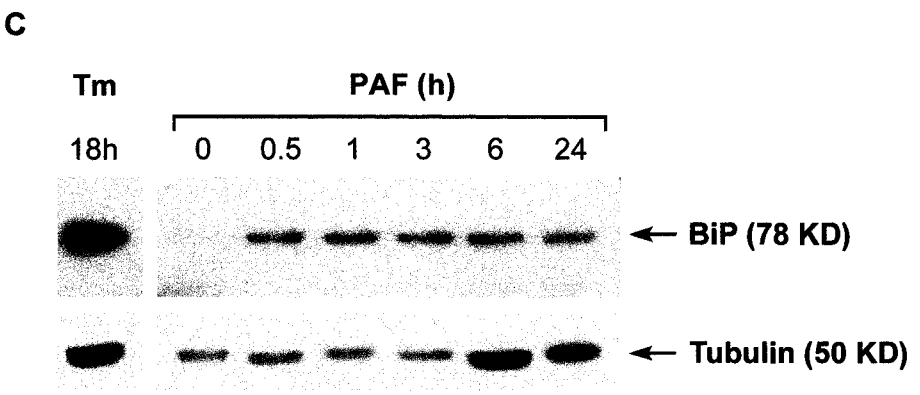


Figure 2.9

**Figure 2.10: Temporal sequence of caspase activation following PAF treatment.** Asterisks (*) indicate a significant increase in substrate cleavage relative to control. Number signs (#) indicate a significant decrease in substrate cleavage relative to cells treated with death ligand in the absence of caspase inhibitor. (A) The caspase-2 inhibitor Z-VDVAD-FMK blocked 1 μM PAF-induced caspase-3/7 activation as measured by DEVD cleavage (** $p<0.01$, ANOVA, *post-hoc* Dunnett's *t* test; ## $p<0.01$, Student's *t* test, PAF vs. PAF + Z-VDVAD-FMK). (B) The caspase-3/7 inhibitor Z-DEVD-FMK did not significantly decrease 1 μM PAF-induced caspase-2 activation as measured by VDVAD cleavage (* $p<0.05$, ANOVA, *post-hoc* Dunnett's *t* test). (C) Both caspase-2 and caspase-3/7 inhibitors reduced 1 μM PAF-induced caspase-9 activation as measured by LEHD cleavage (** $p<0.01$, ANOVA, *post-hoc* Dunnett's *t* test; # $p<0.05$, Student's *t* test, PAF vs. PAF + Z-DEVD-FMK or PAF + Z-VDVAD-FMK). (A) – (C) Data were expressed as the mean $\pm$ SEM (n=72-108 per data point). (D) Schematic representing the sequence of PAF-induced caspase activation in hNTs.

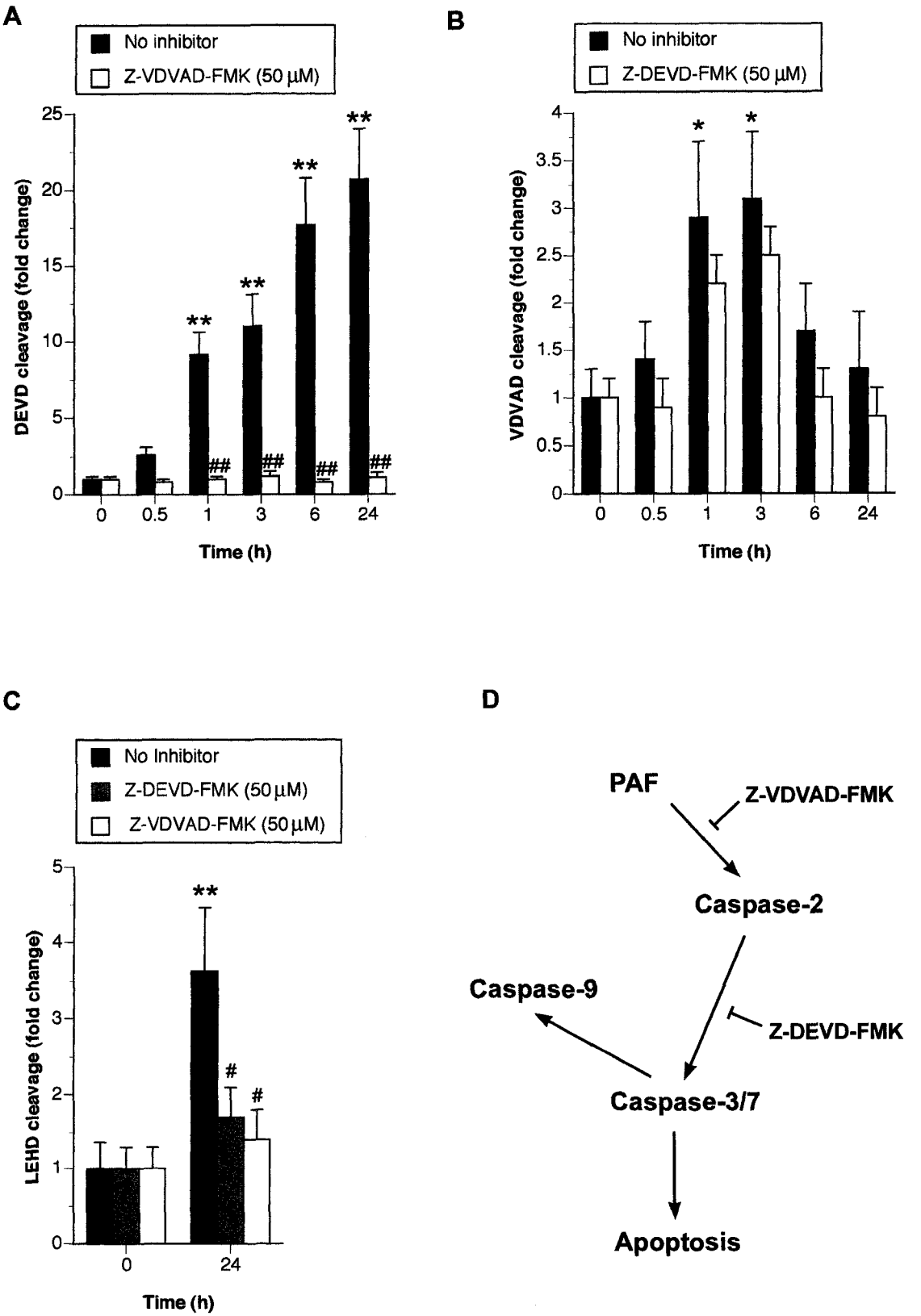


Figure 2.10

(Figure 2.10C). Blocking either caspase-2 or caspase-7 inhibited caspase-9 activation. The sequence of caspase activation is summarized in (Figure 2.10D).

## 2.7 Discussion

The results presented in this chapter are the first to describe PAFR-independent apoptosis in human neurons induced by PAF. Previously, the Bennett lab has demonstrated PAFR-independent, caspase-3-dependent apoptosis in PC12-AC cell line, a clonal derivative of the well-established rat pheochromocytoma PC12 cell line (Bonin et al., 2004; Brewer et al., 2002). While these cells can be reversibly differentiated into a peripheral neuronal-like phenotype, PC12-AC cells are not an appropriate model of human CNS neurons and, in this thesis, an optimal *in vitro* system was established.

### *2.7.1 Validation of the model system*

The cell line used in this study was the NT2/hNT neuronal differentiation model. NT2 neural progenitor cells were clonally derived from a human teratocarcinoma (Pleasure et al., 1992). Upon 4-5 weeks of RA treatment and subsequent mitotic inhibition for 3 weeks, NT2s can be terminally differentiated into human CNS neurons. Unlike other established human cell lines derived from neural tumour tissue, hNT neurons are post-mitotic and do not revert to a proliferative phenotype upon removal of mitotic inhibitors. In the brain, neurons require non-neuronal glial cells for proper function. For this reason, in this thesis, NT2s were differentiated into a mixed culture (hNT) of approximately 80% neurons, and 20% non-neuronal cells. Antigenic analysis of NT2s and hNTs was performed through

immunochemical characterization with the stem cell marker nestin, DNA synthesis marker PCNA, neuronal markers NSE, NF-68, and GAP43, the oligodendrocyte marker myelin PLP, the astrocyte marker GFAP and the intermediate filament vimentin. NT2 cells were nestin-positive, PCNA-positive, vimentin-positive, NSE-negative, NF-68-negative, GAP43-negative, myelin PLP-negative, and GFAP-negative. These data confirmed that the clonal NT2 line employed in this study are stem cell-like cells capable of self-renewal that do not express markers of differentiated CNS cells. Following differentiation, hNT cultures as a whole were nestin-negative, NF-68-positive, GAP43-positive, myelin PLP-positive, and GFAP-negative. Cultures of up to >95% neuronal are obtainable using an extended protocol involving an extra replating step onto Matrigel-coated tissue culture dishes (Pleasure et al., 1992). By eliminating a third replating step, we were able to maintain a higher ratio of non-neuronal cells to neurons compared to this enrichment protocol.

The validity of this cell model in human CNS signalling has been demonstrated in transplantation studies (reviewed in (Newman et al., 2005)). Recently, an improvement in motor skills and memory following hNT transplantation was reported in stroke patients (Kondziolka et al., 2005). Postmortem case studies of a patient who underwent hNT transplantation 27 months prior to death revealed that the hNT grafts contained neurons immunoreactive for neurofilament in the absence of tumours or other abnormalities (Nelson et al., 2002). hNT neurons therefore represent an ideal model system to study the pathological effects of PAF in a post-mitotic human neuronal system.

### *2.7.2 PAF induces ER stress triggering caspase-dependent apoptosis in hNT neurons*

Although the effects of PAF in neurons are assumed to be transduced by PAFR, a growing body of evidence suggests that PAFR-independent signalling also plays an important role in determining neuronal fate following pathophysiological elevation of PAF concentrations (reviewed in Chapter 1). Here, hNT neuronal cultures were found not to express PAFR as determined by RT-PCR with two different primer pairs. We found that PAF triggers PAFR-independent apoptotic cell death in terminally differentiated neurons but not neural precursors.

To provide mechanistic insight, the caspase cascade elicited in hNTs by PAF exposure was identified. As reviewed in Chapter 1, caspases are cysteine proteases responsible for the majority of morphological changes in apoptosis. Despite converging evidence that PAF triggers caspase activity, it had not been determined whether PAF activates caspase in neurons and whether this activation is PAFR-dependent or PAFR-independent. For example, while c-PAF exacerbated ultraviolet radiation-induced apoptosis through cytochrome *c* release and caspase-3 activation in corneal epithelial cells (Ma and Bazan, 2001), caspase inhibitors were not able to protect from PAF-induced cell death in retinovascular endothelial cells (Beauchamp et al., 2002). However, PAF-induced death of cultured astrocytes and oligodendrocytes was found to be caspase-3-dependent (Hostettler et al., 2002). BN 52021, a PAF inhibitor that antagonizes PAFR and accelerates PAF hydrolysis (Bonin et al., 2004; Marcheselli et al., 1990), reduced cytochrome *c* release and caspase-9 cleavage induced by PAF synthesis following ischemia-reperfusion injury in the rat small intestine (Wu et al., 2003) while PAF antagonists have also been

shown to inhibit caspase-3 activation induced by prion proteins in primary mouse cortical neurons (Bate et al., 2004c). However, none of these studies directly assessed the expression of the PAFR and, as such, it is difficult to establish whether multiple pathways are in play in these cell systems.

Here, it is shown, for the first time, that PAF elicits ER stress in human neurons characterized by BiP upregulation within 30 min of PAF exposure resulting in caspase-2 cleavage and caspase-7 activation. Caspase-3 is only transiently activated. Since caspase-7 is an executioner caspase, the simplest explanation is that PAF activates caspase-2 which then activates caspase-7 as has been shown in other cell systems (Ho et al., 2005). However, considering the comparable kinetics of caspase-2 and caspase-7 activation observed in this study, it is also possible that caspase-7 activated caspase-2. Although caspase-2 is categorized as a member of the initiator caspase family along with caspase-8 and caspase-9, its substrate specificity has been shown to be more similar to that of executioner caspases (Dahmer, 2005; Talanian et al., 1997; Thornberry et al., 1997). In fact, some studies have indicated that caspase-2 can function as both an initiator and an executioner caspase (Dahmer, 2005; Kumar and Vaux, 2002; Troy and Shelanski, 2003). Moreover, *in vitro* studies have shown that executioner caspase-3 (and thus caspase -7, given identical target sequences) can cleave caspase-2 (Li et al., 1997; Paroni et al., 2001; Slee et al., 1999). To establish whether caspase-2 or caspase-7 initiates the PAF caspase cascade, a series of caspase inhibitors were used to block downstream caspase activation events. Caspase-3/7 activation by PAF was completely blocked by the caspase-2 inhibitor Z-VDVAD-FMK whereas caspase-2 activation was not significantly affected by the caspase-3/7 inhibitor Z-DEVD-FMK.

Together, these observations demonstrate that PAF-induced caspase-2 activation is required for caspase-7 cleavage following PAF induction of ER stress.

We have yet to identify how PAF triggers ER-mediated events, although both death receptor and mitochondrial pathways have been ruled out. Both ER stress and caspase-2 activation can be triggered by cross-talk between the extrinsic (caspase-8-dependent apoptosis triggered by receptors containing death domains at the plasma membrane) and intrinsic (caspase-9-dependent mitochondrial-driven) pathways (Breckenridge et al., 2003; Wagner et al., 2004). Since caspase-8-dependent apoptosis is initiated by the activation of death receptors (for a review, see Chapter 1), it may be that PAF's ability to enhance TNF$\alpha$ production as reported in peripheral cell types (Cuschieri et al., 2005) could result in caspase-8 auto-activation in hNTs and downstream ER stress. However, no significant caspase-8 activation was detected in hNTs following PAF exposure (Figure 2.7). Cross-talk with mitochondria may also precipitate ER stress. Prior to this study, it has been assumed that PAF primarily triggers apoptosis through the intrinisic pathway (reviewed above). In isolated rat brain mitochondria, PAF induced permeability transition and cytochrome *c* release that was prevented by PAF antagonists (Parker et al., 2002). Surprisingly, PAF-induced apoptosis in hNTs was not initiated at the mitochondrial level. Instead, mitochondrial apoptotic transduction represented a secondary apoptotic pathway as cytochrome *c* release and caspase-9 activity was not detected in hNTs until well after ER stress induction and activation of both caspase-2 and 7. In support of this conclusion, the inhibition of PAF-induced caspase-2 activation by Z-VDVAD-FMK or caspase-7 activation by Z-DEVD-FMK also prevented downstream caspase-9 activation. Together, these data provide

strong evidence that PAF induces ER stress prior to mitochondrial involvement and that caspase-2 is the primary initiator caspase triggering downstream events.

These findings also add support to the hypothesis that caspase-2 is the human "functional homologue" of rodent caspase-12 in human neurons. In rodents, caspase-12 has been shown to be involved in ER stress-induced apoptotic pathways (Nakagawa et al., 2000). Not only is pro-caspase-12 primarily localized to the ER, but it is also cleaved during ER stress (Hitomi et al., 2004). In humans, the gene sequence homologous to mouse caspase-12 has a frameshift mutation resulting in a premature stop codon, and an amino acid substitution within a critical site for caspase enzymatic activity rendering human caspase-12 catalytically inactive (Fischer et al., 2002; Hitomi et al., 2004). It has been suggested that caspase-4 assumes the role of caspase-12 in human cells since it is associated with the ER and has been shown to be activated by ER stress *in vitro* in HeLa cells and mitotic SK-N-SH neuroblastoma cells (Hitomi et al., 2004; Katayama et al., 2004). However, caspase-4 mRNA is not expressed in human brain (Lin et al., 2000) whereas caspase-2 is (Kitamura et al., 1998). Recently, thapsigargin, a known inducer of ER stress, has been shown to activate caspase-2, caspase-3, and caspase-7 in human SH-SY5Y neuroblastoma cells (Dahmer, 2005). Interestingly, caspase-7 had previously been shown to form a complex with caspase-12 and BiP (Rao et al., 2002). Our data are consistent with these findings indicating the caspase-2 is activated by PAF upon ER stress and triggers downstream caspase activation culminating in caspase-7 activation.

### *2.7.3 Summary*

In summary, these studies provide the first evidence that PAF triggers apoptosis in human neurons in the absence of PAFR. PAF is shown to induce ER stress resulting in caspase-2 activation which, in turn, cleaves and activates executioner caspase-7. Mitochondrial effects, specifically cytochrome *c* release resulting in caspase-9 activation, are observed downstream of this primary ER cascade.

# Chapter 3: Caspase-independent, mitochondrial apoptotic pathways mediated by platelet activating factor in human neurons

## 3.1 Publications resulting from studies described in this chapter:

Moffat TC, Wong S, Hozturk E, Migahed L, Paliga A, Hill J, Bennett SAL (2006) Platelet activating factor elicits an endoplasmic reticulum-dependent caspase cascade in human neurons independently of its G-protein coupled receptor, in preparation.

Moffat TC, Whitehead S, Harper ME, Bennett SAL (2006) Role of uncoupling protein-2 in neuronal loss triggered by the bioactive phospholipid platelet activating factor, in preparation.

## 3.2 Statement of author contributions

The experiments presented in this chapter were performed by Tia C. Moffat. All figures and text in this chapter were prepared by Tia C. Moffat with guidance and editorial assistance from Dr. Steffany A.L. Bennett. Additional studies using PAFR null mutant mice were performed by Scott Ryan, a Ph.D. student in the Bennett laboratory, to expand upon the observations reported in this thesis with respect to PAF inducing caspase-3/7-dependent apoptosis in the absence of PAFR. Supplementary studies using UCP2 and PAFR double-null mutant mice were performed by Dr. Shawn Whitehead, a post-doctoral fellow in the Bennett laboratory, to further investigate the role of UCP2 in PAF-induced apoptosis in the absence of

PAFR, based on the PAF-induced UCP2 upregulation reported in this thesis. These data are used in the discussion to interpret the significance of the UCP2 increase observed in PAF-treated hNT neurons and are presented in Appendix 3.

## 3.3 Abstract

In Chapter 2, PAF signalling in hNTs was shown to lead to caspase activation through ER stress and downstream mitochondrial effects. To further explore secondary mitochondrial involvement in PAF-mediated neuronal death, caspase-independent mitochondrial signalling was assessed. The release of mitochondrial proteins such as AIF and endoG are examples of caspase-independent mechanisms possibly affected by PAF-induced ER and mitochondrial cross-talk. Here, it is shown that PAF does not induce mitochondrial release of AIF and endoG as part of the PAFR-independent death pathway in hNTs. ROS were identified as downstream effectors of hNT neuronal death following PAF administration. PAF was also shown to induce expression of mitochondrial uncoupling protein-2 (UCP2), a protein thought to be implicated in the protection from ROS. A surprising role for UCP2 in transducing PAF-mediated apoptosis was demonstrated using primary neuronal culture from $PAFR^{-/-}/UCP2^{-/-}$ mice in collaboration with other members of the Bennett laboratory.

## 3.4 Introduction

Mitochondria play a central role in the regulation of apoptosis elicited through the intrinsic death pathway (reviewed in Chapter 1). In Chapter 2, PAF-mediated neuronal death was shown to trigger neuronal loss through ER stress and elicit

secondary mitochondrial events in a subset of neurons as indicated by cytochrome *c* release and caspase-9 activation. PAF has previously been shown to induce apoptotic-associated mitochondrial signalling events including cytochrome *c* release and changes in $\Delta\Psi_m$ (Lu et al., 2004; Ma and Bazan, 2001; Parker et al., 2002; Perry et al., 2005; Wu et al., 2003). Cross-talk between the ER and the mitochondria influences apoptotic progression and is mediated, in part, through signalling pathways involving Bcl-2 family members and $Ca^{2+}$ release from the ER (Walter and Hajnoczky, 2005).

In this chapter, the secondary mitochondrial involvement in PAF-mediated hNT death was explored. Mitochondrial-mediated death can involve the caspase-independent release of mitochondrial proteins such AIF and endoG into the cytosol (see Chapter 1 for a review). ROS have also been implicated in PAF-induced neuronal death (Feuerstein et al., 1990; Matsuo et al., 1996; Zhu et al., 2004). UCP2, a member of a family of inner mitochondrial membrane proteins involved in uncoupling ATP synthesis from the electron transport chain, is hypothesized to protect cells from ROS (Boss et al., 2000; Mattiasson et al., 2003; Paradis et al., 2003). It has also been suggested that UCP2 offers neuroprotection in models of ischemia, kainic acid injury, epilepsy, and Parkinson's Disease (Andrews et al., 2005; Clavel et al., 2003; Diano et al., 2003; Mattiasson et al., 2003). Conversely, UCP2 has also been hypothesized to contribute directly to induction of cell death (Mills et al., 2002). The roles of AIF, endoG, and UCP2 in PAF signalling have not yet been described. Here, caspase-independent mitochondrial effects such as

release of AIF and endoG, increased ROS production, loss of $\Delta\Psi_m$, and changes in UCP2 protein expression were evaluated.

## 3.5 Materials and Methods

### *3.5.1 Reagents*

Unless otherwise specified, all cell culture reagents were obtained from Invitrogen, and all chemical reagents were obtained from Sigma.

### *3.5.2 Cell Culture*

NT2s and hNTs were cultured and differentiated as described in Section 2.5.2.

### *3.5.3 Cell Treatments*

Cells were treated as described in Section 2.5.3. Agents used in cell treatments were EtOH (0.1%), PAF (1 μM), STS (1 μM), or hydrogen peroxide ($H_2O_2$, 100 μM).

### *3.5.4 Protein Isolation*

Total cell protein isolation, as well as mitochondrial and cytosolic protein fractionation, was performed as described in Section 2.5.9.

### *3.5.5 Western Blotting*

Western blotting was performed as described in Section 2.5.10. Primary antibodies used were goat polyclonal anti-AIF (1:1000, Santa Cruz Biotechnology),

rabbit polyclonal anti-endoG (1:2000, Chemicon), mouse monoclonal anti-COX IV (1:5000, Molecular Probes), mouse monoclonal anti-β-tubulin III (1:10000, Sigma), and rabbit polyclonal anti-UCP2 (1:1000, Calbiochem). Secondary antibodies used were HRP-conjugated anti-goat IgG (1:10000, Jackson Immunoresearch), HRP-conjugated anti-rabbit IgG (1:5000, Jackson Immunoresearch), and HRP-conjugated anti-mouse IgG (1:2000, Jackson Immunoresearch).

### *3.5.6 RT-PCR*

Total RNA isolation, residual DNA digestion, and first strand cDNA synthesis were performed as described in Section 2.5.5. The primer pair used was 854uc2h (sense 5'-CCTACTGCCACTGTGAAGTT-3' and antisense 5-TTCAGCTGCTCATAGGTGAC-3') defining an 854 bp amplicon of human UCP2. cDNA template amplification mixture and cycling protocol were as described in Section 2.5.5. RT-PCR negative controls included a sample treated without RT enzyme to prove the absence of residual genomic contamination, and template amplified with $H_2O$ instead of Taq enzyme to prove the absence of reagent contamination.

### *3.5.7 Immunocytochemistry*

Immunocytochemistry was performed as described in Section 2.2.4. The primary antibody used was rabbit polyclonal anti-UCP2 (1:500, Calbiochem) and the secondary antibody used was Cy3-conjugated anti-rabbit IgG (1:600, Jackson Immunoresearch).

### 3.5.8 *MitoTracker Red CMXRos Mitochondrial Staining*

$\Delta\Psi_m$ / ROS production was measured using a modified protocol from the manufacturer's instructions for mitochondrial staining with MitoTracker Red CMXRos (MTR, Molecular Probes). Cells were cultured in tissue culture dishes containing glass coverslips coated with laminin/poly-D-lysine as described in 2.5.2. Following treatments, cells were washed in 10 mM phosphate-buffered saline (PBS). MTR reagent was reconstituted in dimethyl sulfoxide (DMSO) and diluted in treatment media to give a 200 nM final concentration. Cells were incubated in the diluted MTR for 15 min at 37°C and 5% $CO_2$, and then washed with PBS and fixed for 20 min in 3.7% paraformaldehyde diluted in PBS. Cells were mounted in Vectashield (Vector Laboratories) and analyzed with a Leica DMRXA2 epifluorescent microscope equipped with an ORCA-ER digital camera (Hamamatsu) and with OpenLab 3.17 software (Improvision).

### 3.5.9 *ROS Detection Assay*

The presence of ROS was measured using a modified protocol from the manufacturer's instructions for the 5-(and-6)-carboxy-2′,7′-dichlorodihydrofluorescein diacetate assay (DCFDA, Molecular Probes). Cells were cultured in 96-well black plates with clear bottoms. Following treatments, cells were washed with PBS. DCFDA reagent was reconstituted in DMSO and diluted in PBS to give a 100 µM final concentration. Cells were incubated in the diluted DCFDA (100 µL per well) for 30 min at 37°C and 5% $CO_2$, and then washed with PBS. Cells were immediately analyzed using a Leica DMIL inverted epifluorescent microscope equipped with a Qimaging QICAM fast 1394 digital camera (Quorum Technologies).

Phase contrast and fluorescent photos were taken of ten random fields per treatment in duplicate experiments, with only one random field taken per well due to the photosensitivity of the DCFDA reagent observed under fluorescent wavelengths.

### *3.5.10 Statistical analysis*

Statistical analysis was performed as described in Section 2.5.11.

## 3.6 Results

### *3.6.1 PAF does not induce translocation of AIF or endoG*

In order to assess the release of AIF and endoG from the mitochondria, mitochondrial and cytosolic fractions were isolated from hNTs 0-24 h after 1 μM PAF exposure. Western blots showed that the majority of AIF and endoG remained in the mitochondria following PAF treatment with minimal levels of AIF and endoG present in the cytosol that were not altered by PAF treatment (Figure 3.1).

### *3.6.2 PAF induces ROS production in hNTs*

An increase in the fluorescence intensity of the mitochondrial dye MTR was observed in hNT neurons after 24 h of 1 μM PAF administration as compared to vehicle-treated cells (Figure 3.2A). Since MTR fluorescence intensity can be affected by the presence of ROS (Buckman et al., 2001; Park et al., 2006), these results could be due to PAF-induced ROS production in hNTs or to an increase in $\Delta\Psi_m$ indicative of mitochondrial membrane polarization. To distinguish between these possibilities, the fluorescent DCFDA assay was used to directly measure the presence of ROS in hNTs following a 24 h treatment of 1 μM PAF. PAF induced a

**Figure 3.1: PAF does not elicit translocation of AIF or endoG from the mitochondria to the cytosol.** Western blot analysis of AIF, endoG, COX IV (loading control for mitochondrial fractions) and tubulin (loading control for cytosolic fractions) in mitochondrial (M) and cytosolic (C) fractions extracted from hNTs following 0-24 h of 1 μM PAF treatment. Note that while some cytosolic contamination is present in the mitochondrial fraction (as indicated by tubulin staining), mitochondrial protein was not detected in the cytosolic fraction (as indicated by COX IV staining). No significant increase in AIF or endoG was detected in the cytosolic fractions, indicating that AIF and endoG were not released from the mitochondria.

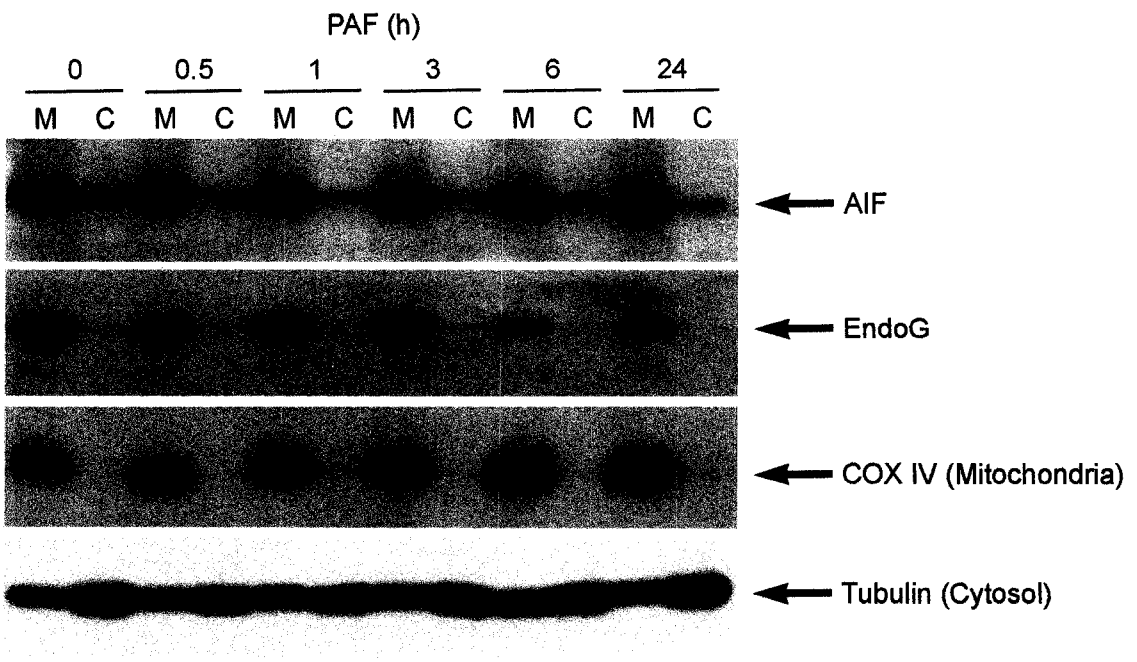


Figure 3.1

**Figure 3.2: PAF induces an increase ROS levels.** (A) hNTs treated for 24 h with either vehicle (a-c) or 1 μM PAF (d-f) were labelled with the mitochondrial dye MTR. Punctate mitochondrial MTR staining is seen throughout the neuritic extensions (b, e) and the neuronal cell bodies (c, f). PAF induced an increase in overall neuronal MTR fluorescence intensity, indicative of an increase in either $\Delta\Psi_m$ or ROS levels. Scale bars for a, d, 50 μm; for b, c, e, f, 10 μm. (B) Representative digital micrographs of the DCFDA assay in hNTs following either 24 h vehicle or 1 μM PAF treatment, or 3 h of 1 μM STS treatment as a positive control for ROS production. Arrows point to representative cells with increased ROS levels. Scale bars, 50 μm. (C) The % of ROS-positive hNTs was quantified using the DCFDA assay. A 24 h treatment of 1 μM PAF induced a 3-fold increase in hNT ROS levels. STS was used as a positive control. Data were expressed as the mean ± SEM (n=20 per data point; **p<0.01, ANOVA, *post-hoc* Dunnett's *t* test).

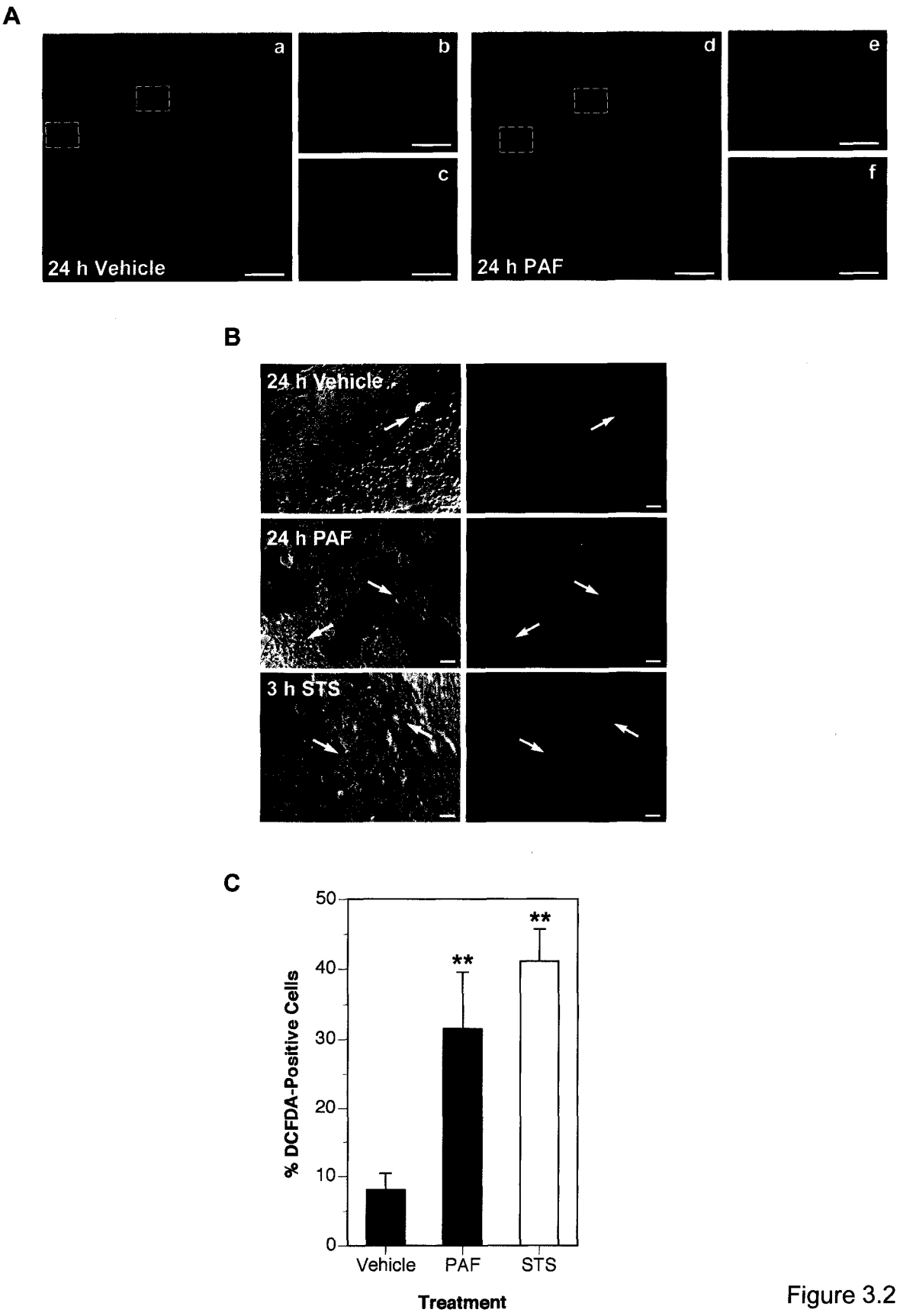


Figure 3.2

significant increase in ROS production as compared to vehicle-treated cells (Figure 3.2B,C). Since STS has previously been shown to induce neuronal ROS production, STS (1 μM) was used as a positive control (Pong et al., 2001).

### *3.6.3 PAF increases UCP2 protein expression in hNTs*

UCP2 mRNA was expressed by hNT cultures as assessed by RT-PCR (Figure 3.3A). GAPDH was amplified from each sample to confirm template integrity. The effect of PAF on UCP2 protein expression in hNTs was evaluated by immunocytochemistry and Western blotting. An increase in UCP2 protein was detected in hNTs 24 h following 1 μM PAF administration (Figure 3.3B,C).

## 3.7 Discussion

The results presented in this chapter indicate that PAF increases mitochondrial ROS production but does not trigger caspase-independent mitochondrial pathways of apoptosis attributed to AIF or endoG in human neurons. Moreover, an increase in mitochondrial UCP2 protein expression was detected 24 h after PAF exposure.

### *3.7.1 AIF and endoG do not play a role in PAF-mediated apoptosis of hNT neurons*

Although the translocation of AIF and endoG have been implicated in models of neurotoxicity (Dawson and Dawson, 2004; Singh et al., 2004; Tanaka et al., 2005), it appears that their translocation is not involved in PAF-induced neuronal apoptosis. As such, the caspase-dependent cascade triggered by ER stress

**Figure 3.3: PAF increases hNT UCP2 protein levels.** (A) RT-PCR analysis demonstrated expression of UCP2 mRNA in hNTs (+RT, top panel). RT-PCR negative controls included a sample treated without RT enzyme (-RT), and template amplified with $H_2O$ instead of Taq enzyme ($H_2O$). cDNA template integrity was confirmed by amplification of GAPDH as an internal standard (bottom panel). (B) Immunocytochemistry of hNTs following 0 and 24 h of 1μM PAF administration. Arrows point to representative cells expressing UCP2 protein. UCP2 protein expression was increased in PAF-treated hNTs. Scale bars, 50 μm. (C) Western blot analysis of UCP2 protein expression in mitochondrial fractions of hNTs following 0 and 24 h of 1μM PAF administration confirmed the PAF-induced upregulation of UCP2 protein. COXIV was used as a loading control.

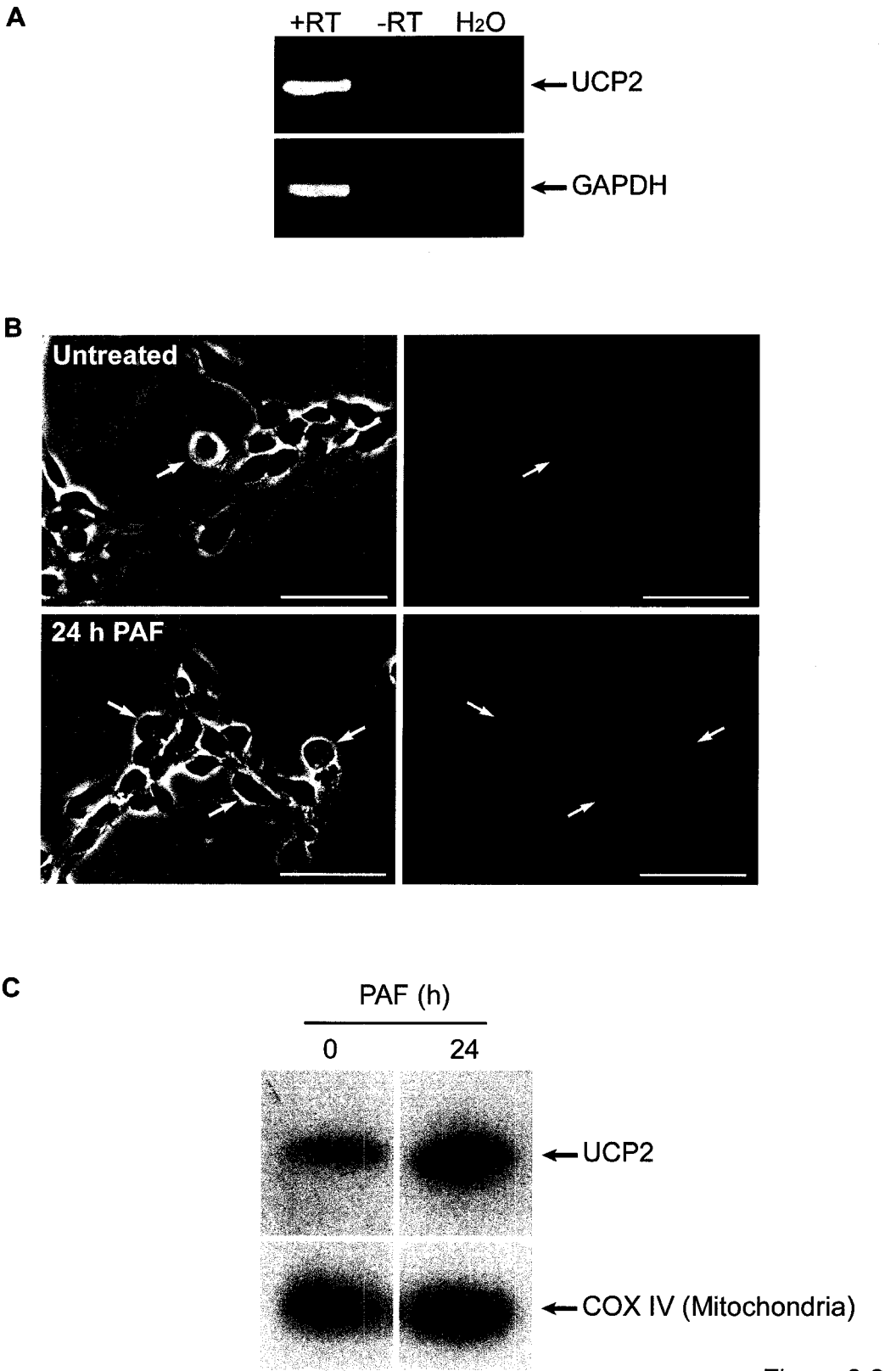


Figure 3.3

described in Chapter 2 is likely the primary neuronal death pathway elicited by PAF independently of PAFR.

### *3.7.2 PAF does not appear to induce $\Delta\Psi_m$ collapse but does induce ROS production in hNTs*

Apoptotic signalling can lead to mitochondrial membrane hyperpolarization as $\Delta\Psi_m$ increases, followed by depolarization as the PTPC is formed, the outer mitochondrial membrane ruptures and, finally, $\Delta\Psi_m$ collapses, allowing the release of mitochondrial apoptogenic factors such as cytochrome *c*, AIF, and endoG (see (Ly et al., 2003) for a review). MTR fluorescence intensity is indicative of $\Delta\Psi_m$, but can also be influenced by the presence of ROS in neurons and astrocytes (Buckman et al., 2001; Park et al., 2006). As such, a decrease in MTR fluorescence intensity could be interpreted as a loss of $\Delta\Psi_m$ and/or a decrease in ROS whereas an increase in MTR fluorescence intensity is most often attributed to ROS production but could also be interpreted as an increase in $\Delta\Psi_m$ (Imoto et al., 2006; Pendergrass et al., 2004). Here, the coincident increase in both DCFDA and MTR fluorescence indicates that PAF increases neuronal ROS production. If, however, the increase in MTR fluorescence intensity is in any way reflective of $\Delta\Psi_m$, then mitochondrial hyperpolarization, an event that often precedes $\Delta\Psi_m$ dissipation involved in releasing apoptogenic factors (Ly et al., 2003), could be involved in signalling PAF-induced apoptosis. The fact that neither AIF nor endoG are released from the mitochondria within 24 h of PAF administration makes this possibility unlikely. Although cytochrome *c* is released by some neurons 24 h after PAF treatment (Figure 2.9),

mitochondrial release of cytochrome *c* into the cytosol can occur without a change in $\Delta\Psi_m$ (see (Ly et al., 2003) for a review). Conclusive evidence that PAF does not impact upon $\Delta\Psi_m$ would require use of a ROS-insensitive/$\Delta\Psi_m$-sensitive dye such as or 5,5',6,6'-tetrachloro-1,1',3,3'-tetraethylbenzimidazolocarbocyanine iodide (JC-1, Molecular Probes) or tetramethylrhodamine methyl ester (TMRM, Molecular Probes).

Data presented here are consistent with previous reports that ROS production is involved in PAF-induced neuronal death (Feuerstein et al., 1990; Matsuo et al., 1996; Zhu et al., 2004). A recent study showed that PAF increases ROS levels and mitochondrial membrane hyperpolarization in rat cortical neurons (Perry et al., 2005). However, in each of these studies, PAFR status was not evaluated. Here, it is shown that PAF-induced neuronal ROS production occurs independently of PAFR. ROS is hypothesized to trigger neuronal apoptosis through cytochrome *c* release and caspase-3 activation (Annunziato et al., 2003).

### *3.7.3 PAF induces UCP2 expression in hNT neurons*

Caspase-independent mitochondrial responses are not confined to the release of AIF and endoG. For example, the upregulation of UCP2 protein observed following PAF treatment in this study poses an interesting question as to the role of UCP2 in PAF-induced neuronal apoptosis. Recent studies have provided evidence of neuroprotection by UCP2 in models of ischemia, kainic acid injury, epilepsy, and Parkinson's Disease (Andrews et al., 2005; Clavel et al., 2003; Diano et al., 2003; Mattiasson et al., 2003). UCP2 expression is hypothesized to either suppress ROS

production occurring through electron transfer from semiquinone radical to molecular oxygen or prevent mitochondrial accumulation of ROS by facilitating the transport of ROS to the cytosol, thereby activating neuroprotective pathways (Boss et al., 2000; Mattiasson et al., 2003; Paradis et al., 2003). However, other studies suggest that elevated UCP2 expression in HeLa cells is associated with cell death (Mills et al., 2002). Therefore, UCP2 may be upregulated in hNTs in response to PAF in an attempt to protect neurons from ROS-mediated damage, or alternatively UCP2 may contribute to secondary neuronal loss.

To clarify the role of UCP2 in PAF-mediated neuronal apoptosis, colleagues in the Bennett laboratory have provided mechanistic insight into the increase of UCP2 following PAF challenge. It was collaboratively hypothesized that if UCP2 plays a protective role in PAF-induced neuronal apoptosis, then neurons with diminished UCP2 levels will be more sensitive to PAF administration. However, if UCP2 upregulation is involved in PAF-induced apoptosis, then neurons devoid of UCP2 should be protected from apoptosis triggered by PAF. As part of my Ph.D. studies, knockdown of UCP2 levels in hNTs was attempted, but RNA interference (RNAi) of either scrambled or specific sequences proved toxic. A double null-mutant mouse model was therefore used to evaluate PAF toxicity in primary culture of mouse cerebellar granule neurons (CGN). CGNs endogenously express PAFR and as shown by the Bennett laboratory, are not susceptible to PAF-induced death (Appendix 2). However, $PAFR^{-/-}$ CGNs are sensitive to PAF and exhibit a 40% decrease in survival as measured by the LIVE/DEAD assay and a 15-fold increase in caspase-3/7 activation as measured by the CaspaTag assay (Appendix 2). To produce an appropriate model that would analyze the effect of UCP2 expression in

the absence of PAFR expression, $PAFR^{-/-}$ and $UCP2^{-/-}$ mice were bred to produce congenic $PAFR^{+/+}/UCP2^{+/+}$, $PAFR^{-/-}/UCP2^{+/+}$ and $PAFR^{-/-}/UCP2^{-/-}$ mice. These studies were initiated during my Ph.D research and continued by others in the Bennett laboratory. As expected, $PAFR^{-/-}/UCP2^{+/+}$ CGNs displayed a decrease in survival following PAF administration as measured by the LIVE/DEAD assay (Appendix 3), as shown previously in $PAFR^{-/-}$ CGNs (Appendix 2). Surprisingly, it was found that $PAFR^{-/-}/UCP2^{-/-}$ CGNs were protected from PAF neurotoxicity (Appendix 3). The lack of neuronal death in the $PAFR^{-/-}/UCP2^{-/-}$ CGNs indicates a controversial pro-apoptotic role for UCP2 in neurons and suggests that UCP2 is a key regulator of the PAFR-independent neuronal apoptotic pathway induced by PAF. The role of UCP2 in modulating PAF-induced death remains to be clarified.

### *3.7.4 Summary*

In summary, these studies more completely delineate the PAFR-independent apoptotic cascade through which PAF transduces neuronal death in hNTs. AIF and endoG do not play a role in PAF-induced apoptosis in human neurons. However, an induction of ROS is observed following exposure to pathophysiological concentrations of PAF. In addition, a controversial pro-apoptotic role for UCP2 is described in collaboration with colleagues in the Bennett laboratory, as UCP2 upregulation appears to contribute to PAF-induced neuronal death.

# Chapter 4: Neuroprotective assessment of PAF inhibitors and other protective compounds in PAFR-independent death and Aβ-mediated neurotoxicity *in vitro*

## 4.1 Publications resulting from studies described in this chapter:

Harris CS, Moffat TC, Ryan SD, Migahed L, Mo F, Midzic, I, Bennett SAL (2006) Plant phenolic compounds protect against amyloid-$\beta_{1-42}$ neurotoxicity - a structure-activity analysis, in preparation.

Moffat TC and Bennett SAL (2006) PAF inhibitors that prevent caspase-dependent apoptosis in human neurons triggered by PAF independently of its G-protein-coupled receptor, in preparation

## 4.2 Statement of author contributions

The experiments presented in this chapter were either carried out or supervised by Tia C. Moffat. All figures and text in this chapter were prepared by Tia C. Moffat with guidance and editorial assistance from Dr. Steffany A.L. Bennett. Screening, identification, and subsequent structure-activity relationships of anti-apoptotic plant phenolics were performed by Cory Harris as part of his Ph.D. research assisted by Fan Mo and Lamiaa Migahed. The affect of these compounds was assessed in hNTs by Tia C. Moffat. The TUNEL experiments were collaboratively double counted by Lamiaa Migahed, Fan Mo, and Ines Midzic. Additional studies of PAFAH I subunit expression in NT2 and hNT cultures by Western blotting were performed by Scott Ryan as part of his Ph.D. research.

## 4.3 Abstract

While it is recognized that PAF signalling is implicated in neurodegenerative disease, it has only been suggested that PAF plays a role in Aβ-induced neuronal apoptosis during AD. To strengthen the hypothesis that PAF and Aβ apoptotic signalling are interrelated, a panel of natural and synthetic compounds, including known PAF inhibitors, was tested for the ability to block PAF and/or Aβ-mediated apoptosis in hNTs. The PAF inhibitors ONO-6240 and RP59227 displayed neuroprotective properties inhibiting both PAF and Aβ-induced toxicity in the absence of PAFR. Surprisingly, FR49175 and BN52021, previously shown to inhibit PAFR-independent death, failed to improve viability of PAF or Aβ-treated hNTs. Four neuroprotective plant phenolics were also screened. Although orsellinic acid did not offer protection of neurons from PAFor Aβ-induced apoptosis, hesperetin blocked both PAF and Aβ-induced neuronal apoptosis, while the neuroprotective effects of quercetin were limited to Aβ-induced apoptosis. Finally, the anti-apoptotic HIV protease inhibitor (PI) nelfinavir (NFV) was shown to reduce both PAF and Aβ-induced neuronal apoptosis likely through inhibition of mitochondrial caspase-9 activation elicited downstream of ER stress.

## 4.4 Introduction

To target PAF-mediated neuronal loss, we next sought to identify agents capable of inhibiting PAF-mediated neurotoxicity in the absence of PAFR. A large number of natural and synthetic agents have been identified as PAF antagonists based on their ability to inhibit PAF-induced platelet aggregation (bioassay) and/or on their affinity for soluble PAF binding proteins (Braquet and Esanu, 1991; Koltai et

al., 1991; Marcheselli et al., 1990; Shen, 1991). The majority of these PAF "inhibitors" were characterized in the early 1990s and, to our knowledge, few (if any) studies have established directly whether these compounds specifically act as PAFR antagonists using a null-mutant model system or a cell line shown to lack PAFR transcript. Because a single G-protein receptor has been identified, it has been assumed that PAF mediates all biological activity through this receptor. However, accumulating evidence points towards additional PAF signalling pathways transduced independently of PAFR (Bratton, 1993; Bratton et al., 1992; Brewer et al., 2002; Marcheselli et al., 1990; Sapir et al., 1997; Tokuoka et al., 2003) and this hypothesis is further supported by the data presented in Chapters 2 and 3 of this thesis. At least three PAF binding sites have been identified pharmacologically in rat synaptosomal preparations (Marcheselli et al., 1990). Moreover, PAF analogs have been shown to enhance cerebellar neuronal migration in a null-mutant background suggesting that other PAF effector proteins are likely expressed in the CNS (Tokuoka et al., 2003). Together, these data suggest that a closer examination of the anti-apoptotic actions of existing PAF antagonists/inhibitors in a PAFR-negative background is warranted.

Here, a panel of ten compounds, made up of known PAF inhibitors, plant/fungal-derived phenolic compounds, and the HIV PI NFV, was evaluated for neuroprotective activity in hNT neurons. Structures are presented in (Figure 4.1). These compounds were chosen based on a preliminary screen of compounds in the PAFR-negative PC12-AC model performed in the Bennett laboratory and by published studies indicating that NFV exhibits anti-apoptotic activity relevant to the

**Figure 4.1: Structures of the compounds tested for the ability to protect hNT neuronal cultures from PAF and Aβ-induced toxicity.** Compounds tested in this study can be categorized as follows: structural PAF analogs (CV3988, ONO6248); PAF inhibitors (BN52021, FR49175, L659-989, RP59227); natural phenolic compounds (quercetin, hesperetin, orsellinic acid); and HIV protease inhibitor (NFV).

**Structural PAF Analogs**

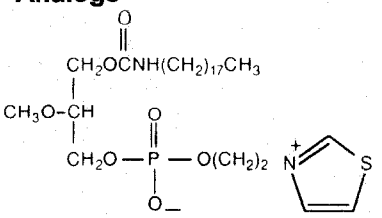

**CV3988**

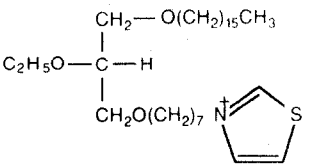

**ONO6248**

**PAF Inhibitors**

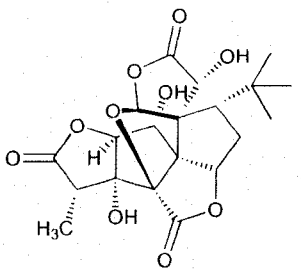

**BN52021**

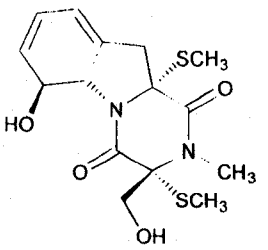

**FR49175**

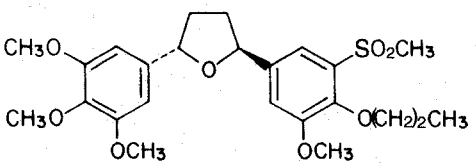

**L659-989**

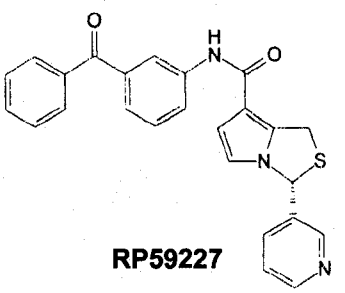

**RP59227**

**Natural Phenolic Compounds**

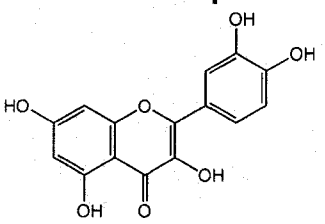

**Quercetin**

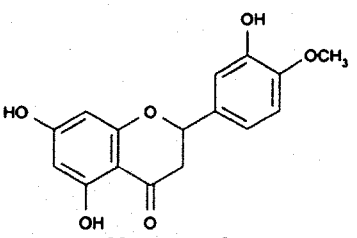

**Hesperetin**

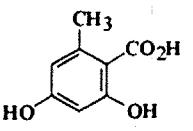

**Orsellinic Acid**

**HIV Protease Inhibitor**

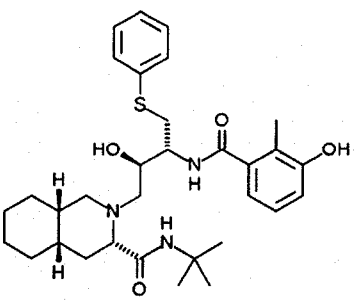

**NFV**

Figure 4.1

treatment of HIV and HIV-dementia (Lau et al., 2005; Phenix et al., 2002; Phenix et al., 2001; Weaver et al., 2005; Zbarsky et al., 2005).

A secondary objective of this chapter was to determine whether agents capable of blocking PAF-induced apoptosis in hNT neurons also inhibit Aβ-induced cell death. As discussed in Chapter 1, imbalances of substrates and enzymes in the PAF synthesis pathways seen in AD are predicted to lead to enhanced PAF production (see Chapter 1 for a review). Thus, it was of interest to prioritize agents that block both PAF-mediated cell death and Aβ-induced apoptotic pathways for future mechanistic assessment.

## 4.5 Materials and Methods

### *4.5.1 Reagents*

Unless otherwise specified, all cell culture reagents were obtained from Invitrogen, and all chemical reagents were obtained from Sigma.

### *4.5.2 Cell culture*

hNTs were cultured and differentiated as described in Section 2.5.2.

### *4.5.3 Cell treatments*

Cells were treated as described in Section 2.5.3. Cells were treated with either EtOH (0.1%), PAF (1 μM), or Aβ (25 μM) in the presence of either DMSO (0.1%) or CV-3988 (10 μM, BioMol), L659-989 (10 μM, Dr. T.Y. Shen, University of Virginia, Charlottesville, Virginia), FR49175 (10 μM, BioMol), BN52021 (50 μM, BioMol), ONO-6240 (10 μM, Dr. T.Y. Shen), RP59227 (10 μM; Dr. T.Y. Shen),

hesperetin (1 μg/mL; Dr. John Thor Arnason, University of Ottawa, Ottawa, ON), quercetin (1 μg/mL; Dr. John Thor Arnason), orsellinic acid (1 μg/mL; Dr. John Thor Arnason), or NFV (7 μM; kind gift of Agouron Pharmaceuticals Inc).

### *4.5.4 TUNEL*

Cells were assessed for DNA fragmentation using the TUNEL assay as described in Section 2.5.7.

### *4.5.5 Statistical analysis*

Statistical analysis was performed as described in Section 2.5.11.

## 4.6 Results

### *4.6.1 PAF inhibitors block PAF- and Aβ-induced death in hNTs*

Compounds were screened for the ability to prevent either PAF or Aβ-induced toxicity of hNTs as measured by the TUNEL assay. CV-3988 and L659-989 were toxic to hNTs and induced a 60% decrease in survival (Figure 4.2). However, both compounds protected hNTs from Aβ. Surprisingly, BN52021 and FR49175, compounds that have previously been shown to protect PAFR-negative PC12-AC cells from PAF-mediated death (Bonin et al., 2004), were unable to protect hNTs from either PAF or Aβ-induced toxicity (Figure 4.3). By contrast, both ONO-6240 and RP59227 protected hNTs from PAF and Aβ-induced toxicity (Figure 4.3).

### *4.6.2 Natural phenolic compounds protect hNTs from PAF- and Aβ-induced death*

Previously, colleagues in the Bennett laboratory screened a library of 54 flavonoids for anti-apoptotic activities in PC12-AC cells (Harris et al., 2006) and tested these compounds for PAF inhibitory effects in PC12 cells (Mo et al., in preparation). Three compounds were capable of inhibiting PAF-induced cell death in PC12 cells and were chosen for analysis in hNTs. Hesperetin, quercetin and orsellinic acid were screened for the ability to prevent either PAF or Aβ-induced toxicity of hNTs as measured by the TUNEL assay. Hesperetin protected hNTs from both PAF and Aβ-induced toxicity (Figure 4.4). Quercetin protected hNTs only from Aβ-induced toxicity, while orsellinic acid was unable to protect hNTs from either PAF or Aβ-induced toxicity (Figure 4.4).

**Figure 4.2: The PAF inhibitors CV-3988 and L659-989 prevent Aβ-induced but not PAF-induced death in hNT neuronal cultures in the absence of PAFR.** hNT neuronal cultures were cotreated for 24 h with either 1 μM PAF or 25 μM Aβ and one of the following PAF inhibitors: 10 μM CV-3988 or 10 μM L659-989. % Survival was measured using the TUNEL assay, and data were expressed standardized to vehicle control. While both CV-3988 and L659-989 were toxic to hNTs, inducing a 60% decrease in survival, both compounds protected hNTs from Aβ, but not from PAF. Asterisks (*) indicate a significant decrease in % survival in cells treated with death ligand relative to vehicle control. Number signs (#) indicate a significant increase or decrease in % survival in cells treated with PAF inhibitors relative to cells treated without PAF inhibitors. Data were expressed as the mean $\pm$ SEM (n=27-45 per data point; ** $p<0.01$, # $p<0.05$, ## $p<0.01$, ANOVA, *post-hoc* Dunnett's *t* test).

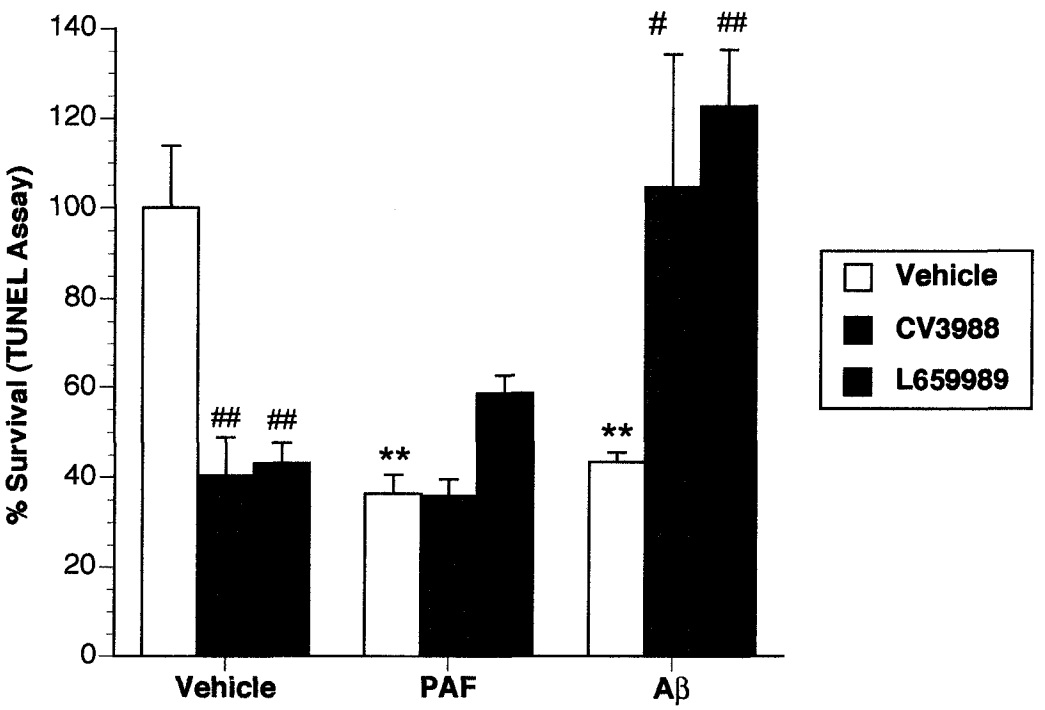


Figure 4.2

**Figure 4.3: The PAF inhibitors ONO-6240 and RP59227 protect hNT neuronal cultures from both PAF and Aβ-induced neurotoxicity in the absence of PAFR.** hNT neuronal cultures were cotreated for 24 h with either 1 μM PAF or 25 μM Aβ and one of the following PAF inhibitors: 50 μM BN52021, 10 μM FR49175, 10 μM ONO6248 or 10 μM RP59227. % Survival was measured using the TUNEL assay, and data were expressed standardized to vehicle control. Both BN52021 and FR49175 did not offer protection from PAF or Aβ-induced toxicity. Both ONO6248 and RP59227 significantly prevented PAF and Aβ-induced neuronal death in hNTs. Asterisks (*) indicate a significant decrease in % survival in cells treated with death ligand relative to vehicle control. Number signs (#) indicate a significant increase in % survival in cells treated with PAF inhibitors relative to cells treated without PAF inhibitors. Data were expressed as the mean $\pm$ SEM (n=27-45 per data point; ** $p<0.01$, # $p<0.05$, ## $p<0.01$, ANOVA, *post-hoc* Dunnett's *t* test).

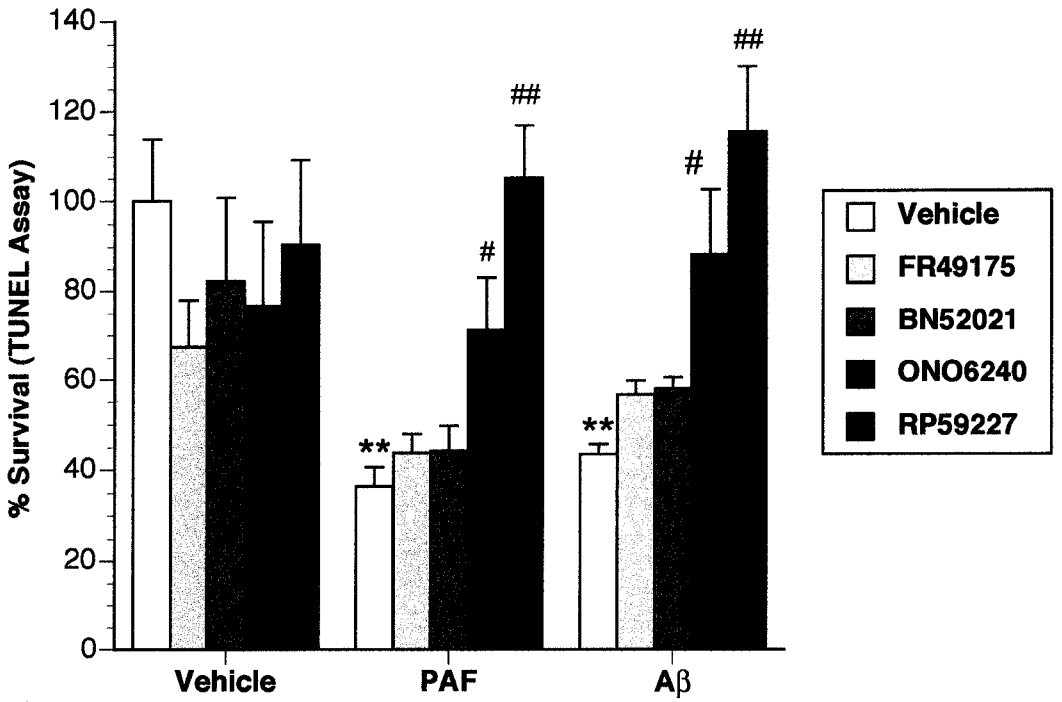


Figure 4.3

**Figure 4.4: Select natural phenolic compounds protect hNT neuronal cultures from PAF- and/or Aβ-induced death in the absence of PAFR.** hNT neuronal cultures were cotreated for 24 h with either 1 μM PAF or 25 μM Aβ and one of the following natural phenolic compounds: 1 μg/mL hesperetin, 1 μg/mL quercetin, or 1 μg/mL orsellinic acid. % Survival was measured using the TUNEL assay, and data were expressed standardized to vehicle control. Hesperetin was able to significantly protect hNTs from both PAF- and Aβ-induced neuronal death, while quercetin significantly protected only from Aβ. Orsellinic acid did not offer protection from PAF- or Aβ-induced neurotoxicity. Asterisks (*) indicate a significant decrease in % survival in cells treated with death ligand relative to vehicle control. Number signs (#) indicate a significant increase in % survival in cells treated with natural phenolic compounds relative to cells treated without natural phenolic compounds. Data were expressed as the mean $\pm$ SEM (n=27-45 per data point; ** $p<0.01$, # $p<0.05$, ANOVA, *post-hoc* Dunnett's *t* test).

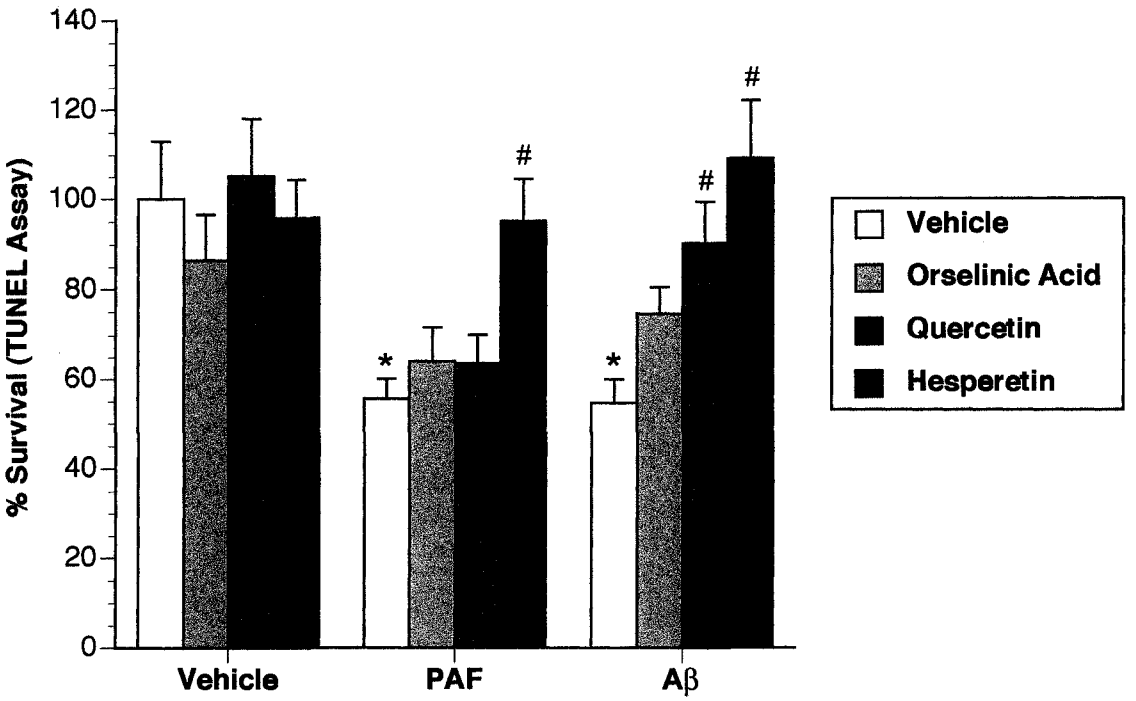


Figure 4.4

### *4.6.3 NFV blocks PAF- and Aβ-induced death in hNTs*

The ability of NFV to protect hNTs from PAF and Aβ was measured by TUNEL reactivity. NFV is soluble in DMSO but the clinical tablet and oral powder formulations available to us contain additional aqueous soluble materials proprietary to Agouron Pharmaceuticals Inc that precipitate in DMSO. It was suggested by Agouron Pharmaceuticals Inc that we filter the DMSO-solubilized product to remove insoluble precipitate but this technique was found by our collaborators to reduce drug concentration. To address toxicity due to this precipitate, the % survival values for vehicle/NFV-treated hNTs were set to 100% and the % survival values for PAF/NFV- and Aβ/NFV-treated hNTs were standardized to this value. While NFV treatment completely blocked Aβ toxicity, the protection of hNTs by NFV from PAF approached significance (Figure 4.5).

## 4.7 Discussion

Many natural and synthetic compounds have been shown to be anti-apoptotic and/or to inhibit PAF toxicity but none of these compounds have been directly assessed for their ability to inhibit PAFR-independent biological activity. A panel of known and suspected PAF inhibitors was screened for their ability to protect neurons from PAF toxicity in order to identify potential therapeutic compounds for the treatment of neuronal disease states that involve PAF signalling in the absence of PAFR. These agents were also used to begin to assess the potential involvement of PAF in the neurodegenerative disease AD by evaluating their ability to block Aβ-induced neuronal death.

**Figure 4.5: The HIV protease inhibitor NFV protects hNT neuronal cultures from PAF- and Aβ-induced death in the absence of PAFR.** hNT neuronal cultures were cotreated for 24 h with either 1 μM PAF or 25 μM Aβ and 7 μM NFV. % Survival was measured using the TUNEL assay, and was expressed standardized to control. % Survival of cells treated without NFV was expressed standardized to vehicle control, while % survival of NFV-treated cells was expressed standardized to NFV control. The protection of hNTs offered by NFV from PAF approached significance, while protection from Aβ was statistically significant. Asterisks (*) indicate a significant decrease in % survival in cells treated with death ligand relative to vehicle control. Tilde (~) indicates an increase in % survival that approaches significance in NFV -treated cells relative to cells treated without NFV. Number signs (#) indicate a significant increase in % survival in NFV -treated cells relative to cells treated without NFV. Data were expressed as the mean $\pm$ SEM (n=27-45 per data point; * $p<0.05$, ~ $p<0.08$, ## $p<0.01$, ANOVA, *post-hoc* Tukey).

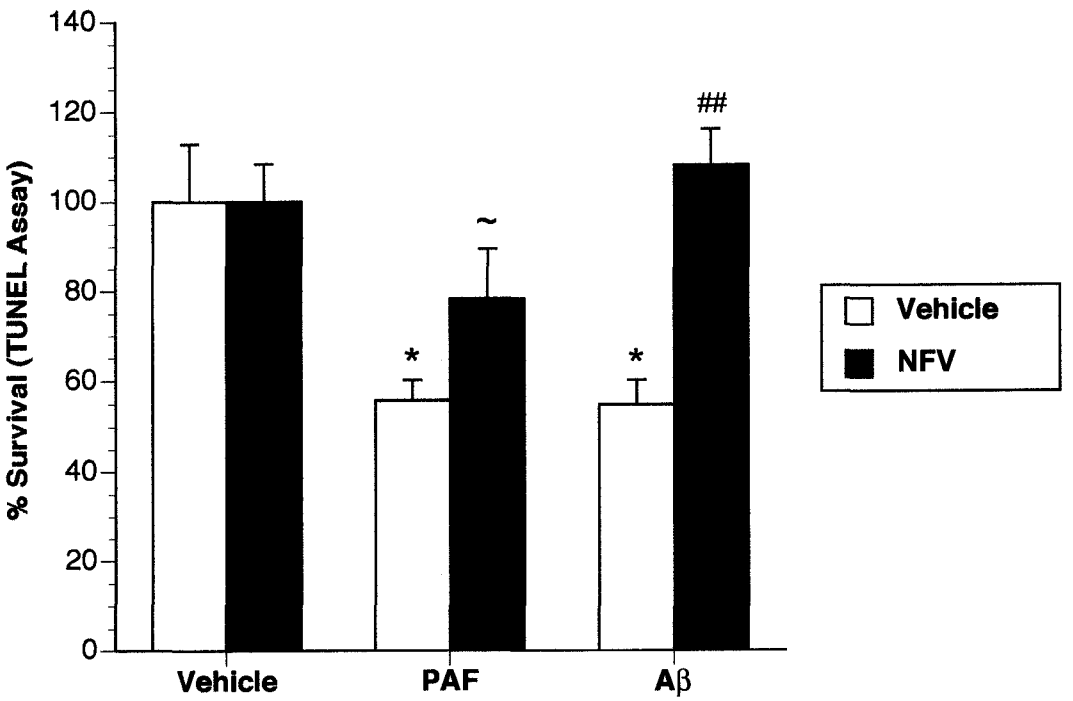


Figure 4.5

*4.7.1 BN52021 and FR49175 protect PC12-AC cells but not hNT neurons from PAF-mediated death*

BN52021, also known as ginkgolide B, is a terpenoid extract from leaves of *Ginkgo biloba* tree that has previously been shown to have antioxidant action as a free radical scavenger, to prevent PAF-induced glutamate release, and to protect neurons from ischemia-reperfusion injury (Yoshikawa et al., 1999). BN52021 is a non-competitive PAF inhibitor that inhibits the binding of PAF to both microsomal and synaptosomal membrane binding sites (Marcheselli et al., 1990). Administration has been shown to increase the survival of SH-SY5Y human neuroblastoma cells following PAF and Aβ, and reduce caspase-3 activity in mouse cortical neurons (Bate et al., 2004b). The neuroprotective properties of ginkgolide B observed *in vitro* and *in vivo* in rodent models led to clinical trials for the treatment of AD, however, these trials have not met with therapeutic success (Le Bars et al., 1997; Le Bars et al., 2000; van Dongen et al., 2003; van Dongen et al., 2000; Wettstein, 2000).

This disconnect is partially addressed in the present study. We show that BN52021 and FR49175 are not able to protect human hNTs from PAF or Aβ-induced death. This finding was surprising given that the Bennett laboratory has previously demonstrated that both BN52021 and FR49175 have the ability to protect rat PC12-AC cells from PAF-induced toxic effects in the absence of PAFR (Bonin et al., 2004; Brewer et al., 2002). Colleagues demonstrated that BN52021 and FR49175 protect rodent cells from PAFR-independent death by accelerating PAF hydrolysis. In PC12-AC cells, BN52021 and FR49175 inhibit PAF-induced death in the absence of PAFR by decreasing the expression of the PAFAH I $\alpha_1$ protein, thereby promoting an $\alpha_2/\alpha_2$ homodimer formation of PAFAH I, which is known to

hydrolyze PAF more efficiently than the $\alpha_1/\alpha_1$ homodimer (Bonin et al., 2004). Interestingly, the expression of the PAFAH I $\alpha_1$ and $\alpha_2$ subunits is under developmental control with $\alpha_1$ predominating in embryonic tissue and $\alpha_2$ predominating in adult brain (Manya et al., 1998). Western blot analysis demonstrated that this pattern is recapitulated in the NT2 model system (Appendix 4). Like PC12-AC cells (Bonin et al 2004), NT2 cells express higher levels of $\alpha_1$ than $\alpha_2$ catalytic subunits whereas hNTs predominantly express $\alpha_2$ with only minimal $\alpha_1$ expression. Since we have previously shown that the mechanism of action of BN52021 and FR49175 is to reduce $\alpha_1$ expression and thereby promote $\alpha_2/\alpha_2$ homodimer formation (Bonin et al., 2004), perhaps in retrospect, it is not surprising that these compounds fail to inhibit PAF-induced hNT death. Likely hNT $\alpha_1$ levels are too low and/or hNT $\alpha_2$ levels are too high for BN52021 and FR49175 to produce a significant increase in $\alpha_2/\alpha_2$ homodimer formation and therefore enhance PAF hydrolysis. It is tempting to speculate that this mechanism, in part, underlies the failure of BN52021 to translate into human clinical benefit.

### *4.7.2 ONO-6240 and RP 59227 are known PAF inhibitors that protect hNT neurons from PAF and Aβ*

ONO-6240 is a structural PAF antagonist that has been shown to reduce PAF-induced airway eosinophil infiltration, suggesting that ONO-6240 may be useful for treating inflammatory respiratory diseases such as asthma (Shi et al., 1995). Since ONO-6240 protected hNTs from both PAF and Aβ toxicity, arguably it deserves further mechanistic assessment. It is curious that this structural analog is able to protect hNTs from PAF challenge, while the other structural analog tested,

CV3988, did not offer any protection. CV3988 has been shown to competitively block PAF binding to a single site localizing to synaptosomal membranes, likely PAFR (Marcheselli et al., 1990). Since hNTs do not express PAFR, it is not surprising that CV3988 failed to protect human neurons from PAF-induced toxicity despite success in PC12-AC cells (Brewer et al., 2002). Thus, since the mechanism of action of ONO-6248 has not been extensively studied, it is possible that this compound impinges on multiple pathways in addition to PAFR.

RP 59227 (N-(3-benzoylphenyl)-3-pyridyl)-1H,3H-pyrrolol [1,2-c] thiazolecarboxamide), or tulopafant, is a member of the triazolobenzodiazepine chemical family (pyrrolo[1,2-c]thiazole derivative) and is one of the most potent PAF inhibitors identified to date (Auchampach et al., 1998; Floch et al., 1991). RP 48740, the parent compound of RP 59227, was the first non-lipid synthetic PAF inhibitor discovered (de Sant' Anna et al., 1996). RP 59227 has the ability to protect from ischemia/reperfusion injury since RP 59227 pretreatment was found to effectively reduce both myocardial infarct size and the incidence of ischemia and reperfusion-induced arrhythmias in anesthetized dogs (Auchampach et al., 1998). These data, combined with the findings shown here that RP 59227 can abrogate the toxic effects of both PAF and Aβ in hNTs, indicate that RP 59227 may be an ideal neuroprotective therapeutic agent for the treatment of stroke and neurodegenerative disease. Validation of this promise will require further mechanistic assessment.

### *4.7.3 Plant-derived phenolic compounds can protect neurons from PAF and Aβ*

Naturally occurring phenolic compounds such as plant-derived flavonoids are potent antioxidants with anti-apoptotic abilities, and have been suggested as

potential therapeutic agents for the treatment of various oxidative stress-related neurodegenerative diseases such as AD (Galli et al., 2002; Mandel and Youdim, 2004). Colleagues in the Bennett laboratory have shown that the flavonoids quercetin and hesperetin are able to prevent a loss of metabolic activity in PAF-treated PC12-AC cells and protect both $PAFR^{-/-}$ mouse CGNs and rat dorsal root ganglion neurons from PAF-induced caspase-3/7-dependent death (data not shown). However, repeated observation that efficacy in rodent models may not translate into human therapeutic benefit underlined the necessity to test quercetin and hesperetin in the hNT system. Since hesperetin was able to protect hNTs from both PAF and Aβ, further studies should address potential therapeutic abilities. Conversely, quercetin only protected hNTs from Aβ and not from PAF. It is therefore likely that quercetin's mechanism of action does not involve the inhibition of PAF signalling; however quercetin may be of use in the treatment of AD with further validation. Orsellinic acid was included as (a) a negative control for PAF involvement as it did not protect PC12-AC cells from PAF-induced cell death but did inhibit etoposide- and ceramide-induced apoptosis (data not shown), and (b) a natural fungal derivative counterpart to the synthetic FR49175 fungal metabolite. Both FR49175 and orsellinic acid failed to protect hNTs from PAF and Aβ toxicity in hNTs.

### *4.7.4 NFV exhibits neuroprotective abilities in the prevention of PAF- and Aβ-induced toxicity*

NFV is an HIV PI used in HIV therapy. Such HIV PIs have been shown to have *in vitro* protective effects in response to diverse apoptotic stimuli (for a review,

see (Phenix et al., 2002)). While many mechanisms of action for these anti-apoptotic effects have been suggested, one proposed mechanism includes the inhibition of caspases. Based on these results, it was hypothesized that NFV could inhibit PAF and/or Aβ-induced neurotoxicity.

Since the NFV formulation could not completely dissolve into its vehicle, many crystals/precipitates of the adjuvants used in the clinical NFV powder were present in the treatment media. Damage to the hNTs due to these crystals is thought to be responsible for the lower cell number present in all NFV treatments. In order to compare the % survival of NFV-treated cells with cells not treated with NFV, % survival of PAF/NFV and Aβ/NFV-treated cells were standardized to the % survival of vehicle/NFV-treated cells. NFV completely blocked Aβ-induced neurotoxicity and offered partial protection from PAF. Our collaborators have previously shown that NFV can protect Jurkat T cells from mitochondrial-dependent apoptosis (Phenix et al., 2001). More recently, they have demonstrated that NFV can block apoptosis *in vitro* through the preservation of mitochondrial integrity by preventing the pore function of the adenine nucleotide translocator (ANT) subunit of the mitochondrial permeability transition pore complex (Weaver et al., 2005)[7]. As described in Chapter 2, mitochondrial apoptosis is a secondary pathway triggered by PAF in hNTs. However, the mitochondrial effects seen in PAF-induced apoptosis in hNTs, specifically cytochrome *c* release resulting in caspase-9 activation, led to the hypothesis that NFV may protect neurons from secondary PAF-induced mitochondrial apoptotic signalling. Given that the mechanism of action of NFV involves the inhibition of the mitochondrial permeability transition pore complex,

[7] My role in this study is described in more detail in Chapter 5.

preventing the loss of $\Delta\Psi_m$ and the activation of caspase-9 and caspase-3, the partial protection of hNTs offered by NFV likely represents abrogation of this later mitochondrial pathway (Weaver et al., 2005). This suggests that following activation of ER stress, downstream mitochondrial events initiated by PAF and participating in Aβ-induced cell death can be targeted by NFV.

### *4.7.5 Implication of PAF production and signalling in AD*

The goal of this chapter was to a) identify PAF inhibitors that could block PAF-induced cell death triggered independently of PAFR in human neurons and b) provide pharmacological evidence that inhibiting PAF signalling can affect Aβ signalling. As described in Chapter 1, an increase in PAF substrate levels and $cPLA_2$ activity in AD brain is hypothesized to lead to enhanced PAF synthesis. PAF and Aβ-induced apoptosis involve similar pathways, including mitochondrial damage, ROS production and caspase activation. Furthermore, while Aβ can increase glycerophospholipid production, glycerophospholipids can enhance Aβ aggregation (Kriem et al., 2005; Mandal et al., 2004). This reciprocal relationship between PAF and Aβ implicates PAF in the progression of AD. Our laboratory is actively pursuing this hypothesis using electrospray ionization tandem mass spectrometry to detect PAF family members in human neurons and microglia following Aβ treatment, and in transgenic mice overexpressing mutated forms of APP. These studies are necessary to confirm the circumstantial evidence provided in this thesis by observation that some pharmacological agents that inhibit PAF-mediated death in human neurons can block Aβ-mediated death.

### *4.7.6 Summary*

In summary, these studies describe the ability of natural and synthetic compounds to protect human neurons from both PAF and Aβ, providing a preliminary pharmacological link between PAF neurotoxicity and the neuronal apoptosis that occurs during AD. The compounds identified as PAF/Aβ inhibitors have unexplored potential as therapeutic agents. In order to move towards clinical trials, *in vivo* testing in mouse models of AD (albeit with the understanding demonstrated in this study that the mouse may not completely model human responses) and validation of PAF synthesis in AD tissue and other neurodegenerative disease states is imperative. As a first step in this direction, Chapter 5 describes the use of NFV to prevent neuronal apoptosis in a mouse model of ischemia.

# Chapter 5: Targeting PAFR-independent death to protect neurons and prevent the associated behavioural impairment *in vivo* following middle cerebral artery occlusion in the mouse

## 5.1 Publications resulting from studies described in this chapter:

Weaver JG, Tarze A, Moffat TC, Lebras M, Deniaud A, Brenner C, Bren GD, Morin MY, Phenix BN, Dong L, Jiang SX, Sim VL, Zurakowski B, Lallier J, Hardin H, Wettstein P, van Heeswijk RP, Douen A, Kroemer RT, Hou ST, Bennett SA, Lynch DH, Kroemer G, Badley AD. (2005) Inhibition of adenine nucleotide translocator pore function and protection against apoptosis in vivo by an HIV PI. J. Clin. Invest. 115(7):1828-38 (see Appendix 5).

## 5.2 Statement of author contributions

The experiments presented in this chapter were carried out as part of a collaborative project resulting in the publication cited above. Mario Morin[1] and Jessica Lallier[1] performed the oral gavages. Bogdan Zurakowski[2] performed all mouse surgeries, behavioural testing 0.5 h post-surgery, sacrifices by lethal injection, and transcardial perfusions. Susan Jiang[2], Jessica Lallier and Tia C. Moffat[1] collaboratively executed the behavioural testing 24 h post-surgery, sacrifices by decapitation, and 2,3,5-triphenyltetrazolium chloride (TTC) staining. Mario Morin

---

[1] Neural Regeneration Laboratory, University of Ottawa, Ottawa, ON, Canada.

2 Experimental Stroke Group, National Research Council Institute for Biological Sciences (NRC/IBS), National Research Council of Canada, Ottawa, ON, Canada.

and Tia C. Moffat sectioned perfused brains with a cryostat. Tia C. Moffat performed the immunohistochemistry. Dr. Steffany A.L. Bennett performed the TUNEL assay. All figures and text in this chapter were prepared by Tia C. Moffat with guidance and editorial assistance from Dr. Steffany A.L. Bennett.

## 5.3 Abstract

HIV PIs have been shown to have anti-apoptotic effects *in vitro* and *in vivo*, yet these effects remain controversial. As demonstrated in Chapter 4, the HIV PI NFV was able to completely block Aβ-induced neurotoxicity and offer some protection from PAF in hNTs, implicating NFV as a potential therapeutic agent in the treatment of neurodegeneration and other apoptotic disease states. As a first step towards testing the efficacy of therapeutic strategies targeting PAF-induced neuronal apoptosis, NFV was chosen for *in vivo* analysis. NFV is already approved for clinical use in the treatment of HIV and, as such, represented the strongest lead compound for subsequent evaluation. In this study, the impact of NFV, boosted with ritonavir (RIT), was evaluated in the mouse using the MCAO model of focal ischemia, a model of non-viral neuronal disease associated with excessive apoptosis and synthesis of neurotoxic concentrations of PAF. NFV/RIT was shown to significantly reduce neuronal apoptotic-like death and improve behavioural recovery in this model.

## 5.4 Introduction

NFV is a member of the HIV PI family of antiretroviral agents currently used to treat HIV infection. While HIV PIs were designed to inhibit viral replication, many of these agents also possess intrinsic anti-apoptotic properties. Numerous studies have described the inhibition of apoptosis by HIV PIs in non-infected cells in response to a variety of stimuli (for a review, see (Phenix et al., 2002)). As such, it has been hypothesized that HIV PIs could offer therapeutic benefit in diseases characterized by apoptosis. When this study was initiated, NFV/RIT had been shown to have *in vivo* anti-apoptotic effects in mouse models of Fas-induced hepatitis and Staphylococcal enterotoxin B-induced shock. These data are presented in (Weaver et al., 2005) (Appendix 5). Specifically, NFV was shown to inhibit mitochondrial-mediated apoptosis by targeting the pore function of one of the PTPC subunits, thereby preventing the release of pro-apoptotic factors from the mitochondria and subsequent caspase activation (Weaver et al., 2005). To extend these studies to the CNS, and based on the *in vitro* data presented in Chapter 4 indicating that NFV can protect human neurons from both PAF and Aβ, the MCAO model of focal ischemia was chosen to establish whether NFV/RIT could be used to inhibit ischemic cell death *in vivo.* Together, these studies formed a complete submission published in the Journal of Clinical Investigation in 2005 (Weaver et al. 2005) (Appendix 5).

## 5.5 Methods

### *5.5.1 Reagents*

Unless otherwise specified, all reagents were obtained from Sigma.

### *5.5.2 Mouse treatments*

C57BL/6 mice (20–23 g) were obtained from Charles River Laboratories. Animal treatments were reviewed and approved by the Mayo Foundation Institutional Animal Care and Use Committee, the NRC/IBS Animal Care Committee, and the University of Ottawa Animal Care Committee. Mice were pretreated by oral gavage with either vehicle (2% EtOH) or a combination of NFV (125 mg/kg; Agouron Pharmaceuticals Inc.) and RIT (13 mg/kg; Abbott Laboratories) 24, 16, and 8 h before sham or MCAO surgery, giving four cohorts: vehicle and sham surgery (n = 7); vehicle and MCAO surgery (n = 10); NFV/RIT and sham surgery, (n = 7); NFV/RIT and MCAO surgery, (n = 10). A fifth cohort received MCAO surgery without vehicle or NFV/RIT pretreatment (n = 5).

### *5.5.3 Cerebral ischemia produced by MCAO*

Following the three oral gavages of either vehicle or NFV/RIT over 24 h, mice were placed under temporary isofluorane anesthesia and subjected to MCAO using an intraluminal filament as previously described (MacManus et al., 2003). After 1 h of MCAO, the filament was withdrawn, blood flow was restored to normal by laser Doppler flowmetry, and wounds were sutured. For sham operations, mice were subjected to all of the aforementioned steps excluding the insertion of the intraluminal filament.

### 5.5.4 *Behavioural testing*

Behavioral impairment following MCAO or sham surgery was assessed at 0.5 h after ischemic surgery when animals had recovered from the anesthetic and 24 h after reperfusion by two independent investigators blind to the gavage and surgical treatments of the mice. A modified 6-point scale was used (Frenkel et al., 2003; Zausinger et al., 2000): 0, normal; 1, mild turning behavior with or without inconsistent curling when picked up by tail and less than 50% attempts to curl to the contralateral side; 2, mild, consistent curling and more than 50% attempts to curl to the contralateral side; 3, strong and immediate consistent curling, mouse holds curled position for more than 1–2 seconds, and mouse's nose almost reaches tail; 4, severe curling progressing into barreling and loss of walking or righting reflex; 5, comatose or moribund. Behavioral scores were averaged within treatment groups for statistical analysis.

### 5.5.5 *Mouse sacrifice*

Following 24 h of reperfusion and behavioural testing, mice were anesthetized with $CO_2$ and sacrificed either by decapitation for TTC experiments, or by lethal injection with sodium pentobarbital and transcardially perfused with 10 mM PBS followed by 3.7% paraformaldehyde in 10 mM PBS for immunocytochemistry and TUNEL experiments.

### 5.5.6 *Measurement of infarct size using TTC viability assay*

In unfixed brain tissue, infarct size was measured by a colorimetric staining method using TTC, as described previously (Preston and Webster, 2000). Viability

was determined by the ability of mitochondrial dehydrogenases to cleave the TTC salt to a red formazan dye. Since necrotic infarct areas remain colourless, loss of TTC staining in the ischemic hemisphere compared to the contralateral hemisphere indicates the size of the infarct. Brains were removed and cut into four 2-mm-thick coronal slices through the forebrain, which were separated into left and right hemispheres. Each hemisphere was stained with 5 ml of 2% TTC for 90 minutes at 37°C. The tissue was rinsed with saline, and the formazan product was solubilized in 5 g of ethanol/DMSO (1:1). After a 24 h incubation in the dark, the red solvent extracts were diluted 1:20 with fresh ethanol/DMSO solvent in triplicate, absorbance was measured at 485 nm in a spectrophotometer, and the values were averaged. Percent decrease in brain TTC staining was calculated using the following equation: percent decrease = [100 – (absorbance of control hemisphere/absorbance of ischemic hemisphere) x 100]; and the values for the ischemic and control brain hemispheres in the same animal were compared.

### *5.5.7 Immunocytochemistry and TUNEL assay*

Perfused brains were postfixed for 24 hours in 3.7% paraformaldehyde in 10 mM PBS and cryoprotected in 20% sucrose solution in 10 mM PBS containing 0.001% sodium azide. Serial coronal sections (10 μm thick) were cut with a cryostat (Leica Microsystems Inc.). Neuronal apoptotic-like death was confirmed in fixed tissue by reaction for TUNEL (Roche Diagnostics Corp.) and immunolabeling for the neuronal nuclear marker NeuN (1:100; Chemicon) using a Cy3-conjugated anti-mouse IgG secondary antibody (1:800; Jackson ImmunoResearch Laboratories Inc.) as described (Melanson-Drapeau et al., 2003). Antibodies were diluted in antibody

buffer (10 mM PBS, 0.3% Triton X-100, and 3% BSA). Sections were mounted in Vectashield (Vector Laboratories) and analyzed with a Leica DMRXA2 epifluorescent microscope equipped with a Hamamatsu ORCA-ER digital camera and OpenLab 3.17 software (Improvision). The total number of NeuN-positive cells and the number of NeuN-positive/TUNEL-positive cells were counted and tissue area was measured using the Advanced Measurements Module of OpenLab 3.17 in two adjacent sections of striatum and cortex from both ischemic and control hemispheres. Means were averaged across treatment groups.

### *5.5.8 Statistical analysis*

Statistical analysis was performed as described in Section 2.5.11.

## 5.6 Results

Mice pretreated with either vehicle or NFV/RIT by oral gavage every 8 h for a total of 24 h followed by either sham or MCAO surgery were assessed for infarct size, neuronal apoptosis, and behavioural impairment.

### *5.6.1 NFV pretreatment decreases infarct size following MCAO as assessed by TTC staining*

Infarct size in the striatum and cortex was assessed by measuring cell viability with TTC staining. Sham-operated mice did not show a decrease in TTC staining between hemispheres (Figure 5.1). After 1 h of MCAO and 24 h of reperfusion, mice that received either vehicle pretreatments or no pretreatment exhibited a 34% decrease in TTC staining in the ischemic hemisphere as compared

**Figure 5.1: NFV reduces infarct size following 1 h of MCAO and 24 h of reperfusion.** (A) Schematic representation of coronal forebrain sections analyzed. Infarct and control hemispheres analyzed by TTC, are indicated in blue. Areas analyzed for NeuN and TUNEL reactivity (see Figure 5.2) are indicated in orange. (B) The infarct size, reflective of the difference in TTC staining between the infarct and control hemispheres, was expressed as % decrease in TTC staining. Following 1 h MCAO and 24 h reperfusion, mice pretreated with NFV/RIT exhibited a smaller infarct (smaller % decrease in TTC staining) relative to mice pretreated with vehicle or untreated mice (* $p<0.05$, Student's *t* test). Number of mice and % decrease in TTC staining in individual mice are indicated for each treatment group (open circles, no pretreatment; closed circles, vehicle pre-treatment; closed squares, NFV/RIT pre-treatment). Sham-operated animals did not show any % decrease in TTC staining. Data were expressed as the mean $\pm$ SEM.

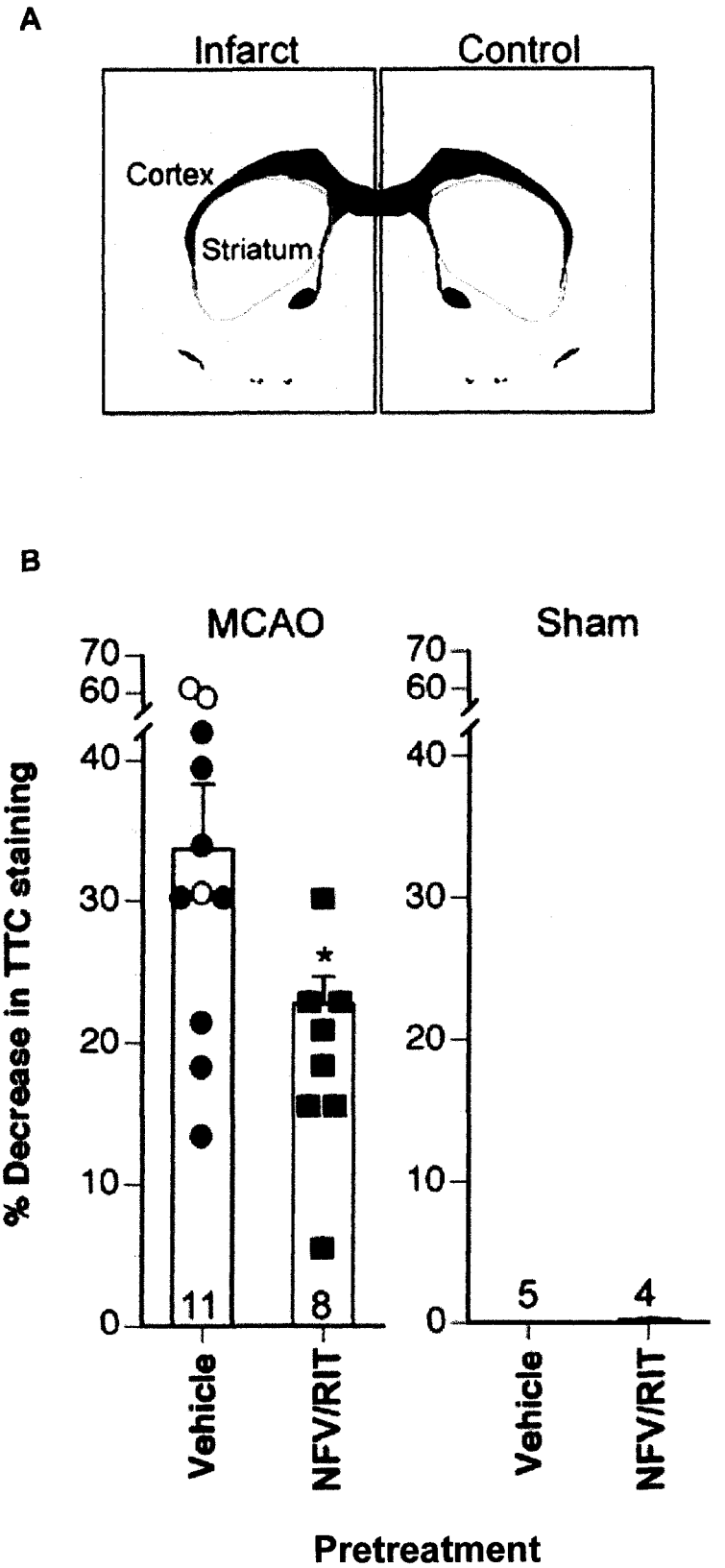


Figure 5.1

to the control hemisphere, while mice in the NFV/RIT pretreatment group showed a 23% decrease in TTC staining in the ischemic hemisphere as compared to the control hemisphere (Figure 5.1). This indicated that pretreatment with NFV/RIT decreased the size of the infarct induced by MCAO.

### *5.6.2 NFV pretreatment protects neurons from apoptotic-like death following MCAO*

Neuronal number in the striatum was assessed by immunodetection of the neuron-specific marker NeuN. Sham-operated mice did not show a difference in neuronal number between hemispheres regardless of pretreatment (Figure 5.2). Both vehicle- and NFV/RIT-treated animals exhibited comparable neuronal loss following 1 h of MCAO and 24 h of reperfusion as shown by approximately 20% loss of NeuN-positive neurons in the ischemic hemisphere as compared to the control hemisphere (Figure 5.2 A,B). However, NFV/RIT pretreatment significantly reduced apoptotic-like death following 1 h of MCAO and 24 h of reperfusion as detected by TUNEL/NeuN double labeling (Figure 5.2 A,C). In vehicle-treated mice, 67% of the remaining NeuN-positive neurons in the striatum were TUNEL-positive, while only 24% of NeuN-positive neurons were TUNEL-positive in NFV/RIT-treated mice (Figure 5.2 C).

### *5.6.3 NFV/RIT pretreatment improves neurological recovery following MCAO*

To determine whether the neuroprotection afforded by NFV/RIT pretreatment manifested in improved behavioural recovery, neurological deficits in motor function were assessed using an expanded 6-point scale (see section 5.5.4). Mice were tested 0.5 h after surgery and again following 24 h of reperfusion. Sham-operated

**Figure 5.2: NFV protects neurons from apoptotic-like death following 1 h of MCAO and 24 h of reperfusion.** (A) Representative digital photos of coronal forebrain sections analyzed for NeuN immunoreactivity and TUNEL reactivity from mice pretreated with either NFV/RIT or vehicle and subjected to 1 h MCAO and 24 h reperfusion. The areas of neuronal damage in the infarct hemispheres are outlined in white. Loss of NeuN-positive neurons following 1 h of MCAO and 24 h of reperfusion was comparable between vehicle and NFV/RIT treatments. In remaining neurons, vehicle-treated mice exhibited apoptotic-like death as detected by TUNEL that also expanded the area of tissue damage (hatched area). Mice pretreated with NFV/RIT displayed little to no TUNEL-positive cells. (B) Quantitation of neuronal loss following 1 h MCAO or sham surgeries and 24 h reperfusion was expressed as number of NeuN-positive neurons / 0.1 $mm^2$. No difference was detected between sham-operated mice pretreated with either NFV/RIT or vehicle so these data were combined for statistical analysis. Both vehicle and NFV/RIT-treated mice exhibited a comparable reduction in neuronal number in the infarct hemisphere following MCAO as compared to the control hemisphere (~ $p=0.08$, * $p<0.05$, ANOVA, *post-hoc* Dunnett's *t* test). Number of mice is indicated for each treatment group. Data were expressed as the mean $\pm$ SEM. (C) Quantitation of TUNEL-positive neurons following 1 h MCAO or sham surgeries and 24 h reperfusion was expressed as % apoptotic. Sham-operated mice did not display any apoptotic-like death. The majority of remaining NeuN-positive cells in vehicle-treated mice were undergoing apoptotic-like death, while TUNEL reactivity was significantly reduced in NFV/RIT-treated mice (** $p<0.01$, ANOVA, *post-hoc* Dunnett's *t* test). Number of mice is indicated for each treatment group. Data were expressed as the mean $\pm$ SEM.

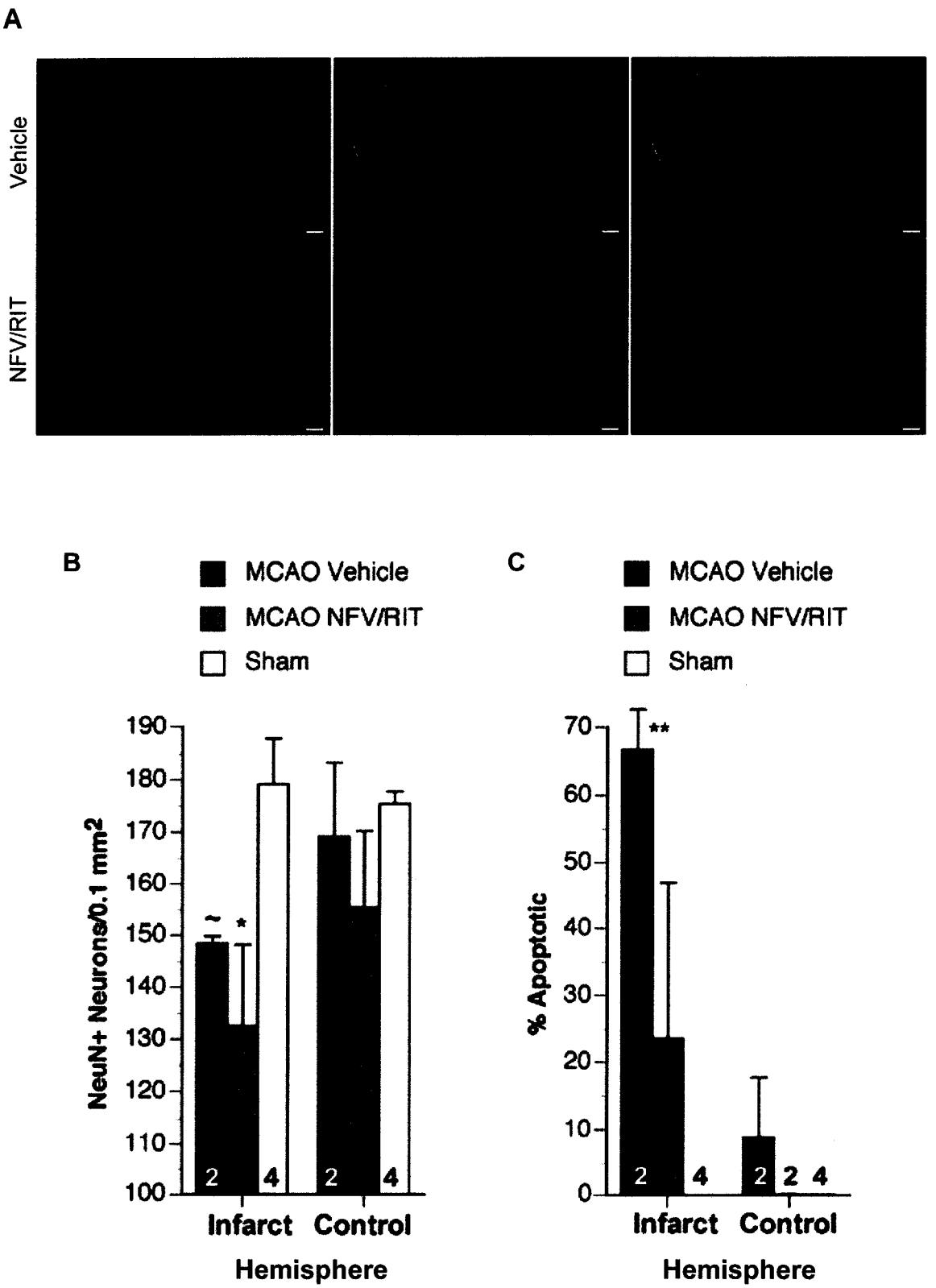


Figure 5.2

mice did not show any motor deficits (Figure 5.3). All MCAO-operated mice exhibited comparable motor deficits 0.5 h after surgery regardless of pretreatment (Figure 5.3). However, behavioural improvement 24 h after MCAO was evident in NFV/RIT-treated mice, while vehicle-treated mice did not show a significant change in behavioural score relative to the 0.5 h timepoint (Figure 5.3). The ability of NFV/RIT to protect neurons was consistent with the reduced infarct size and reduction in neuronal apoptotic loss.

## 5.7 Discussion

The overarching objectives of this thesis were to determine how PAF triggers neuronal loss in human neurons that do not express PAFR and to identify compounds capable of inhibiting this death *in vivo*. To this end, the focus of this chapter was to establish whether a lead compound identified in Chapter 4 (NFV) could reduce neuronal death *in vivo* in a preclinical model of ischemia. NFV was prioritized as it has clinical approval for human therapeutics in HIV and had been shown to elicit a substantial reduction in apoptosis and the improvement in survival in other *in vivo* models of apoptosis as assessed by collaborators of the Bennett laboratory (presented in (Weaver et al., 2005)). As such, NFV represented a "lead" candidate for *in vivo* studies.

Cerebral ischemia is a neuronal model of apoptotic disease leading to the activation of $PLA_2$ and the subsequent induction of pathophysiological PAF production, resulting in neuronal death (Bazan, 1998; Farooqui et al., 2004). Thus, it is likely that NFV/RIT could inhibit mitochondrial-mediated apoptosis triggered by PAF as part of the cascade of neuronal death following ischemia as well as through

**Figure 5.3: NFV improves neurological recovery following 1 h of MCAO and 24 h of reperfusion.** Mice evaluated for TTC staining (Figure 5.1) were also tested for motor deficits using a modified six point scale and results were expressed as behavioural impairment. (A) Representative photos of mice displaying a behavioural score of (a) 1, (b) 2, and (c) 3, as described in Section 5.5.4. (B) Sham-operated mice did not display any behavioural impairment. Mice pretreated with NFV/RIT or vehicle showed equivalent motor deficits when tested at 0.5 h of reperfusion. After 24 h of reperfusion, NFV/RIT-pretreated mice exhibited significant behavioral improvement relative to 0.5 h of reperfusion or to vehicle-treated cells (* $p<0.05$; ** $p<0.01$, ANOVA, *post-hoc* Tukey). Number of mice is indicated for each treatment group. Data were expressed as the mean $\pm$ SEM.

A

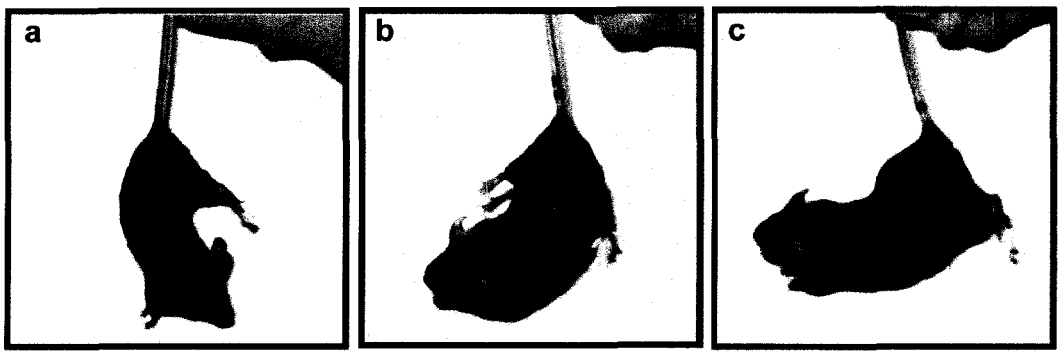


B

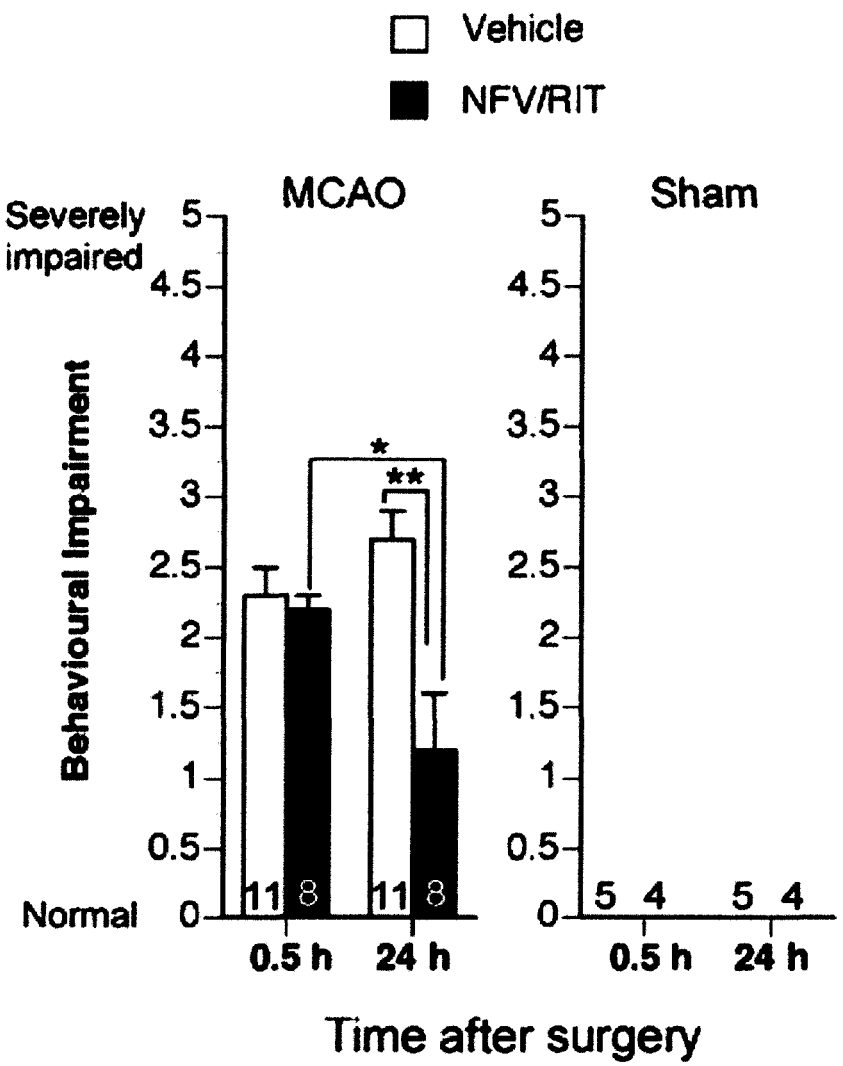


Figure 5.3

other excitotoxic mechanisms. These studies were initiated prior to the complete elucidation of the PAF death cascade in human neurons (Chapters 2 and 3). Given the findings of Kroemer's group indicating that NFV inhibited mitochondrial-mediated apoptosis activation (Phenix et al., 2001; Weaver et al., 2005) it is likely that NFV only participates in reducing the secondary mitochondrial effects triggered by the PAF apoptotic cascade identified in Chapters 2 and 3 as well as inhibiting mitochondrial permeability transition induced by the excitotoxic component of ischemic death. These findings also help to reconcile the partial protection conferred by NFV against PAF-induced cell death observed in Chapter 4. Nevertheless, this chapter represents a first step forward in testing our basic investigations focused on mechanisms underlying neurodegenerative cell death in pre-clinical models of human disease with the ultimate goal of developing new therapeutic strategies to treat brain injury.

With this goal in mind, RIT was chosen to supplement NFV *in vivo* but not *in vitro* to increase bioavailablity. Since the cytochrome P450 enzyme system can convert PIs into their metabolites, which may not retain their PI activity, inhibition of cytochrome P450 enzymes will increase the bioavailability of the PI (Ahonen et al., 1995; Aranko et al., 1994; Bailey et al., 1996). The PI RIT is known to inhibit CYP3A4, a cytochrome P450 isoform largely responsible for PI metabolism (Bailey et al., 1993; Edwards and Bernier, 1996; Erickson, 2001; Phenix et al., 2002). Therefore, when co-administered with other PIs, RIT is able to increase their bioavailability. It is for this reason that NFV was boosted with RIT for the PI pretreatment in this study. It is worthy to note that in an experiment performed by collaborators of the Bennett laboratory, anti-Fas-treated mice pretreated with either

vehicle control or RIT alone died in a dose dependent manner, while mice pretreated with NFV/RIT displayed superior survival as compared to controls (Weaver et al., 2005). This indicated that NFV, and not RIT, was responsible for the observed improvement in survival.

### *5.7.1 NFV/RIT protects neurons from apoptosis in vivo following MCAO*

Here, it is shown that NFV/RIT pretreatment reduced the infarct size following MCAO-induced ischemic injury in the mouse. Although NFV/RIT did not affect the initial necrotic neuronal loss in the ischemic core and, thus, did not improve behavioural indices when mice were tested after recovery from the anesthetic (0.5 h after the 1 h occlusion), NFV/RIT did significantly reduce subsequent apoptotic-like neuronal death observed over the 24 h reperfusion period, markedly improving neurological scores as a consequence.

The ability of PIs to inhibit apoptosis is not without controversy; for a review, see (Phenix et al., 2002). While some have demonstrated the ability of PIs to inhibit apoptosis in HIV-negative cells, others have reported that anti-apoptotic activity is limited to HIV-infected cells. In contrast, some have shown that PIs do not have any effect on apoptosis and others claim that PIs can actually enhance apoptosis. However, the ability of PIs to inhibit apoptosis as shown in this chapter is consistent with previous studies in which treatment with the PIs NFV and saquinavir significantly reduced the spontaneous apoptosis observed in $CD4^+$ and $CD8^+$ T cells in PI therapy-naive HIV-infected patients (Phenix et al., 2000). The ability of NFV to inhibit apoptosis in HIV-negative patients was also recently shown. $CD4^+$ and $CD8^+$ T cells taken from HIV-negative patients prior to, during, and following treatment with

the PIs NFV and combivir did not show any changes, indicating the safety of PIs in non-HIV patients (Cooper et al., 2004). The susceptibility of these $CD4^+$ and $CD8^+$ T cells to *in vitro* apoptosis was significantly inhibited by PI therapy (Cooper et al., 2004).

As described in (Weaver et al., 2005), the effect of NFV/RIT in two other *in vivo* models of apoptosis was investigated by collaborators of the Bennett laboratory in combination with the MCAO study described above. The first model was Fas-induced fatal hepatitis in the mouse by Jo-2 anti-Fas antibody treatment. NFV/RIT pretreatment (24 h) increased % survival of mice, decreased hepatocyte apoptosis as measured by TUNEL, and decreased biochemical and histological evidence of hepatitis. While Jo-2-induced mortality occurred within 72 h, mice pretreated with NFV/RIT survived for 30 days, indicating that NFV/RIT can offer long-term prevention from, rather than delay of, Jo-2-induced death. In the second *in vivo* model of apoptosis, mice were treated with *Staphylococcal enterotoxin B* (SEB), which results in shock and the selective apoptosis of V-β8–positive T cells (Jiang et al., 1995). NFV/RIT prevented apoptosis of Vβ8-positive T cells as measured by TUNEL. SEB injection can also result in death when coadministered with D-galactosamine (D-gal) (Aoki et al., 1995; Miethke et al., 1992). The % survival of SEB/D-gal-treated mice was improved by NFV/RIT pretreatment (24 h) and by treatment with NFV/RIT 4 h following SEB/D-gal treatment, indicating that NFV/RIT can be administered after the apoptosis-initiating event. Although the maximum duration between apoptotic insult and NFV/RIT administration that is still associated with improved outcome remains to be defined, these observations provide

compelling evidence that NFV might afford clinically useful protection from apoptosis-related disease.

### *5.7.2 Anti-apoptotic mechanism of NFV in vitro*

Previously, the anti-apoptotic ability of PIs has been linked to a variety of mechanisms, including caspase inhibition, calpain inhibition, enhanced proliferation, and prevention of $\Delta\Psi_m$ loss (for a review, see (Badley, 2005)). It has recently been demonstrated that the anti-apoptotic mechanism of NFV works through the preservation of mitochondrial integrity, preventing the release of pro-apoptotic factors and subsequent caspase activation (Phenix et al., 2001; Weaver et al., 2005). Using Jurkat T cells, hepatocytes from Jo-2-treated mice, and proteoliposomes reconstituted with PTPC subunits, it was shown that NFV acts to block apoptosis by specifically inhibiting the pore function of the ANT subunit of the PTPC, thus preventing $\Delta\Psi_m$ collapse, cytochrome *c* release, caspase-9 cleavage, and caspase-3 cleavage and activation (Weaver et al., 2005).

### *5.7.3 NFV as a therapeutic target for PAF-related neuronal apoptosis disease states*

Since multiple apoptotic signals converge upon mitochondria, drugs that target mitochondrial regulators of apoptosis, such as NFV, are attractive therapeutic candidates. As described in Chapter 2, the mitochondrial effects seen in PAF-induced apoptosis in hNTs, specifically cytochrome *c* release resulting in caspase-9 activation, are secondary to the ER-related pathway initiated by PAF. While it is

possible that PAF altered $\Delta\Psi_m$ in hNTs, Chapter 3 suggested that this effect is most likely due to ROS production. Despite these findings, NFV did offer protection from PAF neurotoxicity in hNTs that approached significance leading to the hypothesis that NFV can protect neurons from PAF-induced mitochondrial changes elicited downstream of the primary ER stress pathway. To directly test this hypothesis, studies should be performed to establish whether NFV blocks PAF induction of caspase-9 activity observed 24 h after PAF exposure.

The classification of NFV as a drug to treat HIV infection and, in this thesis, a drug to protect neurons from PAF-induced toxicity, may not be coincidental. HIV-dementia is a neurodegenerative condition that occurs when HIV-infected perivascular macrophages and microglia cause neuronal apoptosis by producing neurotoxic compounds (Gonzalez-Scarano and Martin-Garcia, 2005; Mattson et al., 2005). PAF is known to be a proinflammatory mediator synthesized by and released from microglia, and is hypothesized to be a primary mediator of neuronal death in HIV-dementia (Perry et al., 1998). Furthermore, the HIV protein Tat, which is also produced by HIV-infected microglia, can stimulate microglial production of the proinflammatory cytokine TNFα, that can subsequently stimulate further PAF release (Tong et al., 2001). These data substantiate the finding that the HIV PI NFV can offer neuroprotection from PAF-induced apoptosis in neurodegenerative disorders. In addition, the ability of NFV to promote behavioural recovery in a mouse model of cerebral ischemia as shown in this thesis indicates that NFV could offer protection from the neuronal apoptotic pathways that can occur in HIV-dementia.

The studies described in this chapter provided the basis for evaluation of a PAF inhibitor to inhibit apoptosis in a neuronal disease state characterized by

excessive apoptosis. The neuroprotective ability of NFV against PAF- and Aβ-induced toxicity (Chapter 4), and against ischemia-induced neuronal apoptotic-like death described here, together indicate that NFV may be beneficial in reducing neuronal loss in AD. Similar *in vivo* studies in mouse models of AD and other neurodegenerative disease states carried out with PAF inhibitors that offered more significant *in vitro* protection of human neurons from PAF than NFV, such as RP59227, will offer intriguing results and preclinical assessment of potential novel therapies.

### *5.7.4 Summary*

In summary, these studies have shown that NFV, boosted with RIT, can act as an *in vivo* inhibitor of neuronal apoptosis following the MCAO model of focal ischemia in the mouse. NFV/RIT reduced infarct size, inhibited neuronal apoptosis, and improved behavioural recovery. This neuroprotective capacity of NFV/RIT indicates that NFV and other PAF inhibitors have the potential to protect neurons *in vivo* from apoptotic damage in other apoptosis-related neuronal disease states such as AD.

# Chapter 6: General Conclusion: Platelet activating factor in neuronal apoptosis and neurodegenerative disease

## 6.1 Hypothesis and Objectives

This thesis was driven by the hypothesis that PAF-mediated, PAFR-independent signalling underlies, in part, neurotoxicity under multiple pathological conditions and can be targeted *in vitro* and *in vivo* to protect neurons from apoptosis associated with neurodegenerative disease. In order to test this hypothesis, the PAFR-independent neurotoxic pathway induced by PAF in human neurons was delineated (Chapters 2,3), a panel of known PAF inhibitors and potential PAF inhibitors was screened for their ability to protect against PAF- and Aβ -induced neurotoxicity in human neurons (Chapter 4), and the ability of a PAF inhibitor to protect from neurotoxicity and behavioural impairment was tested *in vivo* in a mouse model of focal ischemia (Chapter 5).

## 6.2 A novel PAF-induced human apoptotic pathway relevant to AD

This thesis is the first study to show that PAF elicits apoptosis in the absence of PAFR in human neurons. The implications of describing a PAF-mediated, PAFR-independent apoptotic pathway in human neurons are controversial. Since PAF effects have historically been assumed to be initiated through PAFR (Ishii and Shimizu, 2000), these findings emphasize the reassessment of the role of PAFR in both *in vitro* and *in vivo* models and the contribution of PAF synthesis in neurological disease. Moreover, these findings provide partial explanation as to why PAF-targeted strategies focused on PAFR have met with limited clinical success and suggest a new direction for potential study.

Here, the NT2/hNT human neuronal model was used to investigate the neurotoxic effects of PAF. While both undifferentiated NT2 neural progenitors and terminally differentiated hNT neurons do not express PAFR, only hNTs were sensitive to PAF-induced toxicity (Figures 2.2, 2.3). Using this model, caspase-mediated apoptosis instigated by PAF was re-evaluated. Studies on the role of caspases in PAF signalling have offered contradictory results (Bate et al., 2004c; Beauchamp et al., 2002; Bonin et al., 2004; Hostettler et al., 2002; Ma and Bazan, 2001; Wu et al., 2003). While caspase activity has been indirectly linked to PAF signalling in neurons, this is the first study to directly measure caspase activation as a result of PAF administration in the absence of PAFR in human neurons. Caspase activity assays were used to determine that PAF induces caspase-2 activation early in the human neuronal apoptotic cascade, leading to downstream caspase-9 and caspase-7 activation (Chapter 2). PAF was shown to induce ER stress early in the apoptotic pathway, as measured by an increase in BiP expression, and ER-mitochondrial cross-talk led to downstream mitochondrial effects such as cytochrome *c* release, ROS production, possible changes in $\Delta\Psi_m$, and an increase in UCP2 expression (Chapters 2 and 3). Translocation of the caspase-independent mitochondrial apoptosis regulators AIF and endoG was not observed in this pathway (Chapter 3). While PAF has been previously shown to be involved in mitochondrial-mediated apoptosis (Bazan et al., 2002; Lu et al., 2004; Ma and Bazan, 2001; Wu et al., 2003), the role of PAF in ER apoptotic signalling represents a novel finding.

Aβ has been shown to induce various components of neuronal apoptotic pathways *in vitro*, resulting in caspase activation, dissipation of $\Delta\Psi_m$, ROS

production, alteration of $Ca^{2+}$ homeostasis, chromatin condensation, nuclear damage and DNA fragmentation (Eckert et al., 2003). In addition, postmortem analysis of brain tissue has shown an elevation of DNA fragmentation and caspase expression in AD brain, indicative of apoptosis (Colurso et al., 2003; Pompl et al., 2003). It has been recently suggested that pathways involving both mitochondrial dysfunction and ER stress are fundamental to neuronal apoptosis in AD (Takuma et al., 2005). A number of studies have implicated mitochondrial-mediated apoptosis and mitochondrial dysfunction in AD. The presence of glutamate receptors and $Ca^{2+}$ channels at pre- and post-synaptic membranes results in a high ATP demand (Eckert et al., 2003). To quickly provide high levels of ATP, mitochondria are also concentrated at neuronal synapses and play a key role in synaptic function (Eckert et al., 2003). Since synapses have been postulated to be the location where the neurodegeneration in AD is triggered (Selkoe, 2002), it is likely that mitochondria are involved in the initiation of this detrimental process. A reduction in the activity of cytochrome oxidase (COX), also known as complex IV in the electron transport chain, has been described in the hippocampus of AD patients (Ojaimi and Byrne, 2001). The catalytic COX subunits are encoded by the mtDNA (Eckert et al., 2003). When NT2 mtDNA was replaced with mtDNA from AD patients, the resulting cybrids showed a decrease in COX activity, ATP production, and an increase in ROS compared with cybrids expressing mtDNA from age-matched controls (Cardoso et al., 2004). In addition, the AD cybrids displayed a greater dissipation in $\Delta\Psi_m$ and release of cytochrome *c* than control cybrids upon $A\beta_{1-40}$ administration (Cardoso et al., 2004). Using human primary neurons derived from fetal brain tissue, Aβ was

delivered intracellularly by microinjection and shown to induce Bax-mediated neurotoxicity, an event known to promote cytochrome *c* release (Zhang et al., 2002).

Recent studies have suggested that neurotoxicity induced by Aβ involves ER stress-induced cell death, including ER caspase activation and the dysregulation of $Ca^{2+}$ homeostasis (Katayama et al., 2004; Mattson, 2004). Presenilin-1 (PS1) is an integral membrane protein primarily localized to the ER membrane, and is a component of the γ-secretase complex (Mattson, 2000). PS1 mutations that have been associated with familial forms of AD increase the production of Aβ, activate ER-mediated apoptotic signalling, and enhance the vulnerability of neurons to apoptosis and excitotoxicity by increasing intracellular $Ca^{2+}$ levels (Lleo et al., 2004; Mattson, 2000; Mattson, 2004; Takuma et al., 2005). In primary mouse neurons, Aβ caused caspase-12 activation, while caspase-$12^{-/-}$ neurons exhibited partial protection from Aβ toxicity (Nakagawa et al., 2000). Aβ has also been shown to induce neurotoxicity through ER stress triggered by $Ca^{2+}$ release from the ER (Suen et al., 2003; Takuma et al., 2005). APP can be localized either at the cell surface or intracellularly, within the ER and Golgi membranes (Mattson, 2004). Aβ can therefore be synthesized and accumulate within the ER, allowing for the direct initiation of ER stress and ER-mediated apoptotic pathways (Takuma et al., 2005).

The PAF-induced neuronal apoptotic pathway described in this thesis (Figure 6.1) reflects the mechanism of neuronal loss in AD. Both models of neurotoxicity involve ER stress, mitochondrial dysfunction including ROS production and cytochrome *c* release, caspase activation, and DNA fragmentation. Such convergence indicates that PAF and Aβ activate a similar neuronal apoptotic pathway. These findings provide compelling evidence that these two endogenous

**Figure 6.1: Pathways of PAF-induced neuronal cell death in the absence of PAFR.** The results described in this thesis are summarized in this model figure. In PAFR-negative human neurons, PAF is toxic and generates DNA fragmentation. The primary cell death pathway initiated by PAF signals through the ER stress pathway. PAF induces BiP expression and activates caspase-2 that, in turn, activates caspase-3/7. In addition, PAF induces mitochondrial effects downstream of the ER stress pathway, namely cytochrome *c* release, caspase-9 activation, ROS production and UCP2 expression. ER-mitochondrial cross-talk is apparent by the requirement of caspase-2 to activate caspase-9, and may also occur through Ca2+ signalling or Bcl-2 family members. Other potential mitochondrial effects of PAF in human neurons include changes in $\Delta\Psi_m$ and the opening of the PTPC. The extrinsic apoptotic pathway and the release of AIF or endoG from the mitochondria are not involved in PAF-induced apoptosis in human neurons. The group of tested compounds that protect human neurons from PAF and/or Aβ-induced toxicity consists of ONO-6240, RP59227, hesperetin, quercetin, and NFV.

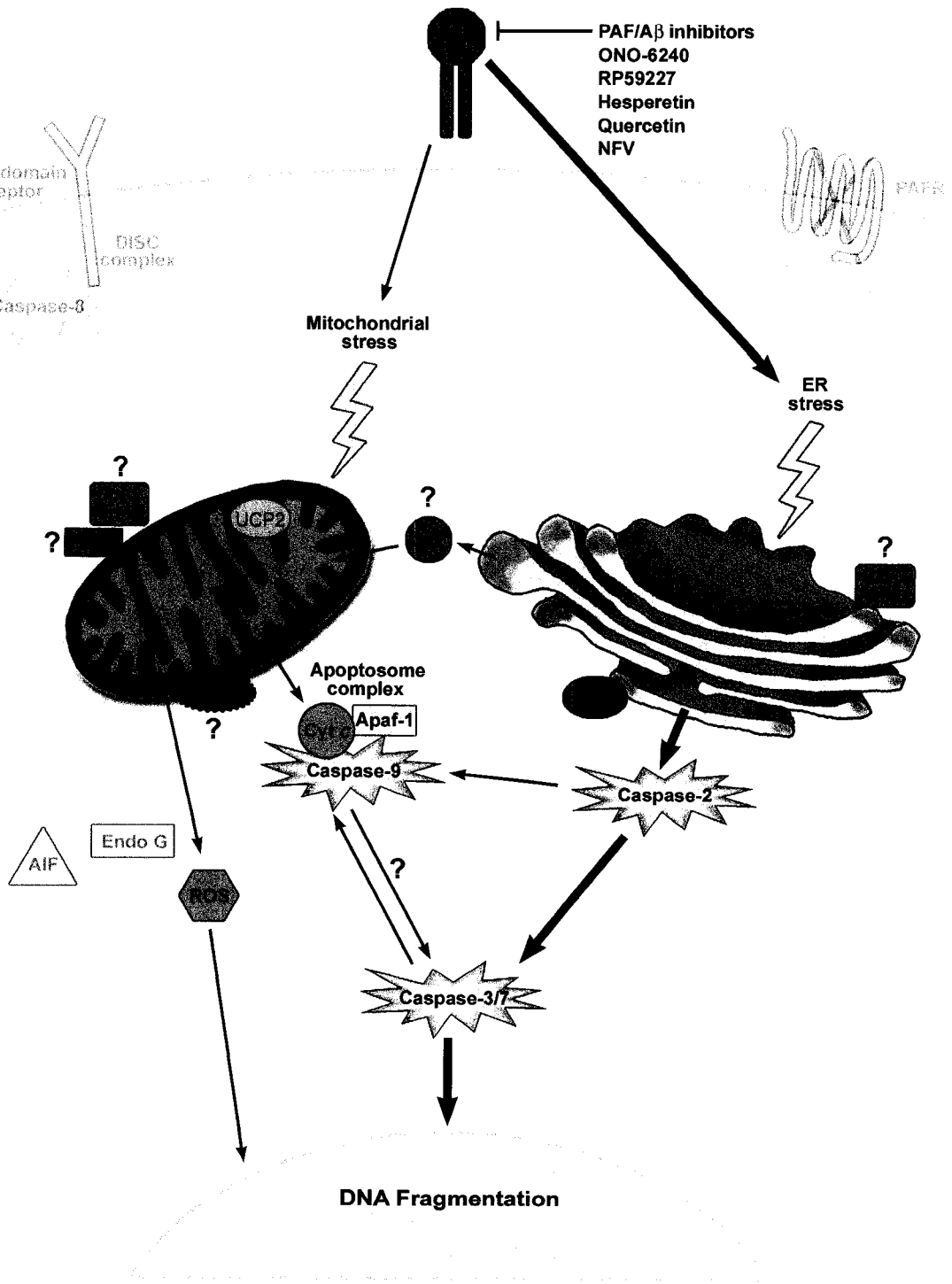


Figure 6.1

neurotoxic agents likely cooperatively induce neuronal loss in AD given increased glycerophospholipid production across the etiology of AD.

## 6.3 The role of UCP2 in PAF-induced, PAFR-independent neuronal apoptosis

Analogous to PAF, the function of UCP2 defines a paradox whereby UCP2 expression has been described as protective in models of neurodegeneration (Andrews et al., 2005; Clavel et al., 2003; Diano et al., 2003; Mattiasson et al., 2003), but can also directly contribute to human cell death (Mills et al., 2002). Here, the involvement of UCP2 in PAF signalling was investigated. The implications of UCP2 upregulation in hNTs following PAF treatment (Chapter 3) was further investigated by my colleagues in the Bennett laboratory by the production of $PAFR^{-/-}$ /$UCP2^{+/+}$ and $PAFR^{-/-}$/$UCP2^{-/-}$ mice. Surprisingly, $PAFR^{-/-}$/$UCP2^{-/-}$ CGNs were not susceptible to PAF neurotoxicity (Appendix 3), indicating a controversial neurotoxic role for UCP2. The lack of neuronal death in the $PAFR^{-/-}$/$UCP2^{-/-}$ CGNs suggests that UCP2 is a crucial mediator of the PAF-induced, PAFR-independent neuronal apoptotic pathway.

## 6.4 Targeting PAF signalling to protect neurons in models of neurodegeneration

Both natural and synthetic compounds have been indirectly shown to have anti-apoptotic effects and/or protect from PAF toxicity, but this is the first study to directly assess the ability of these compounds to inhibit PAF-induced neurotoxicity, in the absence of PAFR. A panel of either known or suspected PAF inhibitors was

screened for their ability to protect human neurons from PAF and Aβ administration. It was found that known synthetic PAF inhibitors (ONO-6240 and RP59227), natural plant-derived phenolic compounds (hesperetin and quercetin), and an HIV-PI (NFV) exhibited neuroprotective abilities against PAF and/or Aβ (Chapter 4). The finding that compounds can protect neurons from both PAF and Aβ strengthens the hypothesis that PAF and Aβ are components of an integrated apoptotic pathway in AD. To link PAF's role in neurodegenerative disorders such as AD, cerebral ischemia and HIV dementia, it was demonstrated that the HIV PI NFV can protect human neurons *in vitro* from Aβ-induced neurotoxicity (Chapter 4), and can protect mouse neurons and improve behavioural recovery in an *in vivo* model of cerebral ischemia (Chapter 5).

Arguably, the implications of the pharmacological results in hNTs will initiate the reassessment of the mechanism of action of these compounds. Many known PAF inhibitors were discovered to have PAF effects through their ability to displace PAF from PAFR or to inhibit PAFR signalling (Marcheselli et al., 1990). Since this thesis and other findings from the Bennett lab (Bonin et al., 2004; Brewer et al., 2002) have now shown that some of these PAF inhibitors inhibit PAF-mediated PAFR-independent signalling through diverse mechanisms, the possibility that multiple PAF signal transduction pathways can be targeted pharmacologically will enable a dissection of the events underling human neuronal loss associated with elevated PAF production.

### *6.4.1 Validity of rodent models of neurodegenerative disorders associated with PAF*

This thesis also underlines the importance of validating rodent results in human *in vitro* model systems. For example, BN52021, or ginkgolide B, exhibited enormous potential as a therapeutic agent due to its neuroprotection in rodent models, that led to clinical trials for the treatment of memory loss and dementia in AD (Le Bars et al., 1997; Le Bars et al., 2000; van Dongen et al., 2003; van Dongen et al., 2000; Wettstein, 2000). However, these clinical trials did not translate into therapeutic benefit. The inability of BN52021 to protect human neurons from either PAF or Aβ-induced toxicity in the absence of PAFR as described in this thesis (Chapter 4) offers an explanation to why these clinical trials did not produce positive results. Considering our unpublished data that neurons in the hippocampus of rodent AD models express PAFR, compared to the PAFR-negative neurons in human hippocampus during AD (Appendix 1), BN52021 is most likely only neuroprotective in the presence of PAFR, such as in rodent models, and is not effective in protecting PAFR-negative neurons in human AD hippocampus. In proposing new therapies for neurodegenerative disease, the results presented in this thesis demonstrate the importance of testing not only *in vivo* using animal models, but also *in vitro* using human cells prior to moving into clinical trials.

## 6.5 Future directions

With further investigation, other components of the PAF-induced human neuronal apoptotic pathway in the absence of PAFR can be defined. Additional molecules most likely to be involved in this pathway are the Bcl-2 family members. Not only are they localized to and function in both the mitochondria and the ER, but

Bcl-2 family members also provide a mechanism of ER-mitochondrial cross-talk during apoptotic signalling (Walter and Hajnoczky, 2005). Other potential links in the pathway for future study include mitochondrial-related effects such as $\Delta\Psi_m$ as measured by TMRM or JC-1, ER-related molecules such as calpains and $Ca^{2+}$, and putative PAF binding proteins localized either at the plasma membrane or intracellularly that could initiate the novel PAFR-independent apoptotic pathway.

Aside from NFV, several potential therapeutic agents targeting PAF and/or Aβ signalling have been identified in this study, as described above. The PAFR-independent mechanism of action of these compounds in the protection of human neurons from PAF and/or Aβ should be delineated *in vitro* by testing the inhibition of caspase activation and mitochondrial and ER effects. As a first step towards clinical applications, these agents should be tested *in vivo* in PAFR-negative mouse models of AD and other *in vivo* models of neurodegenerative disorders, such as the MCAO model of focal ischemia.

## 6.6 Summary

In summary, this thesis has delineated a novel PAF-mediated pathway of PAFR-independent apoptosis in human neurons, and provided evidence that inhibiting PAF signalling may still be therapeutically applicable to neurodegenerative disorders such as AD and stroke despite failure of earlier clinical trials. It is anticipated that future studies built from this thesis will lead to the further characterization of the novel apoptotic pathway relevant to these and other neurodegenerative disorders, and to the development of viable treatments for such devastating diseases.

## References


Ahonen, J., Olkkola, K. T., and Neuvonen, P. J. (1995). Effect of itraconazole and terbinafine on the pharmacokinetics and pharmacodynamics of midazolam in healthy volunteers. Br J Clin Pharmacol *40*, 270-272.

Andrews, Z. B., Horvath, B., Barnstable, C. J., Elsworth, J., Yang, L., Beal, M. F., Roth, R. H., Matthews, R. T., and Horvath, T. L. (2005). Uncoupling protein-2 is critical for nigral dopamine cell survival in a mouse model of Parkinson's disease. J Neurosci *25*, 184-191.

Annunziato, L., Amoroso, S., Pannaccione, A., Cataldi, M., Pignataro, G., D'Alessio, A., Sirabella, R., Secondo, A., Sibaud, L., and Di Renzo, G. F. (2003). Apoptosis induced in neuronal cells by oxidative stress: role played by caspases and intracellular calcium ions. Toxicol Lett *139*, 125-133.

Aoki, Y., Hiromatsu, K., Kobayashi, N., Hotta, T., Saito, H., Igarashi, H., Niho, Y., and Yoshikai, Y. (1995). Protective effect of granulocyte colony-stimulating factor against T-cell-meditated lethal shock triggered by superantigens. Blood *86*, 1420-1427.

Aranko, K., Luurila, H., Backman, J. T., Neuvonen, P. J., and Olkkola, K. T. (1994). The effect of erythromycin on the pharmacokinetics and pharmacodynamics of zopiclone. Br J Clin Pharmacol *38*, 363-367.

Auchampach, J. A., Pieper, G. M., Cavero, I., and Gross, G. J. (1998). Effect of the platelet-activating factor antagonist RP 59227 (Tulopafant) on myocardial ischemia/reperfusion injury and neutrophil function. Basic Res Cardiol *93*, 361-371.

Badley, A. D. (2005). In vitro and in vivo effects of HIV protease inhibitors on apoptosis. Cell Death Differ *12 Suppl 1*, 924-931.

Bailey, D. G., Arnold, J. M., Munoz, C., and Spence, J. D. (1993). Grapefruit juice--felodipine interaction: mechanism, predictability, and effect of naringin. Clin Pharmacol Ther *53*, 637-642.

Bailey, D. G., Bend, J. R., Arnold, J. M., Tran, L. T., and Spence, J. D. (1996). Erythromycin-felodipine interaction: magnitude, mechanism, and comparison with grapefruit juice. Clin Pharmacol Ther *60*, 25-33.

Bate, C., Reid, S., and Williams, A. (2004a). Phospholipase A2 inhibitors or platelet-activating factor antagonists prevent prion replication. J Biol Chem *279*, 36405-36411.

Bate, C., Salmona, M., and Williams, A. (2004b). Ginkgolide B inhibits the neurotoxicity of prions or amyloid-beta1-42. J Neuroinflammation *1*, 4.

Bate, C., Salmona, M., and Williams, A. (2004c). The role of platelet activating factor in prion and amyloid-beta neurotoxicity. Neuroreport *15*, 509-513.

Bazan, N. G. (1998). The neuromessenger platelet-activating factor in plasticity and neurodegeneration. Prog Brain Res *118*, 281-291.

Bazan, N. G. (2005). Lipid signaling in neural plasticity, brain repair, and neuroprotection. Mol Neurobiol *32*, 89-103.

Bazan, N. G., Palacios-Pelaez, R., and Lukiw, W. J. (2002). Hypoxia signaling to genes: significance in Alzheimer's disease. Mol Neurobiol *26*, 283-298.

Beauchamp, M. H., Marrache, A. M., Hou, X., Gobeil, F., Jr., Bernier, S. G., Lachapelle, P., Abran, D., Quiniou, C., Brault, S., Peri, K. G., *et al.* (2002). Platelet-activating factor in vasoobliteration of oxygen-induced retinopathy. Invest Ophthalmol Vis Sci *43*, 3327-3337.

Bennett, S. A., Chen, J., Pappas, B. A., Roberts, D. C., and Tenniswood, M. (1998). Platelet activating factor receptor expression is associated with neuronal apoptosis in an in vivo model of excitotoxicity. Cell Death Differ *5*, 867-875.

Bennett, S. A., Stevenson, B., Staines, W. A., and Roberts, D. C. (1995). Periodic acid-Schiff (PAS)-positive deposits in brain following kainic acid-induced seizures: relationships to fos induction, neuronal necrosis, reactive gliosis, and blood-brain barrier breakdown. Acta Neuropathol (Berl) *89*, 126-138.

Benveniste, J., Henson, P. M., and Cochrane, C. G. (1972). Leukocyte-dependent histamine release from rabbit platelets. The role of IgE, basophils, and a platelet-activating factor. J Exp Med *136*, 1356-1377.

Birkle, D. L., Kurian, P., Braquet, P., and Bazan, N. G. (1988). Platelet-activating factor antagonist BN52021 decreases accumulation of free polyunsaturated fatty acid in mouse brain during ischemia and electroconvulsive shock. J Neurochem *51*, 1900-1905.

Bonin, F., Ryan, S. D., Migahed, L., Mo, F., Lallier, J., Franks, D. J., Arai, H., and Bennett, S. A. (2004). Anti-apoptotic actions of the platelet-activating factor acetylhydrolase I alpha2 catalytic subunit. J Biol Chem *279*, 52425-52436.

Bonventre, J. V., Huang, Z., Taheri, M. R., O'Leary, E., Li, E., Moskowitz, M. A., and Sapirstein, A. (1997). Reduced fertility and postischaemic brain injury in mice deficient in cytosolic phospholipase A2. Nature *390*, 622-625.

Boss, O., Hagen, T., and Lowell, B. B. (2000). Uncoupling proteins 2 and 3: potential regulators of mitochondrial energy metabolism. Diabetes *49*, 143-156.

Boucher, S., and Bennett, S. A. (2003). Differential connexin expression, gap junction intercellular coupling, and hemichannel formation in NT2/D1 human neural progenitors and terminally differentiated hNT neurons. J Neurosci Res *72*, 393-404.

Braquet, P., and Esanu, A. (1991). New trends in PAF antagonist research: a new series of potent hetrapazine-derived PAF antagonists. Agents Actions *32*, 34-36.

Bratton, D. L. (1993). Release of platelet activation factor from activated neutrophils. Transglutaminase-dependent enhancement of transbilayer movement across the plasma membrane. J Biol Chem *268*, 3364-3373.

Bratton, D. L., Dreyer, E., Kailey, J. M., Fadok, V. A., Clay, K. L., and Henson, P. M. (1992). The mechanism of internalization of platelet-activating factor in activated human neutrophils. Enhanced transbilayer movement across the plasma membrane. J Immunol *148*, 514-523.

Breckenridge, D. G., Germain, M., Mathai, J. P., Nguyen, M., and Shore, G. C. (2003). Regulation of apoptosis by endoplasmic reticulum pathways. Oncogene *22*, 8608-8618.

Brewer, C., Bonin, F., Bullock, P., Nault, M. C., Morin, J., Imbeault, S., Shen, T. Y., Franks, D. J., and Bennett, S. A. (2002). Platelet activating factor-induced apoptosis is inhibited by ectopic expression of the platelet activating factor G-protein coupled receptor. J Neurochem *82*, 1502-1511.

Buckman, J. F., Hernandez, H., Kress, G. J., Votyakova, T. V., Pal, S., and Reynolds, I. J. (2001). MitoTracker labeling in primary neuronal and astrocytic cultures: influence of mitochondrial membrane potential and oxidants. J Neurosci Methods *104*, 165-176.

Buxbaum, J. D., Koo, E. H., and Greengard, P. (1993). Protein phosphorylation inhibits production of Alzheimer amyloid beta/A4 peptide. Proc Natl Acad Sci U S A *90*, 9195-9198.

Cardoso, S. M., Santana, I., Swerdlow, R. H., and Oliveira, C. R. (2004). Mitochondria dysfunction of Alzheimer's disease cybrids enhances Abeta toxicity. J Neurochem *89*, 1417-1426.

Chen, C., Magee, J. C., Marcheselli, V., Hardy, M., and Bazan, N. G. (2001). Attenuated LTP in hippocampal dentate gyrus neurons of mice deficient in the PAF receptor. J Neurophysiol *85*, 384-390.

Citron, M. (2002). Alzheimer's disease: treatments in discovery and development. Nat Neurosci *5 Suppl*, 1055-1057.

Clavel, S., Paradis, E., Ricquier, D., and Richard, D. (2003). Kainic acid upregulates uncoupling protein-2 mRNA expression in the mouse brain. Neuroreport *14*, 2015-2017.

Cleary, J. P., Walsh, D. M., Hofmeister, J. J., Shankar, G. M., Kuskowski, M. A., Selkoe, D. J., and Ashe, K. H. (2005). Natural oligomers of the amyloid-beta protein specifically disrupt cognitive function. Nat Neurosci *8*, 79-84.

Colurso, G. J., Nilson, J. E., and Vervoort, L. G. (2003). Quantitative assessment of DNA fragmentation and beta-amyloid deposition in insular cortex and midfrontal gyrus from patients with Alzheimer's disease. Life Sci *73*, 1795-1803.

Cooper, C. L., Phenix, B., Mbisa, G., Lum, J. J., Parato, K., Hawley, N., Angel, J. B., and Badley, A. D. (2004). Antiretroviral therapy influences cellular susceptibility to apoptosis in vivo. Front Biosci *9*, 338-341.

Cuschieri, J., Bulger, E., Garcia, I., Jelacic, S., and Maier, R. V. (2005). Calcium/calmodulin-dependent kinase II is required for platelet-activating factor priming. Shock *23*, 99-106.

Dahmer, M. K. (2005). Caspases-2, -3, and -7 are involved in thapsigargin-induced apoptosis of SH-SY5Y neuroblastoma cells. J Neurosci Res *80*, 576-583.

Darst, M., Al-Hassani, M., Li, T., Yi, Q., Travers, J. M., Lewis, D. A., and Travers, J. B. (2004). Augmentation of chemotherapy-induced cytokine production by expression of the platelet-activating factor receptor in a human epithelial carcinoma cell line. J Immunol *172*, 6330-6335.

Dawson, V. L., and Dawson, T. M. (2004). Deadly conversations: nuclear-mitochondrial cross-talk. J Bioenerg Biomembr *36*, 287-294.

de Sant' Anna, C. M. R., de Alencastro, R. B., Fraga, C. A. M., Barreiro, E. J., and da Motta Netto, J. D. (1996). Molecular modeling on platelet-activating factor (PAF) and new proposed PAF antagonists. Int J Quantum Chem *60*, 1069-1080.

DeCoster, M. A., Mukherjee, P. K., Davis, R. J., and Bazan, N. G. (1998). Platelet-activating factor is a downstream messenger of kainate-induced activation of mitogen-activated protein kinases in primary hippocampal neurons. J Neurosci Res *53*, 297-303.

Degterev, A., Boyce, M., and Yuan, J. (2003). A decade of caspases. Oncogene *22*, 8543-8567.

Diano, S., Matthews, R. T., Patrylo, P., Yang, L., Beal, M. F., Barnstable, C. J., and Horvath, T. L. (2003). Uncoupling protein 2 prevents neuronal death including that occurring during seizures: a mechanism for preconditioning. Endocrinology *144*, 5014-5021.

Dirnagl, U., Iadecola, C., and Moskowitz, M. A. (1999). Pathobiology of ischaemic stroke: an integrated view. Trends Neurosci *22*, 391-397.

Earnshaw, W. C., Martins, L. M., and Kaufmann, S. H. (1999). Mammalian caspases: structure, activation, substrates, and functions during apoptosis. Annu Rev Biochem *68*, 383-424.

Eckert, A., Keil, U., Marques, C. A., Bonert, A., Frey, C., Schussel, K., and Muller, W. E. (2003). Mitochondrial dysfunction, apoptotic cell death, and Alzheimer's disease. Biochem Pharmacol *66*, 1627-1634.

Edwards, D. J., and Bernier, S. M. (1996). Naringin and naringenin are not the primary CYP3A inhibitors in grapefruit juice. Life Sci *59*, 1025-1030.

Eischen, C. M., Kottke, T. J., Martins, L. M., Basi, G. S., Tung, J. S., Earnshaw, W. C., Leibson, P. J., and Kaufmann, S. H. (1997). Comparison of apoptosis in wild-type and Fas-resistant cells: chemotherapy-induced apoptosis is not dependent on Fas/Fas ligand interactions. Blood *90*, 935-943.

Erickson, J. (2001). HIV-1-protease as a target for AIDS therapy. In Protease Inhibitors in AIDS Therapy. Infectious Disease and Therapy, B. Cunha, ed. (New York, Marcel Dekker), pp. 1-25.

Farooqui, A. A., Ong, W. Y., and Horrocks, L. A. (2004). Biochemical aspects of neurodegeneration in human brain: involvement of neural membrane phospholipids and phospholipases A2. Neurochem Res *29*, 1961-1977.

Feuerstein, G., Yue, T. L., and Lysko, P. G. (1990). Platelet-activating factor. A putative mediator in central nervous system injury? Stroke *21*, III90-94.

Fischer, H., Koenig, U., Eckhart, L., and Tschachler, E. (2002). Human caspase 12 has acquired deleterious mutations. Biochem Biophys Res Commun *293*, 722-726.

Floch, A., Tahraoui, L., Sedivy, P., and Cavero, I. (1991). The platelet activating factor receptor antagonist, RP 59227, blocks platelet activating factor receptors mediating liberation of reactive oxygen species in guinea pig macrophages and human polymorphonuclear leukocytes. J Pharmacol Exp Ther *258*, 567-575.

Francescangeli, E., Grassi, S., Pettorossi, V. E., and Goracci, G. (2002). Activation of PAF-synthesizing enzymes in rat brain stem slices after LTP induction in the medial vestibular nuclei. Neurochem Res *27*, 1465-1471.

Frenkel, D., Huang, Z., Maron, R., Koldzic, D. N., Hancock, W. W., Moskowitz, M. A., and Weiner, H. L. (2003). Nasal vaccination with myelin oligodendrocyte glycoprotein reduces stroke size by inducing IL-10-producing CD4+ T cells. J Immunol *171*, 6549-6555.

Galli, R. L., Shukitt-Hale, B., Youdim, K. A., and Joseph, J. A. (2002). Fruit polyphenolics and brain aging: nutritional interventions targeting age-related neuronal and behavioral deficits. Ann N Y Acad Sci *959*, 128-132.

Gau, J. T., Steinhilb, M. L., Kao, T. C., D'Amato, C. J., Gaut, J. R., Frey, K. A., and Turner, R. S. (2002). Stable beta-secretase activity and presynaptic cholinergic markers during progressive central nervous system amyloidogenesis in Tg2576 mice. Am J Pathol *160*, 731-738.

Gelbard, H. A., Nottet, H. S., Swindells, S., Jett, M., Dzenko, K. A., Genis, P., White, R., Wang, L., Choi, Y. B., Zhang, D., and et al. (1994). Platelet-activating factor: a candidate human immunodeficiency virus type 1-induced neurotoxin. J Virol *68*, 4628-4635.

Gonzalez-Scarano, F., and Martin-Garcia, J. (2005). The neuropathogenesis of AIDS. Nat Rev Immunol *5*, 69-81.

Gouras, G. K., Tsai, J., Naslund, J., Vincent, B., Edgar, M., Checler, F., Greenfield, J. P., Haroutunian, V., Buxbaum, J. D., Xu, H., *et al.* (2000). Intraneuronal Abeta42 accumulation in human brain. Am J Pathol *156*, 15-20.

Graham, S. H., and Chen, J. (2001). Programmed cell death in cerebral ischemia. J Cereb Blood Flow Metab *21*, 99-109.

Hardy, J., and Selkoe, D. J. (2002). The amyloid hypothesis of Alzheimer's disease: progress and problems on the road to therapeutics. Science *297*, 353-356.

Harris, C. S., Mo, F., Migahed, L., Chepelev, L., Nozzolillo, C., Wright, J. S., Willmore, W. G., Haddad, P. S., Arnason, J. T., and Bennett, S. A. (2006). A quantitative structure-activity relationship study of the mitogenic, cytoprotective, anti-apoptotic, and cytotoxic activities of phenolic compounds. J Med Chem *(submitted)*.

Hartmann, T. (1999). Intracellular biology of Alzheimer's disease amyloid beta peptide. Eur Arch Psychiatry Clin Neurosci *249*, 291-298.

Hitomi, J., Katayama, T., Eguchi, Y., Kudo, T., Taniguchi, M., Koyama, Y., Manabe, T., Yamagishi, S., Bando, Y., Imaizumi, K., *et al.* (2004). Involvement of caspase-4 in endoplasmic reticulum stress-induced apoptosis and Abeta-induced cell death. J Cell Biol *165*, 347-356.

Ho, P. K., Jabbour, A. M., Ekert, P. G., and Hawkins, C. J. (2005). Caspase-2 is resistant to inhibition by inhibitor of apoptosis proteins (IAPs) and can activate caspase-7. Febs J *272*, 1401-1414.

Honda, Z., Nakamura, M., Miki, I., Minami, M., Watanabe, T., Seyama, Y., Okado, H., Toh, H., Ito, K., Miyamoto, T., and et al. (1991). Cloning by functional expression of platelet-activating factor receptor from guinea-pig lung. Nature *349*, 342-346.

Hostettler, M. E., Knapp, P. E., and Carlson, S. L. (2002). Platelet-activating factor induces cell death in cultured astrocytes and oligodendrocytes: involvement of caspase-3. Glia *38*, 228-239.

Imoto, K., Kukidome, D., Nishikawa, T., Matsuhisa, T., Sonoda, K., Fujisawa, K., Yano, M., Motoshima, H., Taguchi, T., Tsuruzoe, K., *et al.* (2006). Impact of mitochondrial reactive oxygen species and apoptosis signal-regulating kinase 1 on insulin signaling. Diabetes *55*, 1197-1204.

Ishii, S., and Shimizu, T. (2000). Platelet-activating factor (PAF) receptor and genetically engineered PAF receptor mutant mice. Prog Lipid Res *39*, 41-82.

Ivins, K. J., Thornton, P. L., Rohn, T. T., and Cotman, C. W. (1999). Neuronal apoptosis induced by beta-amyloid is mediated by caspase-8. Neurobiol Dis *6*, 440-449.

Jiang, H., Ware, R., Stall, A., Flaherty, L., Chess, L., and Pernis, B. (1995). Murine CD8+ T cells that specifically delete autologous CD4+ T cells expressing V beta 8 TCR: a role of the Qa-1 molecule. Immunity *2*, 185-194.

Kanfer, J. N., Sorrentino, G., and Sitar, D. S. (1998). Phospholipases as mediators of amyloid beta peptide neurotoxicity: an early event contributing to neurodegeneration characteristic of Alzheimer's disease. Neurosci Lett *257*, 93-96.

Katayama, T., Imaizumi, K., Manabe, T., Hitomi, J., Kudo, T., and Tohyama, M. (2004). Induction of neuronal death by ER stress in Alzheimer's disease. J Chem Neuroanat *28*, 67-78.

Kato, K. (1999). Modulation of long-term potentiation in the CA1 area of rat hippocampus by platelet-activating factor. Adv Exp Med Biol *469*, 221-227.

Kaufman, R. J. (1999). Stress signaling from the lumen of the endoplasmic reticulum: coordination of gene transcriptional and translational controls. Genes Dev *13*, 1211-1233.

Kimberly, W. T., Zheng, J. B., Guenette, S. Y., and Selkoe, D. J. (2001). The intracellular domain of the beta-amyloid precursor protein is stabilized by Fe65 and translocates to the nucleus in a notch-like manner. J Biol Chem *276*, 40288-40292.

Kitamura, Y., Shimohama, S., Kamoshima, W., Ota, T., Matsuoka, Y., Nomura, Y., Smith, M. A., Perry, G., Whitehouse, P. J., and Taniguchi, T. (1998). Alteration of proteins regulating apoptosis, Bcl-2, Bcl-x, Bax, Bak, Bad, ICH-1 and CPP32, in Alzheimer's disease. Brain Res *780*, 260-269.

Koltai, M., Hosford, D., Guinot, P., Esanu, A., and Braquet, P. (1991). Platelet activating factor (PAF). A review of its effects, antagonists and possible future clinical implications (Part I). Drugs *42*, 9-29.

Kondziolka, D., Steinberg, G. K., Wechsler, L., Meltzer, C. C., Elder, E., Gebel, J., Decesare, S., Jovin, T., Zafonte, R., Lebowitz, J., *et al.* (2005). Neurotransplantation for patients with subcortical motor stroke: a phase 2 randomized trial. J Neurosurg *103*, 38-45.

Kriem, B., Sponne, I., Fifre, A., Malaplate-Armand, C., Lozac'h-Pillot, K., Koziel, V., Yen-Potin, F. T., Bihain, B., Oster, T., Olivier, J. L., and Pillot, T. (2005). Cytosolic phospholipase A2 mediates neuronal apoptosis induced by soluble oligomers of the amyloid-beta peptide. Faseb J *19*, 85-87.

Kumar, S., and Vaux, D. L. (2002). Apoptosis. A cinderella caspase takes center stage. Science *297*, 1290-1291.

Lau, F. C., Shukitt-Hale, B., and Joseph, J. A. (2005). The beneficial effects of fruit polyphenols on brain aging. Neurobiol Aging *26 Suppl 1*, 128-132.

Le Bars, P. L., Katz, M. M., Berman, N., Itil, T. M., Freedman, A. M., and Schatzberg, A. F. (1997). A placebo-controlled, double-blind, randomized trial of an extract of Ginkgo biloba for dementia. North American EGb Study Group. Jama *278*, 1327-1332.

Le Bars, P. L., Kieser, M., and Itil, K. Z. (2000). A 26-week analysis of a double-blind, placebo-controlled trial of the ginkgo biloba extract EGb 761 in dementia. Dement Geriatr Cogn Disord *11*, 230-237.

Leist, M., and Jaattela, M. (2001). Four deaths and a funeral: from caspases to alternative mechanisms. Nat Rev Mol Cell Biol *2*, 589-598.

Li, H., Bergeron, L., Cryns, V., Pasternack, M. S., Zhu, H., Shi, L., Greenberg, A., and Yuan, J. (1997). Activation of caspase-2 in apoptosis. J Biol Chem *272*, 21010-21017.

Li, H., Zhu, H., Xu, C. J., and Yuan, J. (1998). Cleavage of BID by caspase 8 mediates the mitochondrial damage in the Fas pathway of apoptosis. Cell *94*, 491-501.

Li, L. Y., Luo, X., and Wang, X. (2001). Endonuclease G is an apoptotic DNase when released from mitochondria. Nature *412*, 95-99.

Li, T., Southall, M. D., Yi, Q., Pei, Y., Lewis, D., Al-Hassani, M., Spandau, D., and Travers, J. B. (2003). The epidermal platelet-activating factor receptor augments chemotherapy-induced apoptosis in human carcinoma cell lines. J Biol Chem *278*, 16614-16621.

Lin, X. Y., Choi, M. S., and Porter, A. G. (2000). Expression analysis of the human caspase-1 subfamily reveals specific regulation of the CASP5 gene by lipopolysaccharide and interferon-gamma. J Biol Chem *275*, 39920-39926.

Lleo, A., Berezovska, O., Growdon, J. H., and Hyman, B. T. (2004). Clinical, pathological, and biochemical spectrum of Alzheimer disease associated with PS-1 mutations. Am J Geriatr Psychiatry *12*, 146-156.

Lorenzo, A., and Yankner, B. A. (1994). Beta-amyloid neurotoxicity requires fibril formation and is inhibited by congo red. Proc Natl Acad Sci U S A *91*, 12243-12247.

Lu, J., Caplan, M. S., Saraf, A. P., Li, D., Adler, L., Liu, X., and Jilling, T. (2004). Platelet-activating factor-induced apoptosis is blocked by Bcl-2 in rat intestinal epithelial cells. Am J Physiol Gastrointest Liver Physiol *286*, G340-350.

Ly, J. D., Grubb, D. R., and Lawen, A. (2003). The mitochondrial membrane potential (deltapsi(m)) in apoptosis; an update. Apoptosis *8*, 115-128.

Ma, X., and Bazan, H. E. (2001). Platelet-activating factor (PAF) enhances apoptosis induced by ultraviolet radiation in corneal epithelial cells through cytochrome c-caspase activation. Curr Eye Res *23*, 326-335.

MacManus, J. P., Jian, M., Preston, E., Rasquinha, I., Webster, J., and Zurakowski, B. (2003). Absence of the transcription factor E2F1 attenuates brain injury and improves behavior after focal ischemia in mice. J Cereb Blood Flow Metab *23*, 1020-1028.

Maki, M., Matsukawa, N., Yuasa, H., Otsuka, Y., Yamamoto, T., Akatsu, H., Okamoto, T., Ueda, R., and Ojika, K. (2002). Decreased expression of hippocampal cholinergic neurostimulating peptide precursor protein mRNA in the hippocampus in Alzheimer disease. J Neuropathol Exp Neurol *61*, 176-185.

Mandal, P. K., McClure, R. J., and Pettegrew, J. W. (2004). Interactions of Abeta(1-40) with glycerophosphocholine and intact erythrocyte membranes: fluorescence and circular dichroism studies. Neurochem Res *29*, 2273-2279.

Mandel, S., and Youdim, M. B. (2004). Catechin polyphenols: neurodegeneration and neuroprotection in neurodegenerative diseases. Free Radic Biol Med *37*, 304-317.

Mandelkow, E. M., Stamer, K., Vogel, R., Thies, E., and Mandelkow, E. (2003). Clogging of axons by tau, inhibition of axonal traffic and starvation of synapses. Neurobiol Aging *24*, 1079-1085.

Mannella, C. A., Buttle, K., Rath, B. K., and Marko, M. (1998). Electron microscopic tomography of rat-liver mitochondria and their interaction with the endoplasmic reticulum. Biofactors *8*, 225-228.

Manya, H., Aoki, J., Watanabe, M., Adachi, T., Asou, H., Inoue, Y., Arai, H., and Inoue, K. (1998). Switching of platelet-activating factor acetylhydrolase catalytic subunits in developing rat brain. J Biol Chem *273*, 18567-18572.

Marcelli, M., Marani, M., Li, X., Sturgis, L., Haidacher, S. J., Trial, J. A., Mannucci, R., Nicoletti, I., and Denner, L. (2000). Heterogeneous apoptotic responses of prostate cancer cell lines identify an association between sensitivity to staurosporine-induced apoptosis, expression of Bcl-2 family members, and caspase activation. Prostate *42*, 260-273.

Marcheselli, V. L., Rossowska, M. J., Domingo, M. T., Braquet, P., and Bazan, N. G. (1990). Distinct platelet-activating factor binding sites in synaptic endings and in intracellular membranes of rat cerebral cortex. J Biol Chem *265*, 9140-9145.

Matsuo, Y., Kihara, T., Ikeda, M., Ninomiya, M., Onodera, H., and Kogure, K. (1996). Role of platelet-activating factor and thromboxane A2 in radical production during ischemia and reperfusion of the rat brain. Brain Res *709*, 296-302.

Mattiasson, G., Shamloo, M., Gido, G., Mathi, K., Tomasevic, G., Yi, S., Warden, C. H., Castilho, R. F., Melcher, T., Gonzalez-Zulueta, M., *et al.* (2003). Uncoupling protein-2 prevents neuronal death and diminishes brain dysfunction after stroke and brain trauma. Nat Med *9*, 1062-1068.

Mattson, M. P. (1997). Cellular actions of beta-amyloid precursor protein and its soluble and fibrillogenic derivatives. Physiol Rev *77*, 1081-1132.

Mattson, M. P. (2000). Apoptosis in neurodegenerative disorders. Nat Rev Mol Cell Biol *1*, 120-129.

Mattson, M. P. (2004). Pathways towards and away from Alzheimer's disease. Nature *430*, 631-639.

Mattson, M. P., Haughey, N. J., and Nath, A. (2005). Cell death in HIV dementia. Cell Death Differ *12 Suppl 1*, 893-904.

Melanson-Drapeau, L., Beyko, S., Dave, S., Hebb, A. L., Franks, D. J., Sellitto, C., Paul, D. L., and Bennett, S. A. (2003). Oligodendrocyte progenitor enrichment in the connexin32 null-mutant mouse. J Neurosci *23*, 1759-1768.

Menschik, E. D., and Finkel, L. H. (1998). Neuromodulatory control of hippocampal function: towards a model of Alzheimer's disease. Artif Intell Med *13*, 99-121.

Miethke, T., Wahl, C., Heeg, K., Echtenacher, B., Krammer, P. H., and Wagner, H. (1992). T cell-mediated lethal shock triggered in mice by the superantigen staphylococcal enterotoxin B: critical role of tumor necrosis factor. J Exp Med *175*, 91-98.

Mills, E. M., Xu, D., Fergusson, M. M., Combs, C. A., Xu, Y., and Finkel, T. (2002). Regulation of cellular oncosis by uncoupling protein 2. J Biol Chem *277*, 27385-27392.

Mo, F., Harris, C. S., Migahed, L., Haddad, P. S., Arnason, J. T., and Bennett, S. A. (in preparation). Inhibition of PAF biological activity by plant-derived phenolics.

Mori, M., Aihara, M., Kume, K., Hamanoue, M., Kohsaka, S., and Shimizu, T. (1996). Predominant expression of platelet-activating factor receptor in the rat brain microglia. J Neurosci *16*, 3590-3600.

Morishima, N., Nakanishi, K., Takenouchi, H., Shibata, T., and Yasuhiko, Y. (2002). An endoplasmic reticulum stress-specific caspase cascade in apoptosis. Cytochrome c-independent activation of caspase-9 by caspase-12. J Biol Chem *277*, 34287-34294.

Nakagawa, T., Zhu, H., Morishima, N., Li, E., Xu, J., Yankner, B. A., and Yuan, J. (2000). Caspase-12 mediates endoplasmic-reticulum-specific apoptosis and cytotoxicity by amyloid-beta. Nature *403*, 98-103.

Nakamura, M., Honda, Z., Izumi, T., Sakanaka, C., Mutoh, H., Minami, M., Bito, H., Seyama, Y., Matsumoto, T., Noma, M., and et al. (1991). Molecular cloning and expression of platelet-activating factor receptor from human leukocytes. J Biol Chem *266*, 20400-20405.

Nelson, P. T., Kondziolka, D., Wechsler, L., Goldstein, S., Gebel, J., DeCesare, S., Elder, E. M., Zhang, P. J., Jacobs, A., McGrogan, M., *et al.* (2002). Clonal human (hNT) neuron grafts for stroke therapy: neuropathology in a patient 27 months after implantation. Am J Pathol *160*, 1201-1206.

Newman, M. B., Misiuta, I., Willing, A. E., Zigova, T., Karl, R. C., Borlongan, C. V., and Sanberg, P. R. (2005). Tumorigenicity issues of embryonic carcinoma-derived stem cells: relevance to surgical trials using NT2 and hNT neural cells. Stem Cells Dev *14*, 29-43.

Ojaimi, J., and Byrne, E. (2001). Mitochondrial function and alzheimer's disease. Biol Signals Recept *10*, 254-262.

Orrenius, S., Zhivotovsky, B., and Nicotera, P. (2003). Regulation of cell death: the calcium-apoptosis link. Nat Rev Mol Cell Biol *4*, 552-565.

Paradis, E., Clavel, S., Bouillaud, F., Ricquier, D., and Richard, D. (2003). Uncoupling protein 2: a novel player in neuroprotection. Trends Mol Med *9*, 522-525.

Park, E. S., Gao, X., Chung, J. M., and Chung, K. (2006). Levels of mitochondrial reactive oxygen species increase in rat neuropathic spinal dorsal horn neurons. Neurosci Lett *391*, 108-111.

Parker, M. A., Bazan, H. E., Marcheselli, V., Rodriguez de Turco, E. B., and Bazan, N. G. (2002). Platelet-activating factor induces permeability transition and cytochrome c release in isolated brain mitochondria. J Neurosci Res *69*, 39-50.

Paroni, G., Henderson, C., Schneider, C., and Brancolini, C. (2001). Caspase-2-induced apoptosis is dependent on caspase-9, but its processing during UV- or tumor necrosis factor-dependent cell death requires caspase-3. J Biol Chem *276*, 21907-21915.

Pendergrass, W., Wolf, N., and Poot, M. (2004). Efficacy of MitoTracker Green and CMXrosamine to measure changes in mitochondrial membrane potentials in living cells and tissues. Cytometry A *61*, 162-169.

Perry, S. W., Hamilton, J. A., Tjoelker, L. W., Dbaibo, G., Dzenko, K. A., Epstein, L. G., Hannun, Y., Whittaker, J. S., Dewhurst, S., and Gelbard, H. A. (1998). Platelet-activating factor receptor activation. An initiator step in HIV-1 neuropathogenesis. J Biol Chem *273*, 17660-17664.

Perry, S. W., Norman, J. P., Litzburg, A., Zhang, D., Dewhurst, S., and Gelbard, H. A. (2005). HIV-1 transactivator of transcription protein induces mitochondrial hyperpolarization and synaptic stress leading to apoptosis. J Immunol *174*, 4333-4344.

Phenix, B. N., Angel, J. B., Mandy, F., Kravcik, S., Parato, K., Chambers, K. A., Gallicano, K., Hawley-Foss, N., Cassol, S., Cameron, D. W., and Badley, A. D. (2000). Decreased HIV-associated T cell apoptosis by HIV protease inhibitors. AIDS Res Hum Retroviruses *16*, 559-567.

Phenix, B. N., Cooper, C., Owen, C., and Badley, A. D. (2002). Modulation of apoptosis by HIV protease inhibitors. Apoptosis *7*, 295-312.

Phenix, B. N., Lum, J. J., Nie, Z., Sanchez-Dardon, J., and Badley, A. D. (2001). Antiapoptotic mechanism of HIV protease inhibitors: preventing mitochondrial transmembrane potential loss. Blood *98*, 1078-1085.

Pike, C. J., Walencewicz, A. J., Glabe, C. G., and Cotman, C. W. (1991). Aggregation-related toxicity of synthetic beta-amyloid protein in hippocampal cultures. Eur J Pharmacol *207*, 367-368.

Pleasure, S. J., Page, C., and Lee, V. M. (1992). Pure, postmitotic, polarized human neurons derived from NTera 2 cells provide a system for expressing exogenous proteins in terminally differentiated neurons. J Neurosci *12*, 1802-1815.

Pompl, P. N., Yemul, S., Xiang, Z., Ho, L., Haroutunian, V., Purohit, D., Mohs, R., and Pasinetti, G. M. (2003). Caspase gene expression in the brain as a function of the clinical progression of Alzheimer disease. Arch Neurol *60*, 369-376.

Pong, K., Doctrow, S. R., Huffman, K., Adinolfi, C. A., and Baudry, M. (2001). Attenuation of staurosporine-induced apoptosis, oxidative stress, and mitochondrial dysfunction by synthetic superoxide dismutase and catalase mimetics, in cultured cortical neurons. Exp Neurol *171*, 84-97.

Prescott, S. M., Zimmerman, G. A., Stafforini, D. M., and McIntyre, T. M. (2000). Platelet-activating factor and related lipid mediators. Annu Rev Biochem *69*, 419-445.

Preston, E., and Webster, J. (2000). Spectrophotometric measurement of experimental brain injury. J Neurosci Methods *94*, 187-192.

Rao, R. V., Peel, A., Logvinova, A., del Rio, G., Hermel, E., Yokota, T., Goldsmith, P. C., Ellerby, L. M., Ellerby, H. M., and Bredesen, D. E. (2002). Coupling endoplasmic reticulum stress to the cell death program: role of the ER chaperone GRP78. FEBS Lett *514*, 122-128.

Sapir, T., Elbaum, M., and Reiner, O. (1997). Reduction of microtubule catastrophe events by LIS1, platelet-activating factor acetylhydrolase subunit. Embo J *16*, 6977-6984.

Scorrano, L., Oakes, S. A., Opferman, J. T., Cheng, E. H., Sorcinelli, M. D., Pozzan, T., and Korsmeyer, S. J. (2003). BAX and BAK regulation of endoplasmic reticulum Ca2+: a control point for apoptosis. Science *300*, 135-139.

Selkoe, D. J. (2002). Alzheimer's disease is a synaptic failure. Science *298*, 789-791.

Selkoe, D. J. (2005). Defining molecular targets to prevent Alzheimer disease. Arch Neurol *62*, 192-195.

Shen, T. Y. (1991). Chemical and biochemical characterization of lignan analogs as novel PAF receptor antagonists. Lipids *26*, 1154-1156.

Shi, H., Xu, H., and Liang, G. (1995). [Effects of a platelet-activating factor antagonist ONO-6240 on antigen induced eosinophil infiltration into the airways]. Zhonghua Nei Ke Za Zhi *34*, 753-756.

Shibata, M., Hattori, H., Sasaki, T., Gotoh, J., Hamada, J., and Fukuuchi, Y. (2003). Activation of caspase-12 by endoplasmic reticulum stress induced by transient middle cerebral artery occlusion in mice. Neuroscience *118*, 491-499.

Singh, I. N., Goody, R. J., Dean, C., Ahmad, N. M., Lutz, S. E., Knapp, P. E., Nath, A., and Hauser, K. F. (2004). Apoptotic death of striatal neurons induced by human immunodeficiency virus-1 Tat and gp120: Differential involvement of caspase-3 and endonuclease G. J Neurovirol *10*, 141-151.

Slee, E. A., Harte, M. T., Kluck, R. M., Wolf, B. B., Casiano, C. A., Newmeyer, D. D., Wang, H. G., Reed, J. C., Nicholson, D. W., Alnemri, E. S., *et al.* (1999). Ordering the cytochrome c-initiated caspase cascade: hierarchical activation of caspases-2, -3, -6, -7, -8, and -10 in a caspase-9-dependent manner. J Cell Biol *144*, 281-292.

Southall, M. D., Isenberg, J. S., Nakshatri, H., Yi, Q., Pei, Y., Spandau, D. F., and Travers, J. B. (2001). The platelet-activating factor receptor protects epidermal cells from tumor necrosis factor (TNF) alpha and TNF-related apoptosis-inducing ligand-induced apoptosis through an NF-kappa B-dependent process. J Biol Chem *276*, 45548-45554.

Suen, K. C., Lin, K. F., Elyaman, W., So, K. F., Chang, R. C., and Hugon, J. (2003). Reduction of calcium release from the endoplasmic reticulum could only provide partial neuroprotection against beta-amyloid peptide toxicity. J Neurochem *87*, 1413-1426.

Susin, S. A., Lorenzo, H. K., Zamzami, N., Marzo, I., Snow, B. E., Brothers, G. M., Mangion, J., Jacotot, E., Costantini, P., Loeffler, M., *et al.* (1999). Molecular characterization of mitochondrial apoptosis-inducing factor. Nature *397*, 441-446.

Takuma, K., Yan, S. S., Stern, D. M., and Yamada, K. (2005). Mitochondrial dysfunction, endoplasmic reticulum stress, and apoptosis in Alzheimer's disease. J Pharmacol Sci *97*, 312-316.

Talanian, R. V., Quinlan, C., Trautz, S., Hackett, M. C., Mankovich, J. A., Banach, D., Ghayur, T., Brady, K. D., and Wong, W. W. (1997). Substrate specificities of caspase family proteases. J Biol Chem *272*, 9677-9682.

Tanaka, S., Takehashi, M., Iida, S., Kitajima, T., Kamanaka, Y., Stedeford, T., Banasik, M., and Ueda, K. (2005). Mitochondrial impairment induced by poly(ADP-ribose) polymerase-1 activation in cortical neurons after oxygen and glucose deprivation. J Neurochem *95*, 179-190.

Teather, L. A., Packard, M. G., and Bazan, N. G. (1998). Effects of posttraining intrahippocampal injections of platelet-activating factor and PAF antagonists on memory. Neurobiol Learn Mem *70*, 349-363.

Thornberry, N. A., Rano, T. A., Peterson, E. P., Rasper, D. M., Timkey, T., Garcia-Calvo, M., Houtzager, V. M., Nordstrom, P. A., Roy, S., Vaillancourt, J. P., *et al.* (1997). A combinatorial approach defines specificities of members of the caspase family and granzyme B. Functional relationships established for key mediators of apoptosis. J Biol Chem *272*, 17907-17911.

Tokuoka, S. M., Ishii, S., Kawamura, N., Satoh, M., Shimada, A., Sasaki, S., Hirotsune, S., Wynshaw-Boris, A., and Shimizu, T. (2003). Involvement of platelet-activating factor and LIS1 in neuronal migration. Eur J Neurosci *18*, 563-570.

Tong, N., Sanchez, J. F., Maggirwar, S. B., Ramirez, S. H., Guo, H., Dewhurst, S., and Gelbard, H. A. (2001). Activation of glycogen synthase kinase 3 beta (GSK-3beta) by platelet activating factor mediates migration and cell death in cerebellar granule neurons. Eur J Neurosci *13*, 1913-1922.

Troy, C. M., Rabacchi, S. A., Friedman, W. J., Frappier, T. F., Brown, K., and Shelanski, M. L. (2000). Caspase-2 mediates neuronal cell death induced by beta-amyloid. J Neurosci *20*, 1386-1392.

Troy, C. M., and Shelanski, M. L. (2003). Caspase-2 redux. Cell Death Differ *10*, 101-107.

van Dongen, M., van Rossum, E., Kessels, A., Sielhorst, H., and Knipschild, P. (2003). Ginkgo for elderly people with dementia and age-associated memory impairment: a randomized clinical trial. J Clin Epidemiol *56*, 367-376.

van Dongen, M. C., van Rossum, E., Kessels, A. G., Sielhorst, H. J., and Knipschild, P. G. (2000). The efficacy of ginkgo for elderly people with dementia and age-associated memory impairment: new results of a randomized clinical trial. J Am Geriatr Soc *48*, 1183-1194.

Venable, M. E., Zimmerman, G. A., McIntyre, T. M., and Prescott, S. M. (1993). Platelet-activating factor: a phospholipid autacoid with diverse actions. J Lipid Res *34*, 691-702.

Vila, M., and Przedborski, S. (2003). Targeting programmed cell death in neurodegenerative diseases. Nat Rev Neurosci *4*, 365-375.

Wagner, K. W., Engels, I. H., and Deveraux, Q. L. (2004). Caspase-2 can function upstream of bid cleavage in the TRAIL apoptosis pathway. J Biol Chem *279*, 35047-35052.

Walter, L., and Hajnoczky, G. (2005). Mitochondria and endoplasmic reticulum: the lethal interorganelle cross-talk. J Bioenerg Biomembr *37*, 191-206.

Weaver, J. G., Tarze, A., Moffat, T. C., Lebras, M., Deniaud, A., Brenner, C., Bren, G. D., Morin, M. Y., Phenix, B. N., Dong, L., *et al.* (2005). Inhibition of adenine nucleotide translocator pore function and protection against apoptosis in vivo by an HIV protease inhibitor. J Clin Invest *115*, 1828-1838.

Wertkin, A. M., Turner, R. S., Pleasure, S. J., Golde, T. E., Younkin, S. G., Trojanowski, J. Q., and Lee, V. M. (1993). Human neurons derived from a teratocarcinoma cell line express solely the 695-amino acid amyloid precursor protein and produce intracellular beta-amyloid or A4 peptides. Proc Natl Acad Sci U S A *90*, 9513-9517.

Wettstein, A. (2000). Cholinesterase inhibitors and Gingko extracts--are they comparable in the treatment of dementia? Comparison of published placebo-controlled efficacy studies of at least six months' duration. Phytomedicine *6*, 393-401.

Wu, B., Iwakiri, R., Ootani, A., Fujise, T., Tsunada, S., and Fujimoto, K. (2003). Platelet-activating factor promotes mucosal apoptosis via FasL-mediating caspase-9 active pathway in rat small intestine after ischemia-reperfusion. Faseb J *17*, 1156-1158.

Yoshikawa, T., Naito, Y., and Kondo, M. (1999). Ginkgo biloba leaf extract: review of biological actions and clinical applications. Antioxid Redox Signal *1*, 469-480.

Yue, T. L., and Feuerstein, G. Z. (1994). Platelet-activating factor: a putative neuromodulator and mediator in the pathophysiology of brain injury. Crit Rev Neurobiol *8*, 11-24.

Zamzami, N., Susin, S. A., Marchetti, P., Hirsch, T., Gomez-Monterrey, I., Castedo, M., and Kroemer, G. (1996). Mitochondrial control of nuclear apoptosis. J Exp Med *183*, 1533-1544.

Zausinger, S., Hungerhuber, E., Baethmann, A., Reulen, H., and Schmid-Elsaesser, R. (2000). Neurological impairment in rats after transient middle cerebral artery occlusion: a comparative study under various treatment paradigms. Brain Res *863*, 94-105.

Zbarsky, V., Datla, K. P., Parkar, S., Rai, D. K., Aruoma, O. I., and Dexter, D. T. (2005). Neuroprotective properties of the natural phenolic antioxidants curcumin and naringenin but not quercetin and fisetin in a 6-OHDA model of Parkinson's disease. Free Radic Res *39*, 1119-1125.

Zhang, Y., McLaughlin, R., Goodyer, C., and LeBlanc, A. (2002). Selective cytotoxicity of intracellular amyloid beta peptide1-42 through p53 and Bax in cultured primary human neurons. J Cell Biol *156*, 519-529.

Zhu, P., DeCoster, M. A., and Bazan, N. G. (2004). Interplay among platelet-activating factor, oxidative stress, and group I metabotropic glutamate receptors modulates neuronal survival. J Neurosci Res *77*, 525-531.

Zhuang, J., Dinsdale, D., and Cohen, G. M. (1998). Apoptosis, in human monocytic THP.1 cells, results in the release of cytochrome c from mitochondria prior to their ultracondensation, formation of outer membrane discontinuities and reduction in inner membrane potential. Cell Death Differ *5*, 953-962.

**Appendix 1: Hippocampal PAFR expression pattern is species-dependent.** A) PAFR is expressed by CA3 pyramidal neurons in the mouse hippocampal formation. We raised a polyclonal antibody to a conserved antigenic peptide sequence in human, mouse, and rat PAFR. Specificity was confirmed using PAFR KO control brain. Scale bars, 100 μm. B) Human hippocampal neurons do not express PAFR. Cells with microglial morphology (arrows) are detected in the hippocampus. Some cells with neuronal morphology (arrowheads) in the posterior cortex are PAFR-positive. Scale bars, 50 μm.

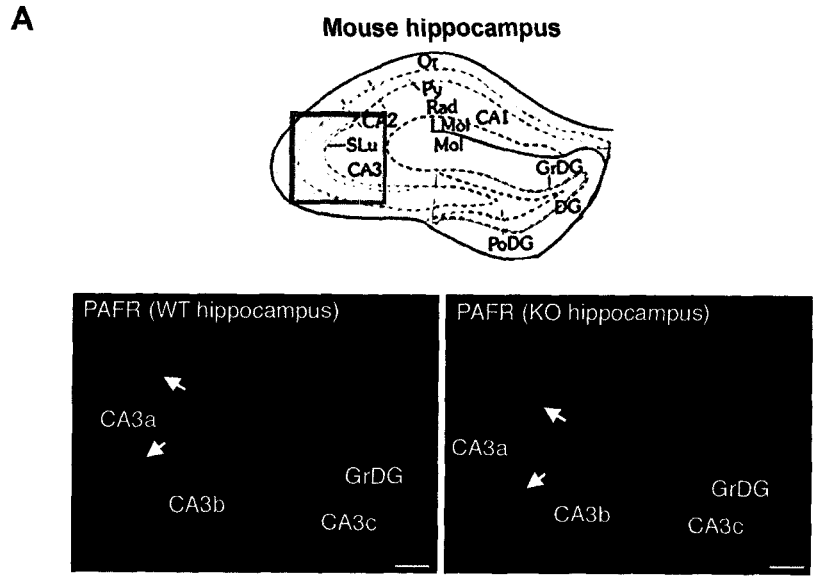


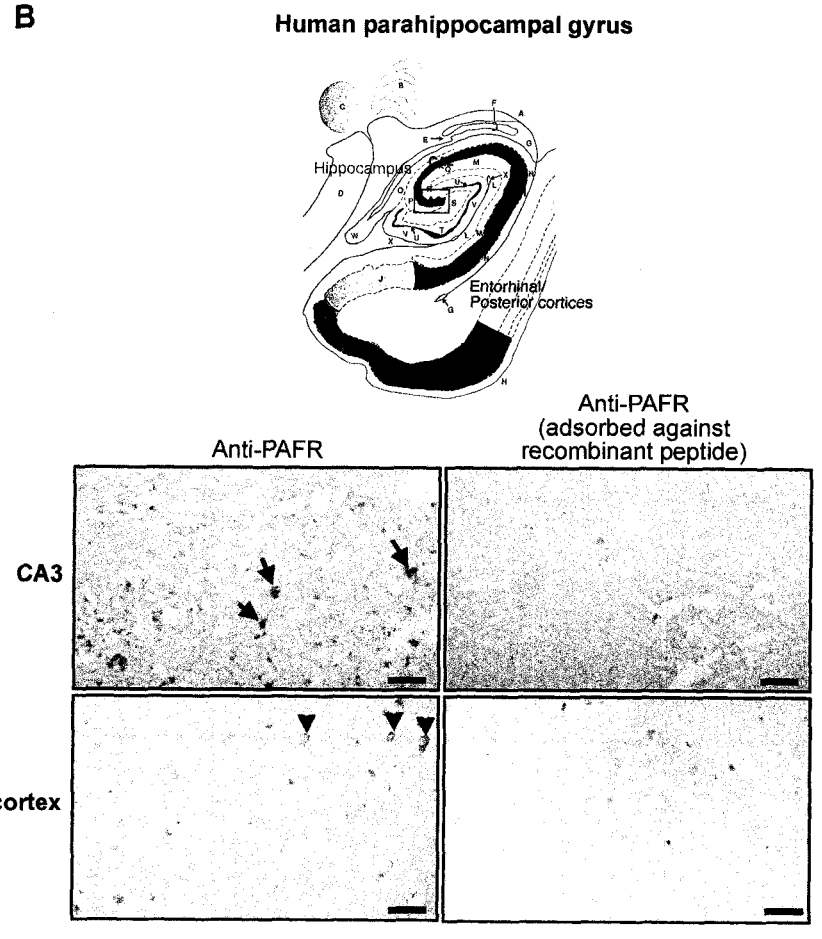


Appendix 1

**Appendix 2: Lack of PAFR expression renders mouse CGNs susceptible to PAF-induced apoptosis.** A) Following a 24 h treatment with 1 μM PAF, CGNs from PAFR KO mice exhibited a decrease in survival (**p<0.01, ANOVA, *post hoc* Tukey), but WT mouse CGNs were not affected. B) Using the CaspaTag assay, cells were labelled with FAM-DEVD-FMK, a fluorescent substrate specific for caspase-3 and -7. A 24 h treatment with 1 μM PAF induced caspase-3/7 activation in CGNs derived from PAFR KO mice but not WT. Etop (25 μM) was used as a positive control for caspase-3/7 activation (**p<0.01, ANOVA, *post hoc* Tukey).

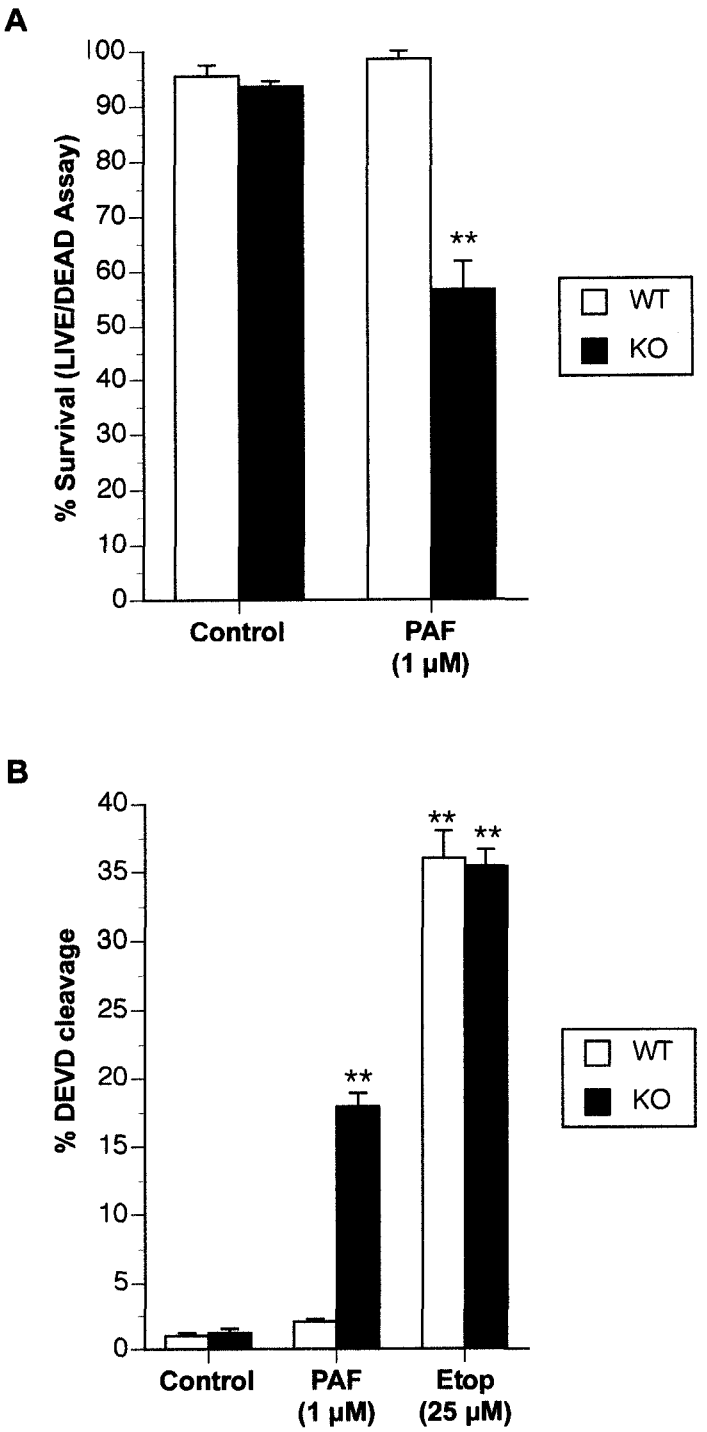


Appendix 2

**Appendix 3: Lack of UCP2 expression renders mouse CGNs resistant to PAF neurotoxicity in the absence of PAFR.** Following a 24 h treatment with 1 μM PAF, CGNs from $PAFR^{+/+}/UCP2^{+/+}$ mice were not susceptible to PAF-induced death. In comparison, $PAFR^{-/-}/UCP2^{+/+}$ mouse CGNs exhibited a decrease in survival (**$p<0.01$, ANOVA, *post hoc* Tukey), but CGNs from $PAFR^{-/-}/UCP2^{-/-}$ mice were protected from PAF-induced toxicity.

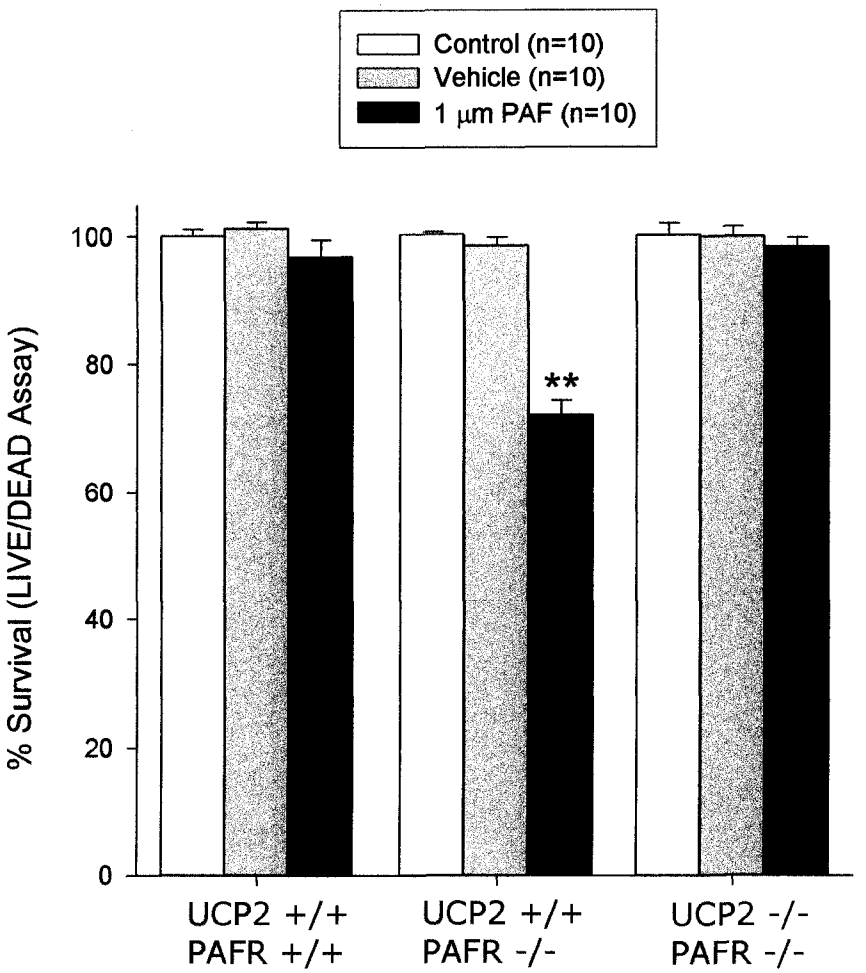


Appendix 3

**Appendix 4: Expression of PAFAH I subunits in NT2s and hNTs.**
Western blot analysis showed that PAF-AH I α2 and LIS1 subunits predominate in hNTs, while NT2s primarily express the α1 subunit. Coomassie blue-staining of total protein was used as a loading control since both actin and tubulin protein levels change as NT2 cells terminally commit to an hNT neuronal lineage.

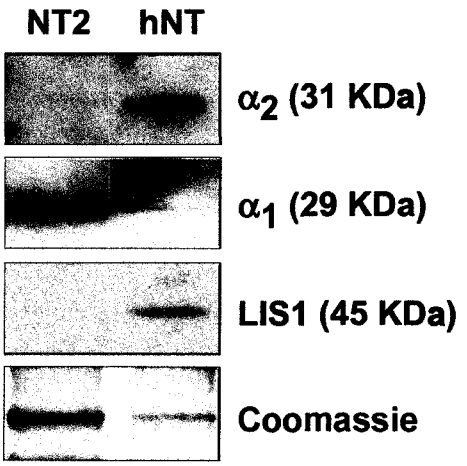


Appendix 4

**Appendix 5**: Weaver JG, Tarze A, Moffat TC, Lebras M, Deniaud A, Brenner C, Bren GD, Morin MY, Phenix BN, Dong L, Jiang SX, Sim VL, Zurakowski B, Lallier J, Hardin H, Wettstein P, van Heeswijk RP, Douen A, Kroemer RT, Hou ST, Bennett SA, Lynch DH, Kroemer G, Badley AD (2005) Inhibition of adenine nucleotide translocator pore function and protection against apoptosis in vivo by an HIV protease inhibitor. J Clin Invest 115:1828-1838.

# Inhibition of adenine nucleotide translocator pore function and protection against apoptosis in vivo by an HIV protease inhibitor

Joel G.R. Weaver,[1,2,3] Agathe Tarze,[4] Tia C. Moffat,[5] Morgane LeBras,[4] Aurelien Deniaud,[4] Catherine Brenner,[4] Gary D. Bren,[2] Mario Y. Morin,[5] Barbara N. Phenix,[3] Li Dong,[3,6] Susan X. Jiang,[7] Valerie L. Sim,[8] Bogdan Zurakowski,[7] Jessica Lallier,[5] Heather Hardin,[9] Peter Wettstein,[9] Rolf P.G. van Heeswijk,[3] Andre Douen,[3] Romano T. Kroemer,[10] Sheng T. Hou,[7] Steffany A.L. Bennett,[5] David H. Lynch,[11] Guido Kroemer,[12] and Andrew D. Badley[2,13]

[1]Division of General Surgery, University of Ottawa, Ottawa, Ontario, Canada. [2]Division of Infectious Diseases, Mayo Clinic and Foundation, Rochester, Minnesota, USA. [3]Ottawa Health Research Institute, University of Ottawa, Ottawa, Ontario, Canada. [4]Université de Versailles Saint-Quentin-en-Yvelines, Versailles, France. [5]Neural Regeneration Laboratory, Department of Biochemistry, Microbiology, and Immunology, and [6]Department of Pathology, University of Ottawa, Ottawa, Ontario, Canada. [7]Experimental Stroke Group, National Research Council Institute for Biological Sciences (NRC/IBS), National Research Council of Canada, Ottawa, Ontario, Canada. [8]Division of Neurology, Ottawa Hospital, Ottawa, Ontario, Canada. [9]Department of Surgery and Immunology, Mayo Clinic, Rochester, Minnesota, USA. [10]Sanofi Aventis, Centre de Recherche de Paris, Vitry-sur-Seine, France. [11]Amnis Corp., Seattle, Washington, USA. [12]Institut Gustave Roussy, Villejuif, France. [13]Translational Program in Immunology and Biodefense, Mayo Clinic and Foundation, Rochester, Minnesota, USA.

**Inhibitors of HIV protease have been shown to have antiapoptotic effects in vitro, yet whether these effects are seen in vivo remains controversial. In this study, we have evaluated the impact of the HIV protease inhibitor (PI) nelfinavir, boosted with ritonavir, in models of nonviral disease associated with excessive apoptosis. In mice with Fas-induced fatal hepatitis, *Staphylococcal enterotoxin B*–induced shock, and middle cerebral artery occlusion–induced stroke, we demonstrate that PIs significantly reduce apoptosis and improve histology, function, and/or behavioral recovery in each of these models. Further, we demonstrate that both in vitro and in vivo, PIs block apoptosis through the preservation of mitochondrial integrity and that in vitro PIs act to prevent pore function of the adenine nucleotide translocator (ANT) subunit of the mitochondrial permeability transition pore complex.**

## Introduction

The abnormal regulation of apoptosis is thought to contribute to a variety of pathologic disease processes in vivo. HIV-induced CD4 T cell depletion and consequent immunodeficiency is one such disease state in which excessive apoptosis has been implicated. Current therapies for HIV not only reduce HIV replication but may also directly impact apoptosis; indeed, many groups have now reported that HIV protease inhibitors (PIs) can inhibit apoptosis at concentrations similar to those that are commonly seen in the plasma of patients receiving such treatments (reviewed in ref. 1). Paradoxically, such agents may also induce apoptosis, particularly of transformed cells, when used at higher doses (2–5).

Studies by several groups have investigated the potential mechanisms by which PIs may inhibit apoptosis, yielding different results. Proposed mechanisms include altered transcriptional regulation of key apoptosis regulatory proteins (5–7) and/or direct inhibition of the apoptosis enzyme ICE (8, 9) and/or calpain (10). Such theories cannot fully account for the ability of PIs to inhibit diverse apoptotic stimuli (reviewed in ref. 1) or the lack of enzymatic inhibition of recombinant caspases in vitro (11). According to another proposed mechanism to account for apoptosis inhibition, PIs alter the propensity of mitochondria to transduce apoptotic signals. This latter model is supported by the findings that PIs are able to block Fas-induced apoptosis involving mitochondrial signaling but not Fas-induced apoptosis that is mitochondria independent (11) and that PIs are able to rescue cells from apoptosis induced by mitochondriotoxic agents (5, 12).

Despite these in vitro findings, it remains controversial whether PI therapy for HIV-infected patients offers additional benefits in terms of CD4 T cell reconstitution compared with non-PI–containing regimens of equal antiviral potency (13, 14). Most studies that demonstrate enhanced CD4 T cell improvements in patients receiving PI therapy were retrospective, post-hoc analyses (15), which raises concerns about the methodologies used. Consequently, at least one study was designed to compare CD4 T cell number, activation profile, memory and naive T cell subsets, and apoptosis between patients receiving PI-continuing or PI-sparing regimens (16). No differences were observed between groups regarding CD4 T cell number, activation, or memory or naive subsets; however, within the first week of therapy, significantly less apoptosis was seen in CD4 T cells of patients receiving PI therapy than in patients who did not receive PI therapy (16). Such data are consistent with the postulated antiapoptotic effects of PIs.

The objectives of this study were, first, to evaluate whether PIs were antiapoptotic in vivo by evaluating apoptotic changes in animal models of disease that are associated with excessive apopto-

**Nonstandard abbreviations used:** $\Delta\Psi_m$, membrane permeability; ANT, adenine nucleotide translocator; AST, aspartate amino transferase; ATR, atractyloside; D-gal, D-galactosamine; MCAO, middle cerebral artery occlusion; NFV, nelfinavir; PBR, benzodiazepine receptor; PI, protease inhibitor; PTPC, permeability transition pore complex; RIT, ritonavir; RT, room temperature; SEB, *Staphylococcal enterotoxin B*; STS, staurosporine; TTC, 2,3,5-triphenyltetrazolium; VDAC, voltage-dependent anion channel.

**Conflict of interest:** The authors have declared that no conflict of interest exists.

**Citation for this article:** *J. Clin. Invest.* 115:1828–1838 (2005). doi:10.1172/JCI22954.

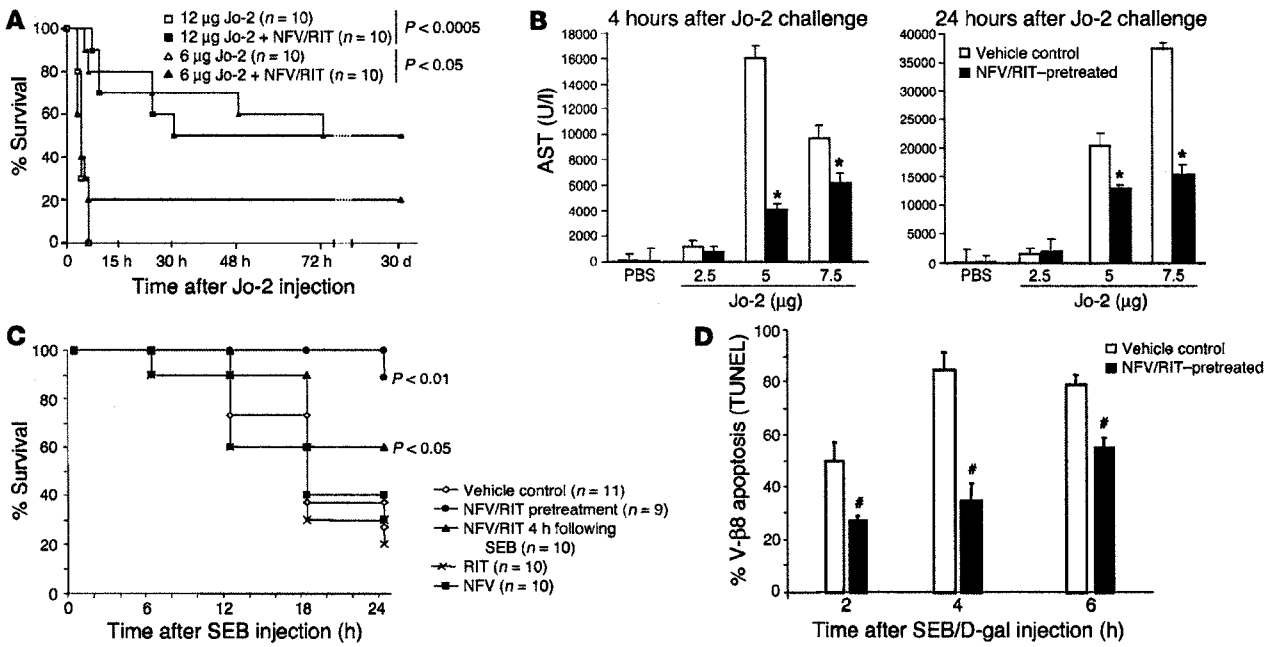


**Figure 1**

Effects of NFV/RIT on Jo-2–induced hepatitis or SEB-induced shock. **(A)** Mice treated with varying doses of Jo-2 antibody in the presence or absence of NFV/RIT were followed for 30 days and analyzed for survival. **(B)** In parallel, mice treated in a similar manner were sacrificed at 4 or 24 hours and analyzed for serum AST level. $^*P < 0.05$. **(C)** Five mice per group were treated with SEB/D-gal with or without NFV/RIT before or 4 hours after SEB or with NFV alone or RIT alone before SEB. Twenty-four-hour survival was monitored (cumulative data from 4 independent experiments are shown). **(D)** Mice treated with SEB/D-gal with NFV/RIT or control were analyzed for V-β8 T cell apoptosis by TUNEL assay (cumulative data from 4 independent experiments are shown). $^{\#}P < 0.01$.

sis but that do not depend upon viral replication and, second, to evaluate the mechanisms involved.

## Results

As mouse metabolism of PIs differs from that of humans, we first performed pharmacokinetic studies of mice treated with nelfinavir (NFV) at doses used in human therapy. Within 1 hour of dosing, mice had undetectable levels of NFV. Therefore, we co-dosed mice with ritonavir (RIT), another PI known to increase PI levels in humans (17). Ultimately, a dose of 125 mg/kg NFV and 13 mg/kg RIT resulted in drug levels similar to those of humans treated with NFV alone (see Methods). This dose was used for in vivo testing.

First, we evaluated the impact of NFV/RIT treatment on CD95/Fas-induced hepatic failure (18–20). Mice received NFV/RIT or vehicle control pretreatment for 24 hours followed by treatment with 6 or 12 μg of IV Jo-2 anti-Fas antibody. Control animals died in a dose-dependent manner, whereas NFV/RIT-pretreated animals displayed superior survival compared with controls (Figure 1A). Moreover, survival of mice treated with RIT (13 mg/kg) was similar to that of controls, which indicates that NFV was responsible for the observed improved survival. Importantly, all mice that died did so within 72 hours, which indicates that NFV/RIT truly prevents rather than delays Jo-2–induced hepatotoxicity and death. In parallel, groups of 10 mice received 2.5, 5, or 7.5 μg of IV Jo-2 with or without NFV/RIT pretreatment. Mice were sacrificed at 4 or 24 hours and analyzed for serum biochemistry, H&E histology, and apoptosis by TUNEL staining. Serum glucose, blood urea nitrogen, creatinine, phosphorus, total protein, albumin, globulin, bilirubin, and cholesterol levels were similar in the 2 groups (data not shown). However, NFV/RIT-pretreated mice had attenuated elevations in serum aspartate amino transferase (AST) at both 4 and 24 hours compared with control mice ($P < 0.03$; Figure 1B), reduced evidence of hepatitis at 48 hours on H&E histology, and a reduced quantity of TUNEL-positive hepatocytes from a mean of 50% to 15% (measured in 5 mice per group; $P = 0.002$; data not shown).

To assess whether NFV/RIT protection extended to other apoptotic disease processes, we treated mice with the bacterial superantigen *Staphylococcal enterotoxin B* (SEB) in the presence or absence of NFV/RIT. Systemic treatment with SEB results in shock and the selective apoptosis of V-β8–positive T cells (21). When coadministered with D-galactosamine (D-gal), SEB injection also results in death (22, 23). Following administration of SEB, apoptosis was measured by TUNEL assay in the V-β8 and V-β3 subsets of splenocytes. Four hours following SEB treatment, 72.6% of V-β8 cells were TUNEL positive, whereas 21.7% of V-β3 cells were TUNEL positive ($n = 3$; $P < 0.05$), which indicates that SEB selectively induced death in V-β8 cells. Parallel groups of mice were pretreated for 24 hours with NFV/RIT, vehicle control, NFV alone, or RIT alone, followed by treatment with 20 mg D-gal and 6.5 μg SEB. NFV/RIT-treated mice had improved survival compared with vehicle control (89%, $n = 9$ vs. 27%, $n = 11$; $P < 0.01$). Survival of vehicle-treated mice was not significantly different from that of mice treated with NFV alone (30%; $n = 10$; $P = 0.25$) or RIT alone (20%; $n = 10$; $P = 0.25$). In addition, NFV/RIT, when given 4 hours after SEB/D-gal, was associated with improved survival compared with control (60%; $n = 10$; $P < 0.05$; Figure 1C). NFV/RIT treatment was also associated with reduced V-β8 T cell apoptosis compared with vehicle control (Figure 1D).

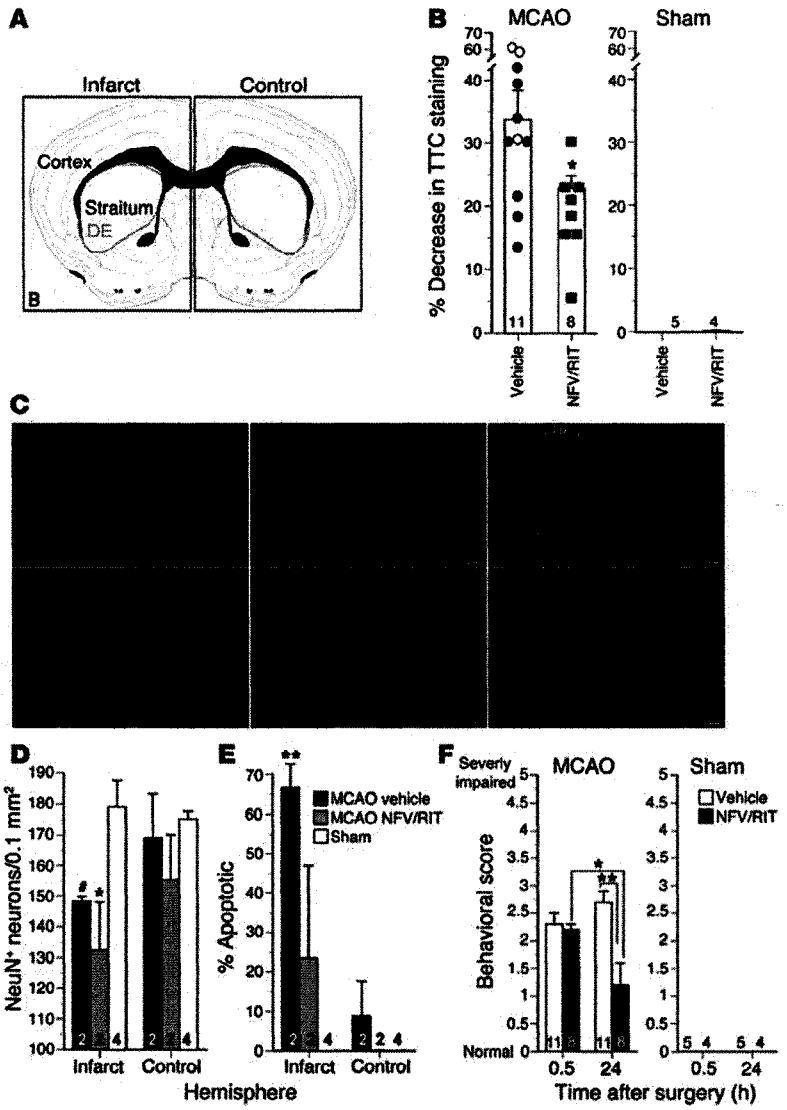


**Figure 2**
Effects of NFV/RIT on infarct size, neuronal loss, and behavioral impairment following 1 hour of MCAO and 24 hours of reperfusion. (**A**) Schematic representation of coronal forebrain sections were analyzed. Infarcted and control hemispheres are indicated. DE, diencephalon. The tissue areas analyzed by TTC as shown in **B** are indicated in blue. The areas analyzed for NeuN and TUNEL reactivity as shown in **D** and **E** are indicated in orange. (**B**) Mice pretreated with NFV/RIT exhibit a smaller infarct 24 hours after surgery, as assessed by TTC staining, relative to mice pretreated with vehicle or control (sham) mice (*$P < 0.05$, Student's $t$ test). Open circles, no pretreatment; filled circles, vehicle pretreatment; filled squares, NFV/RIT pretreatment. (**C**) NFV/RIT protects neurons from apoptotic-like death. (**D**) Quantitation of overall neuronal loss following MCAO or sham surgery. Both vehicle- and NFV/RIT-treated animals exhibit a comparable reduction in neuronal number following MCAO (#$P = 0.08$, *$P < 0.05$, ANOVA, post-hoc Dunnett $t$ test). (**E**) NFV/RIT-treated animals are protected from apoptotic-like death following MCAO surgery. The majority of remaining NeuN-positive cells in vehicle-treated mice are apoptotic, while TUNEL reactivity is significantly reduced in NFV/RIT-treated animals (**$P < 0.01$, ANOVA, post-hoc Dunnett $t$ test). (**F**) NFV/RIT improves neurological recovery following MCAO. Animals tested immediately after MCAO surgery (0.5 hours) show equivalent motor deficits. After 24 hours of reperfusion, NFV/RIT exhibit significant behavioral improvement relative to 0.5 hours or vehicle-treated cells. *$P < 0.05$; **$P < 0.01$, ANOVA, post-hoc Tukey test. Data represent mean ± SEM.

Given the substantial reduction in apoptosis and the improvement in survival afforded by NFV/RIT in the Jo-2 and SEB models, we next assessed the impact of NFV/RIT on cerebral injury in the middle cerebral artery occlusion (MCAO) model of focal ischemia. C57BL/6 mice were pretreated by oral gavage with either NFV/RIT or vehicle (2% EtOH) 24, 16, and 8 hours before sham or MCAO surgery (vehicle control, sham surgery, $n = 7$; vehicle control, MCAO, $n = 10$; NFV/RIT, sham surgery, $n = 7$; NFV/RIT, MCAO surgery, $n = 10$). A fifth cohort received MCAO surgery without NFV/RIT or vehicle pretreatment ($n = 5$). Infarct size in the striatum and cortex was assessed by 2,3,5-triphenyltetrazolium (TTC) staining (Figure 2A). After 1 hour of MCAO followed by 24 hours of reperfusion, vehicle-treated animals or mice that were not orally gavaged exhibited a 34% reduction in TTC staining (Figure 2B). Infarct size as measured by TTC staining was 23% ($P < 0.05$ compared with control) in the NFV/RIT treatment group (Figure 2B). We next assessed neuronal number in the striatum by immunodetection of the neuron-specific marker NeuN (24). Both vehicle- and NFV/RIT-treated animals exhibited a comparable, approximately 20% loss of NeuN-positive neurons after 1 hour of MCAO and 24 hours of reperfusion (Figure 2, C and D). However, NFV/RIT significantly reduced apoptotic-like death, as detected by TUNEL/NeuN double labeling (Figure 2, C and E). In vehicle-treated animals, 67% of the remaining NeuN-positive neurons in the striatum were actively undergoing DNA fragmentation 24 hours after surgery (Figure 2, C and E); however, only 24% ($P < 0.01$) of NeuN-positive neurons were TUNEL reactive in NFV/RIT-treated mice (Figure 2, C and E). Finally, we determined whether the neuroprotection afforded by NFV/RIT pretreatment manifested in improved behavioral recovery. Neurological deficits in motor function were assessed using an expanded 6-point scale modified from refs. 25, 26 (see Methods). Animals were tested immediately after 0.5 hours of MCAO and again 24 hours after reperfusion. NFV/RIT-pretreated animals exhibited comparable motor deficits after 1 hour of MCAO compared with vehicle-treated or control animals (no pretreatments) but evident behavioral improvement 24 hours after surgery (Figure 2F), consistent with the reduction in apoptotic loss and reduced infarct size.

To analyze the antiapoptotic mechanism of NFV/RIT in vivo, we compared apoptotic signaling in Jurkat T cells stimulated in

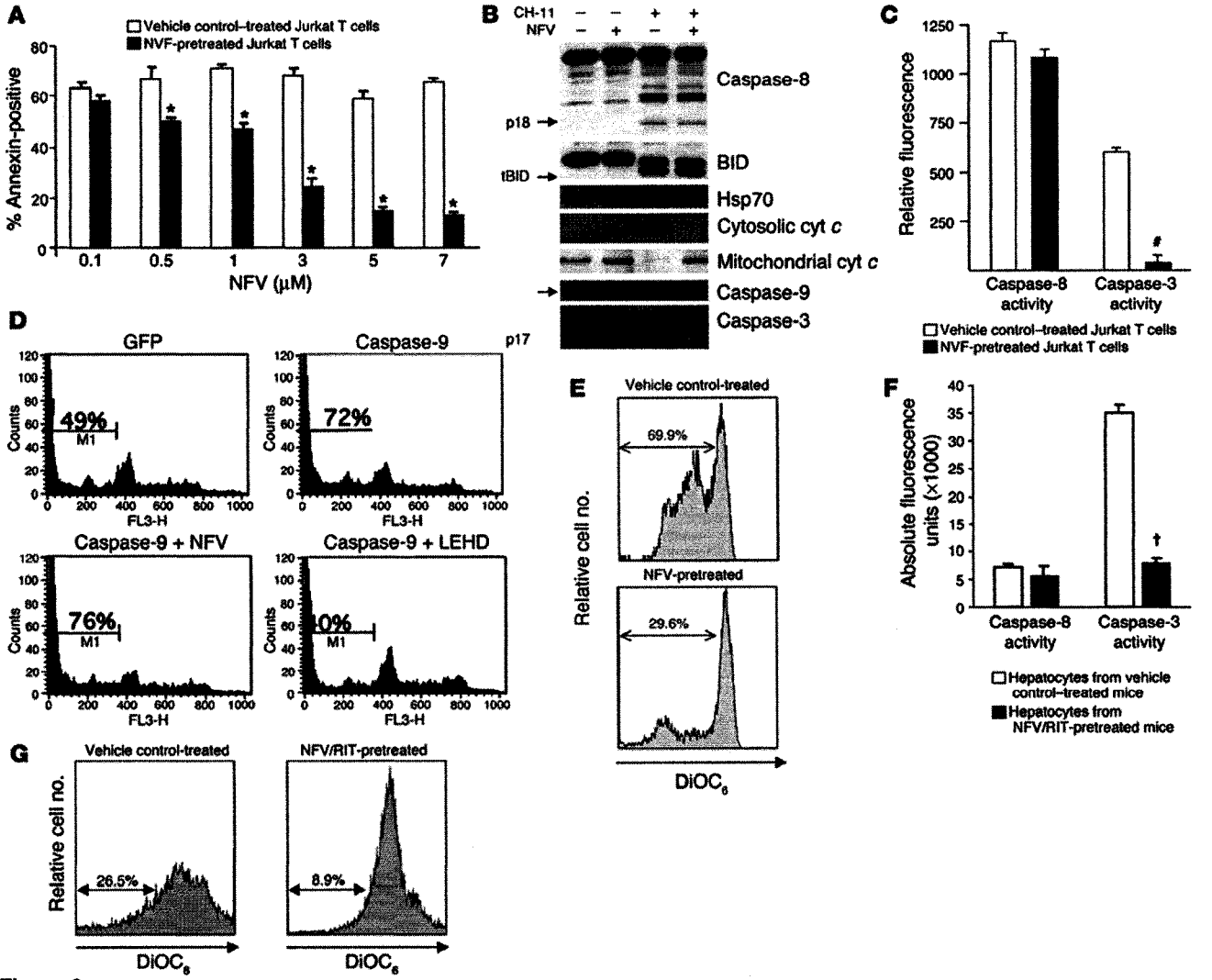


**Figure 3**

Effect of NFV on apoptotic signaling events in vitro and in vivo. (**A**) Jurkat T cells were stimulated with agonistic anti-Fas antibody (CH-11) in the presence or absence of varying concentrations of PI and analyzed for annexin positivity. *$P < 0.05$. (**B**) Western blot analysis of the Fas signaling events of caspase-8, -9, and -3 cleavage, BID cleavage, or cytosolic translocation of cytochrome *c* (cyt *c*) in Jurkat T cells treated or not treated with CH-11 with or without NFV. tBID, truncated BID. (**C**) Caspase-8 and caspase-3 activity was also assessed in Jurkat T cells stimulated with CH-11 in the presence or absence of NFV. #$P < 0.01$. (**D**) Jurkat cells were transiently transfected by a GFP plasmid or a caspase-9 GFP plasmid, treated or not treated with 7 μM NFV or 100 μM LEHD, cultured for 6 hours, stained with PI, and analyzed by cytofluorometry for hypoploidy. (**E**) Jurkat cells stimulated with CH-11 in the presence or absence of NFV were analyzed for loss of $DiOC_6$ retention. Hepatocytes isolated from mice receiving Jo-2 with NFV/RIT or control (as in Figure 1) were also analyzed for caspase-8 and caspase-3 activity (**F**) and loss of $DiOC_6$ retention (**G**). †$P < 0.005$.

vitro with CH-11 anti-Fas antibody with the apoptotic signaling in hepatocytes isolated from mice treated in vivo with IV Jo-2 anti-Fas antibody. In vitro pretreatment of Jurkat T cells with NFV followed by stimulation with CH-11 resulted in a dose-dependent reduction in apoptosis (Figure 3A). NFV-pretreated Jurkat T cells had similar caspase-8 cleavage and activity and Bid cleavage as seen in vehicle control cells. However, mitochondrial membrane permeability ($\Delta\Psi_m$), cytochrome *c* release, caspase-9 cleavage, and caspase-3 cleavage and activity were all reduced by NFV pretreatment (Figure 3, B–E), which suggests that NFV inhibition of apoptosis occurs upstream of caspase-9 in the apoptotic pathway. Moreover, transient expression of caspase-9 in Jurkat T cells resulted in hypoploidy that was not inhibited by NFV yet was inhibited by the caspase-9 inhibitor, LEHD, which confirms that NFV blocks apoptosis upstream of caspase-9 activation. Similar analyses were performed ex vivo on hepatocytes isolated from mice pretreated with either NFV/RIT or vehicle control and subsequently challenged with IV Jo-2. In these cells, caspase-8 activation was unaltered by NFV/RIT pretreatment, whereas caspase-3 activity was significantly ($P < 0.005$) inhibited (Figure 3F). Additionally, loss of $\Delta\Psi_m$ was evident in vehicle control hepatocytes but was blocked in the hepatocytes of mice that received NFV/RIT pretreatment (Figure 3G). Therefore, in vitro and in vivo, PIs inhibit mitochondrial $\Delta\Psi_m$ and subsequent postmitochondrial signaling events.

To confirm that the effect of NFV localizes to mitochondria, we treated isolated mitochondria with Vpr, atractyloside (ATR), Bax

and determined that NFV inhibits mitochondrial swelling induced by all 3 stimuli (Figure 4A). Inhibition of Bax-induced apoptosis might indicate a loss of Bax activation and translocation or a lack of effect of Bax on $\Delta\Psi_m$ (reviewed in refs. 27, 28). We therefore directly assessed whether NFV inhibited mitochondrial translocation and activation of Bax. We stimulated cells through the Fas receptor in the presence of NFV or DMSO vehicle control and analyzed them for nuclear morphology using Hoechst 33342 staining and for Bax activation by immunofluorescence using an antibody specific for the activated conformation of Bax. Control (untreated) cells had no evidence of Bax activation and had intact nuclei. Fas-stimulated cells exhibited both Bax activation with punctate Bax staining and fragmented nuclei, consistent with apoptosis. NFV-pretreated cells showed punctate staining for activated Bax, yet no nuclear fragmentation was observed (Figure 4B).

Furthermore, we induced apoptosis by overexpression of Bax. Bax was cotransfected with GFP, and consequently apoptosis was assessed specifically in the GFP-positive cell populations. NFV treatment inhibited $\Delta\Psi_m$ loss induced by the overexpression of Bax (Figure 4C). Together, therefore, our data indicate that the antiapoptotic action of NFV occurs at the level of mitochondria, downstream of Bax translocation and activation, but invoking mitochondrial $\Delta\Psi_m$.

Mitochondrial loss of $\Delta\Psi_m$ is coincident with the opening of the mitochondrial permeability transition pore complex (PTPC). These events allow the release of cytochrome *c* into the cytosolic compartment, which, in the presence of dATP, results in the formation of a complex between Apaf-1 and procaspase-9 known as the apoptosome. This results in activation of procaspase-9 (29, 30), which in turn activates the downstream effector caspase-3 (31). A key regulator in this process, therefore, is the mitochondrial PTPC, which is composed of the peripheral benzodiazepine receptor (PBR), adenine nucleotide translocator (ANT), voltage-dependent anion channel (VDAC), as well as other proteins (32). We therefore assessed apoptosis in the presence or absence of NFV in WT yeast or yeast deficient in both isoforms of VDAC or all 3 isoforms of ANT. HIV Vpr initiates apoptosis through binding ANT with affinities in the nanomolar range (33), whereas Vpr does not bind to VDAC in vitro (33). Consistent with prior reports, Vpr was able to induce yeast death only if ANT was present (Figure 5, A and B). Since VDAC and ANT physically interact, and form the principal pore channel of PTPC in a cooperative manner (34, 35), absence of VDAC also abrogated the ability of Vpr to cause death (Figure 5A). $H_2O_2$ also induces apoptosis in an ANT-dependent manner, potentially through oxidation of thiol groups within ANT (36–38). Like Vpr, $H_2O_2$ only induced apoptosis if ANT was present, and VDAC was required as well (Figure 5A). Next, we assessed the ability of NFV to inhibit apoptosis in WT yeast following stimulation with Vpr or $H_2O_2$. WT yeast underwent Vpr- and $H_2O_2$-induced apoptosis, which was inhibited in a dose-dependent manner by NFV treatment (Figure 5B), arguing that NFV requires the presence of ANT, VDAC, or both.

To further examine the involvement of the components of the PTPC in NFV-mediated inhibition of apoptosis, we next used chemical ligands that selectively interact with different components of the PTPC, causing it to open and resulting in subsequent loss of $\Delta\Psi_m$. PK11195 is an agonist of the PBR (39, 40), ATR is an agonist of ANT (41), and staurosporine (STS) is an agonist of VDAC (42, 43). Jurkat T cells were pretreated with NFV or vehicle control and subsequently treated with these agonists and analyzed for apoptosis. Treatment with PK11195 or STS resulted in apoptosis (Figure 6A), loss of $\Delta\Psi_m$ (Figure 6B), cytochrome *c* release, caspase-9 cleavage, caspase-3 cleavage and activation, and poly (ADP-ribose) polymerase (PARP) cleavage (Figure 6, C and D) that were not altered by NFV, which suggests that NFV does not alter PBR or VDAC-initiated loss of $\Delta\Psi_m$. Repeating these experiments with the ANT-specific agonist ATR resulted in a loss of $\Delta\Psi_m$, cytochrome *c* release, caspase-9 cleavage, caspase-3 cleavage, PARP cleavage, and caspase-3 activation that were inhibited by NFV (Figure 6, A–D). These differential results suggest that NFV acts as an inhibitor of ANT-dependent PTPC opening.

To confirm that NFV can act specifically with ANT to inhibit its pore function, we used proteoliposomes reconstituted with either entire PTPC or with ANT alone, which release a fluorescent dye following pore opening (44). Consistent with our cellular data, treatment of PTPC liposomes with ATR results in significant fluorescence release that was progressively inhibited by a range (0.1–10 μm) of increasing doses of NFV (Figure 7A). We

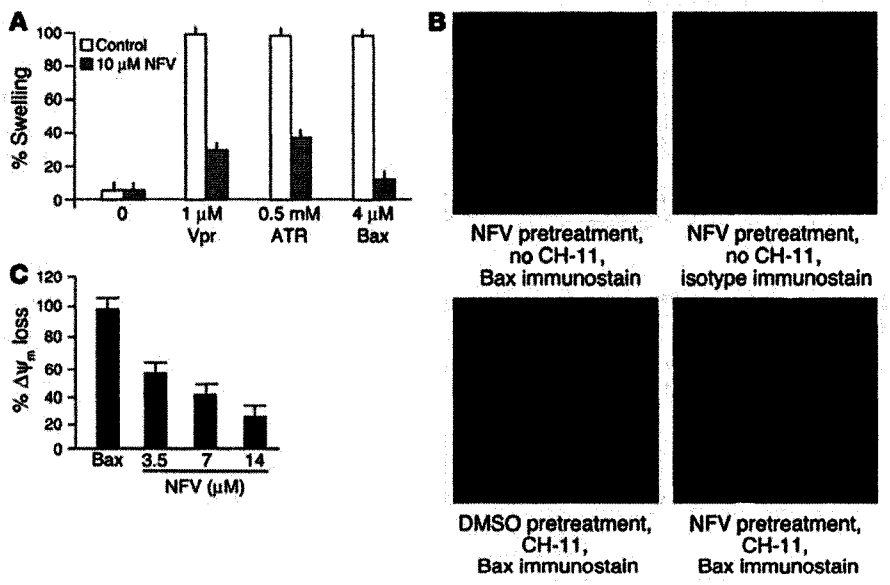


**Figure 4**

NFV blocks Bax-induced apoptosis but not Bax activation. **(A)** Mouse liver mitochondria were incubated with 10 μM of NFV followed by 1 μM Vpr-derived peptide, 0.5 mM ATR, or 4 μM Bax while absorption was assessed at 545 nm. The loss of absorption induced by 0.5 mM ATR within 20 minutes was considered at 100% of large amplitude swelling. All experiments were reproduced 3 times. **(B)** Jurkat T cells were treated with an agonistic anti-Fas antibody in the presence or absence of NFV and stained with Hoechst 33342 for nuclear morphology, an antibody (or isotype control) specific for activated Bax, and an Alexa Fluor–conjugated secondary antibody. All cells were stained with Hoechst and varying combinations of NFV or DMSO, CH-11, and anti-Bax or isotype antibody as indicated. **(C)** Jurkat T cells were transfected with Bax, and immediately following transfection, NFV or control was added and $\Delta\Psi_m$ was assessed.

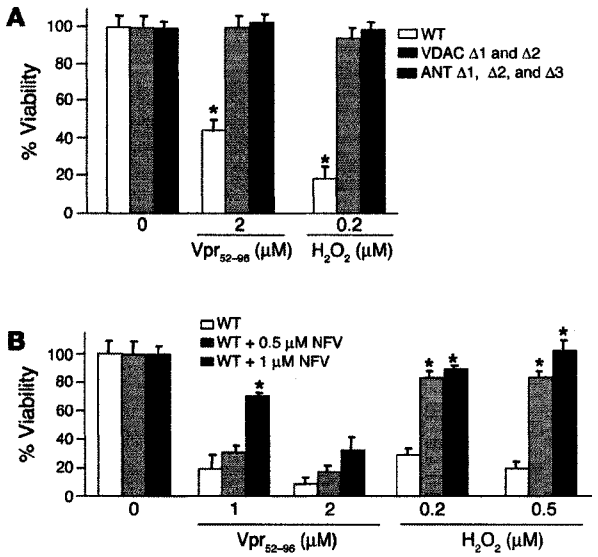


**Figure 5**
Effects of NFV on apoptosis in yeast. (**A**) WT yeast or yeast deficient in both isoforms of VDAC (VDAC Δ1 and Δ2) or 3 isoforms of ANT (ANT Δ1, Δ2, and Δ3) were treated with the apoptosis-inducing agents Vpr peptide (residues 52–96) or $H_2O_2$ and analyzed for viability. (**B**) WT yeast treated with varying doses of NFV was treated with the same apoptosis inducers and analyzed for viability. Results are representative of 3 independent experiments. *$P < 0.05$.

next assessed whether NFV could act directly upon ANT to inhibit its pore function. ANT liposomes were created and treated with 2 distinct ANT ligands, ATR (Figure 7B) and Vpr (Figure 7C). Each ligand resulted in a dose-dependent release of fluorescence from the ANT liposomes that in turn was inhibited ($P < 0.05$) in a dose-responsive manner by NFV.

## Discussion

Here we provide evidence that HIV PIs have the ability to meaningfully impact apoptosis in vivo in a variety of animal models and that this effect localizes to mitochondrial release of proapoptotic factors. Moreover, our in vitro data suggest that NFV acts to inhibit the pore function of the ANT subunit of the mitochondrial PTPC. This effect of NFV permits the premitochondrial signaling events of death receptor–initiated apoptosis yet inhibits mitochondrial loss of $\Delta\Psi_m$ and the subsequent formation of the apoptosome and activation of caspase-9 and caspase-3.

This mechanism of action offers insight into the question of whether cells that have undergone some changes of apoptosis (e.g., caspase-8 activation) but not others (e.g., $\Delta\Psi_m$) will still be fated to death. Hepatocytes from Jo-2–treated mice dosed with NFV/RIT maintained caspase-8 activation but not the mitochondrial and postmitochondrial signaling events. Consequently, analysis of these mice affords an opportunity to address the long-term outcome of tissues rescued from death by NFV/RIT treatment. First, since no mortality was observed between days 3 and 30, NFV/RIT treatment prevents rather than delays death. Second, serum AST remains lower in NFV/RIT-treated mice, which suggests maintenance of hepatocyte viability and function. Third, hepatic histology of NFV/RIT-treated mice is preserved at day 30, which demonstrates a lack of delayed tissue damage in mice surviving as a consequence of NFV/RIT therapy. Comparable results were

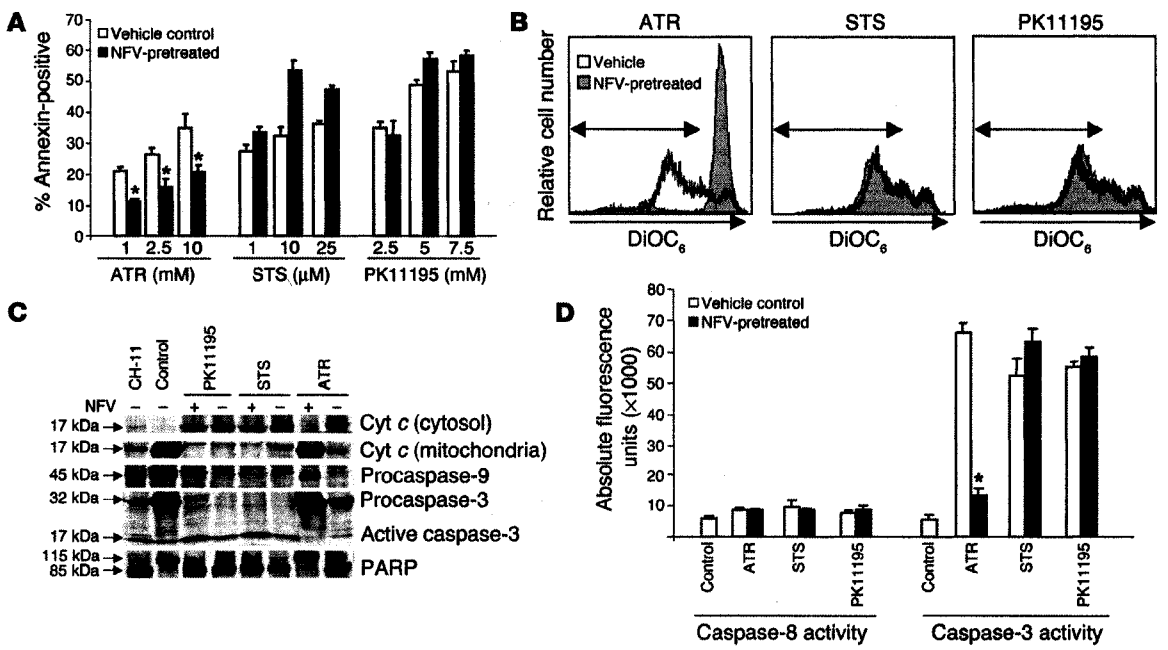


**Figure 6**
Effects of NFV on the apoptosis-inducing abilities of the selective PTPC agonists. Jurkat T cells were treated with either the ANT agonist ATR, VDAC agonist STS, or PBR agonist PK11195, in the presence or absence of PI, and analyzed for annexin positivity (**A**), loss of $DiOC_6$ retention (**B**) caspase-9, caspase-3, and poly (ADP-ribose) polymerase (PARP) cleavage and cytosolic release of cytochrome *c* (**C**), and caspase-8 and caspase-3 activity (**D**). Results are representative of 3 independent experiments. *$P < 0.01$.

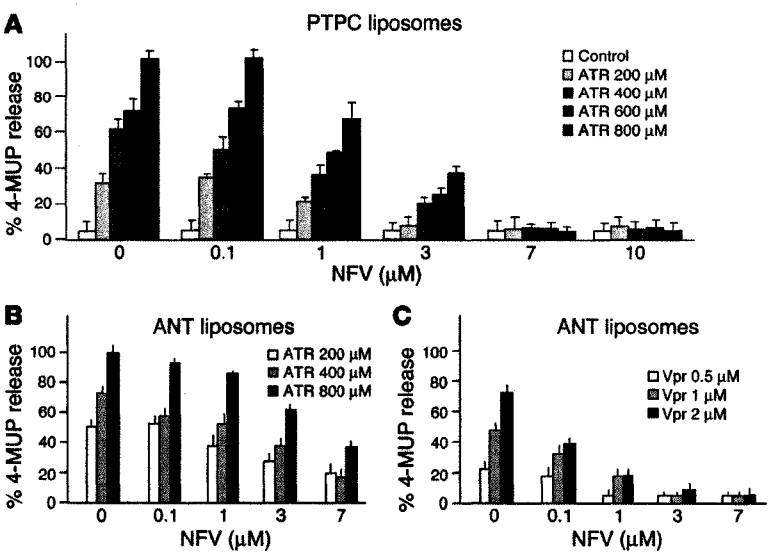


**Figure 7**
Effects of NFV on PTPC or ANT pore function. (**A**) Proteoliposomes containing PTPC complexes were treated with NFV, stimulated with ATR, and analyzed for fluorescence release. Proteoliposomes containing ANT were treated with NFV and analyzed for fluorescence release following stimulation with ATR (**B**) or Vpr peptide (residues 52–96) (**C**). Results are representative of 3 independent experiments.

observed in the MCAO model of focal ischemia. NFV/RIT did not affect necrotic loss or neuronal damage in the ischemic core, nor did pretreatment improve behavioral indices when animals were tested after recovery from the anesthetic, 30 minutes after the 1-hour occlusion. However, NFV/RIT significantly reduced subsequent apoptotic-like death observed over the 24-hour reperfusion period, markedly improving neurological scores as a consequence. Therefore, blocking the mitochondrial events of apoptosis represents a viable approach to preventing rather than delaying cell death and a potential means of improving function in pathologic processes involving exaggerated apoptosis.

It is noteworthy that the antiapoptotic effects of NFV/RIT persist even if administered after the apoptosis-initiating event in mice receiving SEB/D-gal, and survival is improved when NFT/RIT is administered 4 hours later. Although the maximum duration between apoptotic insult and NFV/RIT administration that is still associated with improved outcome remains to be defined, these observations suggest the increased likelihood that such agents might afford clinically useful protection.

Recently, the role of ANT in mitochondrial permeability transition has been questioned. Whereas ANT has been widely regarded as being essential for mitochondrial depolarization and consequent cytochrome *c* release, apoptosome formation, and apoptosis, a recent report directly challenges that role. Mice were constructed with a complete deficiency in both isoforms of ANT within liver tissues (45). Hepatocytes from these mice had compensatory upregulation of cytochrome *c* and of cytochrome *c* oxidase. Mitochondria from these livers contain functional PTPCs, which release cytochrome *c*; however, 3-fold more calcium signal was required to induce the permeability transition than in WT cells. Thus, although the knockout of ANT-1 and ANT-2 genes in hepatocytes does not abolish mitochondrial outer membrane permeabilization induced by calcium in absolute terms, it does significantly reduce the sensitivity of these mitochondria to calcium-induced PTPC opening. Our current data are consistent with some findings discussed in that report; both inhibition of ANT by PIs and genetic absence of ANT result in abrogated mitochondrial response to ANT ligands, including ATR. However, unlike cells from ANT-deficient livers, which remain sensitive to apoptosis induced by Fas ligand and TNF-α, PI-treated cells acquire resistance to Fas signaling. It is not clear to what extent adaptive responses involving expression of other mitochondrial carrier proteins (which might assume the functions of ANT) may compensate for the defect in ANT-1 and ANT-2, at either the bioenergetic level or the cell death regulatory level (46). By no means do the data from the knockout model exclude the possibility that pharmacologic apoptosis modulation can be achieved through inhibition of ANT function.

Examining the x-ray crystal structure of ANT, we studied whether NFV can be predicted to interact with ANT. Computer simulations of the interactions of NFV with ANT indicated a putative binding site on the matrix side of the transporter protein. Based on this simulation, NFV is predicted to bind close to helices 3 and 5 of ANT (Figure 8). Binding also involves part of the loop connecting helices 3 and 4 (loop M2 in Figure 8), which has been proposed as the ADP binding site (37). Several hydrogen bonds appear to be made between NFV and ANT, in particular with residues K162, G242 (backbone), M239 (backbone), and R243 (Figure 8). Hydrophobic contacts between NFV and ANT constitute the segment around S166 as well as the side chain of R139.

Since multiple apoptotic signals, including death receptor ligation, chemotherapeutics, BH3-only Bcl2 family members, UV radiation, and others converge upon mitochondria, drugs that target mitochondrial regulators of apoptosis, such as NFV, are attractive therapeutic candidates. Our data provide the basis for the evaluation of NFV or related compounds as in vivo inhibitors of apoptosis in non-HIV disease states characterized by excessive apoptosis.

## Methods

### *Mouse treatments*

Mice received either NFV/RIT in 2% ethanol or vehicle control (2% ethanol) by oral gavage every 8 hours. Animal treatments were reviewed and approved by the Mayo Foundation Institutional Animal Care and Use Committee, the NRC/IBS Animal Care Committee, and the University of Ottawa Animal Care Committee. Plasma concentrations of NFV and RIT were measured simultaneously using liquid chromatography with tandem mass spectrometry. The lower limit of quantitation for NFV and RIT was 2.5 ng/ml. The accuracy of quality control samples analyzed simultaneously with the study samples ranged from 83.7% to 107.5% for NFV and 105.0% to 116.5% for RIT. The within-run variability for 3 replicative analyses of the quality control samples was less than 9.7% for both NFV and RIT. This assay has been cross-validated as part of the International Interlaboratory Quality Control Program for Therapeutic Drug Monitoring in HIV Infection (47). To determine a dosing regimen that would result in relevant plasma concentrations, we treated 6- to 8-week-old BALB/c and C57BL/6 mice with 250 mg/kg of NFV (Agouron Pharmaceuticals Inc.) every 8 hours, yet plasma concentrations were undetectable 6 hours after dosing. Since coadministration of RIT in humans significantly increases

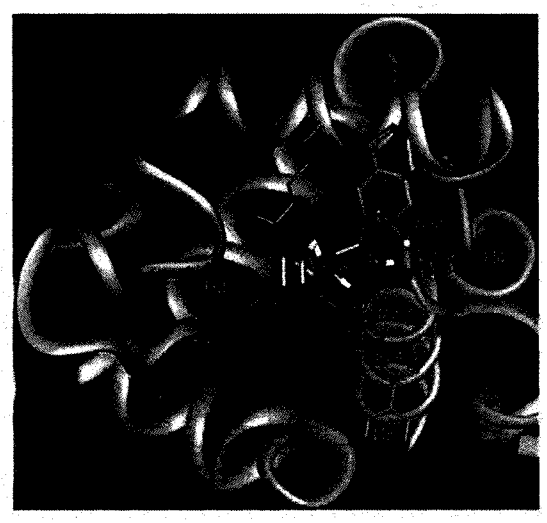

**Figure 8**
**Computer-simulated model of NFV interaction with ANT. Close-up of the proposed binding mode of NFV to the matrix side of ANT. Parts of helices 1, 3, 4, and 5 (H1, H3, H4, and H5) are shown. Loop M2, connecting helices 3 and 4, is shown in red. Hydrogen bonds are displayed as dotted lines. Side chains or backbone atoms of selected residues are shown (see Methods). The PI is colored according to atom types: C, green; O, red; N, blue; S, yellow.**

NFV levels compared with NFV alone (48), we treated mice every 8 hours with 125 mg/kg NFV and 13 mg/kg RIT (Abbott Laboratories). Eight-hour NFV trough levels, ranging from 1,199 to 1,258 ng/ml, were comparable to concentrations observed in HIV-infected patients using NFV. We also assessed whether C57BL/6 mice treated with this dose of NFV/RIT achieved detectable drug levels in the brain. NFV and RIT concentrations in brain tissues were determined after the tissues were washed extensively with PBS, blotted dry with filter paper, placed in 5 ml of 0.1 M phosphoric acid, and homogenized using a polytron. Supernatants were analyzed as described above for drug level determination. Analysis of whole brains revealed levels of NFV between 682 and 986 μg/g of brain tissue. We therefore opted to assess the in vivo antiapoptotic effects of the combination of NFV and RIT using this dosing regimen.

### *Fas-induced liver failure*

Six-week-old female C57BL/6 mice (Charles River Laboratories) received the indicated doses of Jo-2 anti-Fas antibody (BD Biosciences – Pharmingen) by tail vein injection. Moribund animals, or animals who survived until the indicated time points, were sacrificed by $CO_2$ asphyxiation. Clinical chemistries were performed on serum obtained from 3 mice from each treatment group at 4 and 24 hours after Jo-2 injection. Quantitation of hepatocyte apoptosis by TUNEL assay (Roche Diagnostics Corp.) was averaged from results analyses performed in a blinded manner by 4 reviewers.

### *SEB-induced shock*

Six-week-old female BALB/c mice (Harlan) received 20 mg D-gal (Sigma-Aldrich) and 6.5 μg SEB (Toxin Technology Inc.) intraperitoneally. Animals were euthanized if they became moribund, laterally recumbent, or hypothermic (rectal temperature <32°C) at the indicated time points. Spleens were harvested and splenocytes isolated mechanically with plastic mesh. Following red cell lysis and removal of B cells by incubation with nylon wool (1 hour, 37°C; Accurate Chemical and Scientific Corp.), purified T cells were stained with monoclonal anti-mouse V-β8-FITC antibody (clone F23.1), V-β3-FITC antibody (Clone KJ25), or appropriate isotype control (BD Biosciences – Pharmingen) and then washed with PBS and fixed with 1% paraformaldehyde. Dual staining with TUNEL-TMR red (Roche Diagnostics Corp.) was performed as per the manufacturer's instructions.

### *Cerebral ischemia produced by MCAO*

C57BL/6 mice (20–23 g) were obtained from Charles River Laboratories. Under temporary isofluorane anesthesia, mice were subjected mice to MCAO using an intraluminal filament as previously described (49). After 1 hour of MCAO, the filament was withdrawn, blood flow restored to normal by laser Doppler flowmetry, and wounds sutured. Beginning 24 hours before surgery, mice received 3 oral gavages, 8 hours apart, of either NFV/RIT or vehicle. Following 24 hours of reperfusion, mice were anesthetized with $CO_2$ and sacrificed by either decapitation or lethal injection with sodium pentobarbital and transcardially perfused with 10 mM PBS (10 mM sodium phosphate and 154 mM NaCl) followed by 3.7% paraformaldehyde in 10 mM PBS. Behavioral impairment following MCAO was assessed at 30 minutes after ischemic surgery when animals had recovered from the anesthetic and 24 hours after reperfusion by 2 investigators blind to the treatment of the mice. A modified 6-point scale was used (25, 26): 0, normal; 1, mild turning behavior with or without inconsistent curling when picked up by tail and less than 50% attempts to curl to the contralateral side; 2, mild, consistent curling and more than 50% attempts to curl to the contralateral side; 3, strong and immediate consistent curling, mouse holds curled position for more than 1–2 seconds, and mouse's nose almost reaches tail; 4, severe curling progressing into barreling and loss of walking or righting reflex; 5, comatose or moribund. Behavioral scores were averaged within treatment groups for statistical analysis. In unfixed tissue, infarct size was measured by a colorimetric staining method using TTC, as described previously (50). Brains were removed and cut into three 2-mm-thick coronal slices through forebrain, which were separated into left and right hemispheres and stained with 5 ml of 2% TTC per hemisphere for 90 minutes at 37°C. The tissue was rinsed with saline, and the formazan product solubilized in ethanol/DMSO (1:1). After a 24-hour incubation in the dark, the red solvent extracts were diluted 1:20 with fresh ethanol/DMSO solvent in triplicate, absorbance was measured at 485 nm in a spectrophotometer, and the values were averaged. Percent decrease in brain TTC staining was calculated using the following equation: percent decrease = [100 – (absorbance of contralateral hemisphere/absorbance of ischemic hemisphere) × 100]; and the values for the ischemic and contralateral sides of the brain in the same animal were compared. Perfused brains were postfixed for 24 hours in 3.7% paraformaldehyde in 10 mM PBS and cryoprotected in 20% sucrose solution in 10 mM PBS containing 0.001% sodium azide. Serial coronal sections (10 μm) were cryostat cut (Leica Microsystems Inc.). Neuronal apoptosis was confirmed in fixed tissue by reaction for TUNEL (Roche Diagnostics Corp.) and immunolabeling for the neuronal nuclear marker NeuN (Chemicon International) using a Cy3-conjugated anti-mouse IgG secondary antibody (Jackson ImmuoResearch Laboratories Inc.) as described (51). Antibodies were diluted in antibody buffer (10 mM PBS, 0.3% Triton X-100, and 3% BSA). We evaluated immunofluorescence using on a DMRXA2 microscope (Leica Microsystems Inc.) equipped for epifluorescence. The number of NeuN-positive/TUNEL-negative cells was counted and tissue area was measured using the Advanced Measurements Module of OpenLab version 3.17 (Improvision) in 2 adjacent sections of both ipsilateral and contralateral striatum and cortex. Means were averaged across treatment groups.

### *Cell culture and apoptosis induction in vitro*

Jurkat T cells (ATCC) were cultured in RPMI media (Mediatech Inc.), supplemented with 10% heat-inactivated FBS (Atlanta Biologicals), and peni-

cillin/streptomycin (Invitrogen Corp.) at 37°C in 5% $CO_2$. Where indicated, cells were incubated with 7 μM NFV or 20 μM z-VAD-fmk (R&D Systems) or vehicle (DMSO) overnight prior to induction of apoptosis with indicated doses of CH-11 anti-Fas antibody (Upstate), ATR (Sigma-Aldrich), STS (Calbiochem), or PK11195 (Sigma-Aldrich).

### *Transfection experiments*

Transient transfection of Jurkat cells with vectors containing a pEGFP gene (pEGFP-N2; BD Biosciences), a Bax-GFP gene (kindly provided by Shigemi Matsuyama, Research Center for Allergy and Immunology, Kanagawa, Japan; ref. 52), and caspase-9-GFP (kindly provided by P. Mehlen, Apoptosis Cancer and Development Laboratory, Lyon, France; ref. 53). Cells were cultured in RPMI 1640, 10% FBS, and 1% L-glutamine without antibiotics. Two days before transfection, cells were passed at $1.5 \times 10^5$ cells/ml. For electroporation, $1 \times 10^7$ cells were pelleted, resuspended in 250 μl of 10% FBS-RPMI 1640, mixed with 250 μl of 20 μg DNA, and incubated for 10 minutes at room temperature (RT). The DNA/cell suspension was transferred to a 4-mm cuvette, and electroporation was performed at 10 ms/325 V using a square wave electroporator (Bio-Rad Laboratories). After 10 minutes at RT, cells were diluted to 20 ml in complete medium without antibiotics and cultured at 37°C under 5% $CO_2$. NVF, DEVD (Bachem), and LEHD (Bachem) were added following electroporation (54).

### *Hepatocyte isolation*

Four hours after treatment with 7.5 μg of Jo-2 antibody, mice were euthanized with pentobarbital (60 mg/kg; Abbott Laboratories) and hepatocytes isolated via a 2-step collagenase digestion (55). Following red cell lysis, hepatocytes were enumerated and evaluated for apoptosis through loss of $\Delta\Psi_m$ and caspase-8 and caspase-3 activity.

### *Assays of apoptotic signaling: TUNEL*

Briefly, $1 \times 10^6$ cells were fixed with 2% paraformaldehyde, permeabilized with 0.1% Triton X-100 and 0.1% citrate, and stained with TUNEL as per the manufacturer's directions (Roche Diagnostics Corp.).

### *DNA content*

For cell cycle analysis, cells ($5 \times 10^5$/ml) were spun down and fixed in 70% ice-cold ethanol/PBS, added dropwise while vortexing, kept at -20°C, and centrifuged. Cells were resuspended in 1 ml PBS containing RNAse and 50 μg/ml propidium iodide (Invitrogen Corp.) and analyzed in a cytofluorometer (56).

*Annexin V and propidium iodide staining.* Fifty microliters of annexin binding buffer (BD Pharmingen) was added to $1 \times 10^6$ cells in 500 μl of media followed by 2 μl of annexin V-FITC (BD Pharmingen) and 1 μl of propidium iodide (Sigma-Aldrich). The mixture was vortexed and incubated for 30 minutes at 37°C and then subjected to FACS analysis.

*Western blot analysis.* We subjected 40–60 μg of protein from whole cell lysates to SDS-PAGE. Following transfer, PVDF membranes (Millipore) were probed with antibodies to caspase-3 (1 μg/ml; Gene Therapy Systems Inc.), caspase-9 (1 μg/ml; Medical & Biological Laboratories Co.), cytochrome *c* (1 μg/ml; BD Biosciences — Pharmingen), or PARP (1 μg/ml; BD Biosciences — Pharmingen). Following incubation with goat anti-mouse HRP (1:10,000; Amersham Biosciences), an enhanced chemiluminescence assay (Amersham Biosciences) was used to detect the proteins of interest. Where indicated, mitochondria were separated from cytosols for subcellular detection of cytochrome *c*, as previously described (57). Briefly, cell lysates were harvested and centrifuged twice at 15,000 *g* (4°C) for 15 minutes to fractionate the cytosolic (supernatant) fraction from the mitochondrial pellet. Aliquots of cytosolic or mitochondrial protein (200 μg) were separated by 4–15% gradient SDS-PAGE and probed with monoclonal antibody against cytochrome *c*.

*Fluorometric caspase-8 and caspase-3 activity.* We resuspended 150-μg aliquots of whole cell lysates in reaction buffer with the appropriate fluorogenic caspase substrate (IETD for caspase-8 and DEVD for caspase-3) (R&D Systems). Activity was determined with a fluorescence plate reader (BIOTEK Inc.) at an excitation wavelength of 400 nm and emission of 505 nm.

*$DiOC_6$ staining.* We incubated $1 \times 10^6$ intact cells with 40 nM $DiOC_6$ (Invitrogen Corp.) for 30 minutes at 37°C prior to FACS analysis.

### *Mitochondrial swelling*

Mitochondria were purified from BALB/c mouse livers on a Percoll gradient (58) and were stored on ice for up to 4 hours. For determination of large amplitude swelling, 5 μl of mitochondria (0.5 mg protein/ml) was added to 200 μl of swelling buffer [0.2 M saccharose, 10 mM TRIS-3-(N-morpholino)-propanesulfonic acid, 5 mM propidium iodide, 1 mM EGTA, 0.35 mM rotenone, pH 7.4], and light absorption was recorded for 20 minutes at 545 nm in a microtiter plate (TECAN GENios). The loss of absorption induced by 0.5 mM ATR was used as a positive control to define maximal large amplitude swelling. For inhibition experiments, NFV or control was always added before the swelling inducers, Vpr-derived peptide, and ATR.

### *Yeast strains and clonogenic assays*

We pretreated $10^4$ cells/ml of *Saccharomyces cerevisiae* M 22-2-1 (genotype *MATa ade2 leu2 lys2 his4 trpl ura3 Canr, por1:LEU2, por2:TRP1*; gift from M. Forte, Vollum Institute, Portland, Oregon, USA) (59, 60), *S. cerevisiae* W301-1B control strain (*MATa ade2, leu2, his3, trpl, ura3, can1*), and JL1-3 (genotype like W301-1B, *aac1:LEU2 aac2:HIS3, aac3:URA*; gift from T. Drgon, NIH, Bethesda, Maryland, USA) (61), with NFV, which was followed by treatment with a Vpr-derived peptide (Genemed Synthesis Inc.) as described (62) or $H_2O_2$ (1 hour, 28°C). This was followed by plating on standard YPD agarose medium (200 yeasts/plate) and quantification of the percentage of surviving clones after 48 hours of culture at 28°C.

### *Liposome technology*

PTPC (1 mg/ml) was separated from rat brains and ANT (0.1 mg/ml) from rat heart mitochondria as previously described (44, 63). Immediately after purification, pure proteins were reconstituted into proteoliposomes (phosphatidylcholine/cholesterol [5:1; wt/wt] for PTPC and phosphatidylcholine/cardiolipin [45:1; wt/wt] for ANT) (64). After extensive dialysis to eliminate the surfactants, proteoliposomes were loaded with 4-methyllumbelliferyl-phosphate (4-MUP) in 10 mM KCl, 10 mM HEPES, 125 mM saccharose (pH 7.4), by sonication (25%, 22 seconds on ice) using a Misonix 550 sonicator (Misonix Inc.), washed on Sephadex PD-10 columns (Amersham Biosciences) and dispensed in 96-well microtiter plates (64). We incubated 25 μl of proteoliposomes with the indicated agents (30 minutes for NFV and 60 minutes for ATR and $Vpr_{52-96}$ at RT). External 4-MUP was then converted to 4-methylumbelliferone (4-MU) by the addition of alkaline phosphatase in the presence of $MgCl_2$ for 15 minutes at 37°C. The release of 4-MU was measured by spectrofluorometry (excitation 360 nm, emission 450 nm). The maximum 4-MUP release was determined by adding 5% Triton X-100 to proteoliposomes. The percentage of 4-MUP release induced by treatment of liposomes by ATR was determined as [(ATR - treated liposome fluorescence - untreated liposome fluorescence)/(TX-100-treated liposome fluorescence - untreated liposomes fluorescence)] × 100. The maximal fluorescence induced by 800 μM ATR was then identified as 100% 4-MUP release, and the fluorescence induced by the treatment of liposomes by another product or another dose was calculated as a percentage of ATR-induced 4-MUP release.

### *Activated Bax immunofluorescence*

Jurkat T cells were treated overnight with NFV or vehicle control before being induced to undergo apoptosis with 0.3 μg/ml of CH-11. Teflon-

coated 10-well immunofluorescence slides (Fischer Scientific International) were pretreated with poly-L-lysine (Polysciences Inc.) for 1 hour at RT, washed with water, and allowed to air dry. Fifty microliters of a $0.5 \times 10^6$ cell suspension was aliquoted to each well and allowed to adhere for 1 hour at 37°C. Following 1 wash with PBS, cells were fixed with 2% paraformaldehyde and washed again with PBS. Cells were then treated with 1:250 of mouse anti-Bax (clone 6A7; BD Biosciences — Pharmingen) or mouse isotype in antibody (Santa Cruz Biotechnology Inc.) in PBS with 1 mg/ml BSA and 100 μg/ml digitonin for 1 hour at RT, followed by 2 washes with PBS. Cells were then incubated for an additional hour at RT in 1:500 of goat anti-mouse Alexa Fluor 633 (Invitrogen Corp.) and 1 mg/ml Hoechst 33342 (Invitrogen Corp.) in PBS with 1 mg/ml BSA and 100 μg/ml digitonin. Cells then underwent a final wash, were coverslipped, and imaged with laser scanning confocal microscopy (LSM510; Zeiss) at an absorption/emission wavelength of 632/647 nm and 340/450 nm for Alexa Fluor 633 and Hoechst 33342, respectively.

### *Computer modeling*

Docking of NFV to ANT was carried out with the program QXP (65), using the FULLDOCK+ algorithm implemented in the 2003 version of the program. The recently published crystal structure of ANT (66) was used as the target structure. During docking, both NFV and the protein side chains were treated as totally flexible, and the backbone atoms of the protein were allowed to move under constraints.

### *Statistics*

Data were analyzed using the Student's *t* test for normally distributed data, ANOVA for binary variables, and the post hoc Tukey test for assessing multiple treatment groups.


## Acknowledgments

A.D. Badley is supported by grants from the NIH (R01 AI62261-01-1 and R01 AI40384) and the Burroughs Wellcome Award for Translational Research (ID#1005160). S.A.L. Bennett is supported by grants from Alzheimer Society of Canada, the Canadian Institutes of Health Research (CIHR), and the Alzheimer Society of Saskatchewan. S.A.L. Bennett is a CIHR New Investigator and an Ontario Mental Health Foundation Intermediate Investigator. G. Kroemer is supported by grants from Agence Nationale de Recherché sur le Sida and Sidaction. S.T. Hou is supported by grants from the Heart and Stroke Foundation of Canada. C. Brenner is supported by grants from the Foundation pour la Recherche Medical, the French Ministry of Science, the Centre National pour la Recherche Scientifique, and the Association pour la Recherche sur le Cancer. A. Tarze received a fellowship from the French Ministry of Science. T.C. Moffat received an Alzheimer Society of Canada/CIHR doctoral fellowship. The authors gratefully acknowledge the administrative expertise of A. Carisse and T. Hoff and the technical assistance of A. Desbois and offer special thanks to S. Kilborn and J. Keyte for veterinary assistance and advice.

Received for publication August 5, 2004, and accepted in revised form April 14, 2005.



Address correspondence to: Andrew D. Badley, Division of Infectious Diseases, Mayo Clinic College of Medicine, 200 First Street NW, Rochester, Minnesota 55905, USA. Telephone: (507) 284-3747; Fax: (507) 284-3757; E-mail: badley.andrew@mayo.edu.



1. Phenix, B.N., Cooper, C., Owen, C., and Badley, A.D. 2002. Modulation of apoptosis by HIV protease inhibitors. *Apoptosis.* **7**:295–312.
2. Zhong, D.S., et al. 2002. HIV protease inhibitor ritonavir induces cytotoxicity of human endothelial cells. *Arterioscler. Thromb. Vasc. Biol.* **22**:1560–1566.
3. Gaedicke, S., et al. 2002. Antitumor effect of the human immunodeficiency virus protease inhibitor ritonavir: induction of tumor-cell apoptosis associated with perturbation of proteasomal proteolysis. *Cancer Res.* **62**:6901–6908.
4. Pajonk, F., Himmelsbach, J., Riess, K., Sommer, A., and McBride, W.H. 2002. The human immunodeficiency virus (HIV)-1 protease inhibitor saquinavir inhibits proteasome function and causes apoptosis and radiosensitization in non-HIV-associated human cancer cells. *Cancer Res.* **62**:5230–5235.
5. Estaquier, J., et al. 2002. Effects of antiretroviral drugs on human immunodeficiency virus type 1-induced CD4(+) T-cell death. *J. Virol.* **76**:5966–5973.
6. Sloand, E.M., Young, N.S., Sato, T., Kim, S., and Maciejewski, J.P. 1998. Inhibition of interleukin-1beta-converting enzyme in human hematopoietic progenitor cells results in blockade of cytokine-mediated apoptosis and expansion of their proliferative potential. *Exp. Hematol.* **26**:1093–1099.
7. Weichold, F.F., et al. 1999. HIV-1 protease inhibitor ritonavir modulates susceptibility to apoptosis of uninfected T cells. *J. Hum. Virol.* **2**:261–269.
8. Sloand, E.M., et al. 1999. Human immunodeficiency virus type 1 protease inhibitor modulates activation of peripheral blood CD4(+) T cells and decreases their susceptibility to apoptosis in vitro and in vivo. *Blood.* **94**:1021–1027.
9. Sloand, E.M., et al. 2000. Protease inhibitors stimulate hematopoiesis and decrease apoptosis and ICE expression in CD34(+) cells. *Blood.* **96**:2735–2739.
10. Ghibelli, L., et al. 2003. Anti-apoptotic effect of HIV protease inhibitors via direct inhibition of calpain. *Biochem. Pharmacol.* **66**:1505–1512.
11. Phenix, B.N., Lum, J.J., Nie, Z., Sanchez-Dardon, J., and Badley, A.D. 2001. Anti-apoptotic mechanism of HIV protease inhibitors: preventing mitochondrial transmembrane potential loss. *Blood.* **98**:1078–1085.
12. Matarrese, P., et al. 2003. Mitochondrial membrane hyperpolarization hijacks activated T lymphocytes toward the apoptotic-prone phenotype: homeostatic mechanisms of HIV protease inhibitors. *J. Immunol.* **170**:6006–6015.
13. Barreiro, P., Soriano, V., Casas, E., and Gonzalez-Lahoz, J. 2002. Different degree of immune recovery using antiretroviral regimens with protease inhibitors or non-nucleosides. *AIDS.* **16**:245–249.
14. Benito, J.M., et al. 2002. Differences in cellular activation and apoptosis in HIV-infected patients receiving protease inhibitors or nonnucleoside reverse transcriptase inhibitors. *AIDS Res. Hum. Retroviruses.* **18**:1379–1388.
15. Kravcik, S., et al. 2001. Comparative CD4 T-cell responses of reverse transcriptase inhibitor therapy with or without nelfinavir matched for viral exposure. *HIV Clin. Trials.* **2**:160–170.
16. Landay, A.L., et al. 2003. Immune reconstitution is comparable in antiretroviral-naive subjects after 1 year of successful therapy with a nucleoside reverse-transcriptase inhibitor- or protease inhibitor-containing antiretroviral regimen. *J. Infect. Dis.* **188**:1444–1454.
17. Zeldin, R.K., and Petruschke, R.A. 2004. Pharmacological and therapeutic properties of ritonavir-boosted protease inhibitor therapy in HIV-infected patients. *J. Antimicrob. Chemother.* **53**:4–9.
18. Zender, L., et al. 2003. Caspase 8 small interfering RNA prevents acute liver failure in mice. *Proc. Natl. Acad. Sci. U. S. A.* **100**:7797–7802.
19. Song, E., et al. 2003. RNA interference targeting Fas protects mice from fulminant hepatitis. *Nat. Med.* **9**:347–351.
20. Kovalovich, K., et al. 2001. Interleukin-6 protects against Fas-mediated death by establishing a critical level of anti-apoptotic hepatic proteins FLIP, Bcl-2, and Bcl-xL. *J. Biol. Chem.* **276**:26605–26613.
21. Jiang, H., et al. 1995. Murine CD8+ T cells that specifically delete autologous CD4+ T cells expressing V beta 8 TCR: a role of the Qa-1 molecule. *Immunity.* **2**:185–194.
22. Miethke, T., et al. 1992. T cell-mediated lethal shock triggered in mice by the superantigen staphylococcal enterotoxin B: critical role of tumor necrosis factor. *J. Exp. Med.* **175**:91–98.
23. Aoki, Y., et al. 1995. Protective effect of granulocyte colony-stimulating factor against T-cell-meditated lethal shock triggered by superantigens. *Blood.* **86**:1420–1427.
24. Mullen, R.J., Buck, C.R., and Smith, A.M. 1992. NeuN, a neuronal specific nuclear protein in vertebrates. *Development.* **116**:201–211.
25. Zausinger, S., Hungerhuber, E., Baethmann, A., Reulen, H., and Schmid-Elsaesser, R. 2000. Neurological impairment in rats after transient middle cerebral artery occlusion: a comparative study under various treatment paradigms. *Brain Res.* **863**:94–105.
26. Frenkel, D., et al. 2003. Nasal vaccination with myelin oligodendrocyte glycoprotein reduces stroke size by inducing IL-10-producing CD4+ T cells. *J. Immunol.* **171**:6549–6555.
27. Martinou, J.-C., and Green, D.R. 2001. Breaking the mitochondrial barrier. *Nat. Rev. Mol. Cell Biol.* **2**:63–67.
28. Zamzami, N., and Kroemer, G. 2001. The mitochondrion in apoptosis: how Pandora's box opens. *Nat. Rev. Mol. Cell Biol.* **2**:67–71.
29. Zou, H., Hanzel, W.J., Liu, X., Lutschg, A., and Wang, X. 1997. Apaf-1, a human protein homologous to C. elegans CED-4, participates in cytochrome c-dependent activation of caspase-3. *Cell.* **90**:405–413.

30. Zou, H., Li, Y., Liu, X., and Wang, X. 1999. An APAF-1 cytochrome c multimeric complex is a functional apoptosome that activates procaspase-9. *J. Biol. Chem.* **274**:11549–11556.
31. Srinivasula, S.M., Ahmad, M., Fernandes-Alnemri, T., and Alnemri, E.S. 1998. Autoactivation of procaspase-9 by Apaf-1-mediated oligomerization. *Mol. Cell.* **1**:949–957.
32. Vieira, H.L.A., et al. 2000. Permeabilization of the mitochondrial inner membrane during apoptosis: impact of the adenine nucleotide translocator. *Cell Death Differ.* **7**:1146–1154.
33. Jacotot, E., et al. 2001. Control of mitochondrial membrane permeabilization by adenine nucleotide translocator interacting with HIV-1 viral protein rR and Bcl-2. *J. Exp. Med.* **193**:509–519.
34. Halestrap, A.P., and Brenner, C. 2003. The adenine nucleotide translocase: a central component of the mitochondrial permeability transition pore and key player in cell death. *Curr. Med. Chem.* **10**:1507–1525.
35. Verrier, F., et al. 2004. Dynamic evolution of the adenine nucleotide translocase interactome during chemotherapy-induced apoptosis. *Oncogene.* **23**:8049–8064.
36. Kanno, T., et al. 2004. Oxidative stress underlies the mechanisms for Ca2+-induced permeability transition of mitochondria. *Free Radic. Res.* **38**:27–35.
37. Halestrap, A.P., Woodfield, K.Y., and Connern, C.P. 1997. Oxidative stress, thiol reagents, and membrane potential modulate the mitochondrial permeability transition by affecting nucleotide binding to the adenine nucleotide translocase. *J. Biol. Chem.* **272**:3346–3354.
38. Nakagawa, Y. 2004. Initiation of apoptotic signal by the peroxidation of cardiolipin of mitochondria. *Ann. N. Y. Acad. Sci.* **1011**:177–184.
39. Decaudin, D., et al. 2002. Peripheral benzodiazepine receptor ligands reverse apoptosis resistance of cancer cells in vitro and in vivo. *Cancer Res.* **62**:1388–1393.
40. Hirsch, T., et al. 1998. PK11195, a ligand of the mitochondrial benzodiazepine receptor, facilitates the induction of apoptosis and reverses Bcl-2-mediated cytoprotection. *Exp. Cell Res.* **241**:426–434.
41. Haouzi, D., et al. 2002. Mitochondrial permeability transition as a novel principle of hepatorenal toxicity in vivo. *Apoptosis.* **7**:395–405.
42. Duan, S., et al. 2003. Mitochondrial outer membrane permeability change and hypersensitivity to digitonin early in staurosporine-induced apoptosis. *J. Biol. Chem.* **278**:1346–1353.
43. Cheng, E.H.-Y., Sheiko, T.V., Fisher, J.K., Craigen, W.J., and Korsmeyer, S.J. 2003. VDAC2 inhibits BAK activation and mitochondrial apoptosis. *Science.* **301**:513–517.
44. Brenner, C., Marzo, I., de Araujo Vieira, H.L., and Kroemer, G. 2000. Purification and liposomal reconstitution of permeability transition pore complex. *Methods Enzymol.* **322**:243–252.
45. Kokoszka, J.E., et al. 2004. The ADP/ATP translocator is not essential for the mitochondrial permeability transition pore. *Nature.* **427**:461–465.
46. Halestrap, A.P. 2004. Mitochondrial permeability: dual role for the ADP/ATP translocator? *Nature.* **430**:984.
47. Aarnoutse, R.E., et al. 2002. International interlaboratory quality control program for measurement of antiretroviral drugs in plasma. *Antimicrob. Agents Chemother.* **46**:884–886.
48. Raines, C.P., et al. 2000. Safety, tolerability, and antiretroviral effects of ritonavir- nelfinavir combination therapy administered for 48 weeks. *J. Acquir. Immune Defic. Syndr.* **25**:322–328.
49. MacManus, J.P., et al. 2003. Absence of the transcription factor E2F1 attenuates brain injury and improves behavior after focal ischemia in mice. *J. Cereb. Blood Flow Metab.* **23**:1020–1028.
50. Preston, E., and Webster, J. 2000. Spectrophotometric measurement of experimental brain injury. *J. Neurosci. Methods.* **94**:187–192.
51. Melanson-Drapeau, L., et al. 2003. Oligodendrocyte progenitor enrichment in the connexin32 null-mutant mouse. *J. Neurosci.* **23**:1759–1768.
52. Sawada, M., et al. 2003. Ku70 suppresses the apoptotic translocation of Bax to mitochondria. *Nat. Cell Biol.* **5**:320–329.
53. Forcet, C., et al. 2001. The dependence receptor DCC (deleted in colorectal cancer) defines an alternative mechanism for caspase activation. *Proc. Natl. Acad. Sci. U. S. A.* **98**:3416–3421.
54. Trushin, S.A., et al. 2003. Protein kinase Calpha (PKCalpha) acts upstream of PKCtheta to activate IkappaB kinase and NF-kappaB in T lymphocytes. *Mol. Cell. Biol.* **23**:7068–7081.
55. Seglen, P.O. 1976. Preparation of isolated rat liver cells. *Methods Cell Biol.* **13**:29–83.
56. Zamzami, N., et al. 1995. Reduction in mitochondrial potential constitutes an early irreversible step of programmed lymphocyte death in vivo. *J. Exp. Med.* **181**:1661–1672.
57. Nie, Z., et al. 2002. HIV-1 protease processes procaspase 8 to cause mitochondrial release of cytochrome c, caspase cleavage and nuclear fragmentation. *Cell Death Differ.* **9**:1172–1184.
58. Susin, S.A., Larochette, N., Geuskens, M., and Kroemer, G. 2000. Purification of mitochondria for apoptosis assays. *Methods Enzymol.* **322**:205–208.
59. Blachly-Dyson, E., et al. 1993. Cloning and functional expression in yeast of two human isoforms of the outer mitochondrial membrane channel, the voltage-dependent anion channel. *J. Biol. Chem.* **268**:1835–1841.
60. Blachly-Dyson, E., Song, J., Wolfgang, W.J., Colombini, M., and Forte, M. 1997. Multicopy suppressors of phenotypes resulting from the absence of yeast VDAC encode a VDAC-like protein. *Mol. Cell. Biol.* **17**:5727–5738.
61. Drgon, T., Sabova, L., Nelson, N., and Kolarov, J. 1991. ADP/ATP translocator is essential only for anaerobic growth of yeast Saccharomyces cerevisiae. *FEBS Lett.* **289**:159–162.
62. Macreadie, I.G., Arunagiri, C.K., Hewish, D.R., White, J.F., and Azad, A.A. 1996. Extracellular addition of a domain of HIV-1 Vpr containing the amino acid sequence motif H(S/F)RIG causes cell membrane permeabilization and death. *Mol. Microbiol.* **19**:1185–1192.
63. Marzo, I., Brenner, C., and Kroemer, G. 1998. The central role of the mitochondrial megachannel in apoptosis: evidence obtained with intact cells, isolated mitochondria, and purified protein complexes. *Biomed. Pharmacother.* **52**:248–251.
64. Belzacq, A.S., et al. 2003. Bcl-2 and Bax modulate adenine nucleotide translocase activity. *Cancer Res.* **63**:541–546.
65. McMartin, C., and Bohacek, R.S. 1997. QXP: powerful, rapid computer algorithms for structure-based drug design. *J. Comput. Aided Mol. Des.* **11**:333–344.
66. Pebay-Peyroula, E., et al. 2003. Structure of mitochondrial ADP/ATP carrier in complex with carboxyatractyloside. *Nature.* **426**:39–44.

## FUNDING

| Year | Award | Type | Amount |
|---|---|---|---|
| 2005 - 2006 | Admission Scholarship (tuition fees) | Institutional | $5,535 |
| 2004 - 2005 | Admission Scholarship (tuition fees) | Institutional | $5,535 |
| 2003 - 2004 | Excellence Scholarship (tuition fees) | Institutional | $5,535 |
| 2002 - 2003 | Ontario Graduate Scholarship, declined | Provincial Government | $15,000 |
| 2002 - 2004 | Alzheimer Society of Canada/CIHR Doctoral Award | Granting Council | $39,060 |
| 2002 - 2003 | Excellence Scholarship (tuition fees) | Institutional | $5,465 |
| 2001 - 2002 | Ontario Graduate Scholarship | Provincial Government | $15,000 |
| 2001 - 2002 | Excellence Scholarship (tuition fees) | Institutional | $5,358 |
| 2000 - 2001 | Ontario Graduate Scholarship in Science and Technology | Provincial Government/Institutional | $15,000 |
| 2000 - 2001 | Admission Scholarship (tuition fees) | Institutional | $4,928 |
| 2000 | Biochemistry Program Entrance Award | Institutional | $4,000 |
| 2000 | NSERC USRA | Granting Council | $5,000 |
| 1999 | NSERC USRA | Granting Council | $5,000 |
| 1999 | E.W.R. Steacie Scholarship | Institutional | $750 |
| 1999 | Heather & Ross Hamlin Bursary | Institutional | $1,000 |
| 1998 | J. Lorne Gray Scholarship | Institutional | $750 |
| 1997 | Dr. Frederick William Charles Mohr Scholarship | Institutional | $750 |

## SCHOLARLY AND PROFESSIONAL ACTIVITIES

### Invited Speaker Presentations

2005 Novel phospholipids targets for neurodegenerative disease. Department of Biochemistry, Microbiology, and Immunology Seminar Series, University of Ottawa, Ottawa, ON, Canada.

2003 A novel platelet activating factor apoptotic signaling pathway implicated in Alzheimer-like neuropathology. Department of Biochemistry, Microbiology, and Immunology Student Seminar Series, University of Ottawa, Ottawa, ON, Canada.

2002 A Time to Die: Platelet activating factor-induced apoptosis of human neurons, but not neural precursors. Minisymposium on Cell Signaling and Neuronal Survival, Louisiana State University, Neuroscience Center of Excellence, New Orleans, LA, USA.

Pathways of lipid mediator-induced neuronal apoptosis. Department of Biochemistry, Microbiology, and Immunology Student Seminar Series, University of Ottawa, Ottawa, ON, Canada.

2001 Role of mitochondrial uncoupling proteins in neural cell fate. International Symposium on Mitochondrial Defects in Pathology and Aging, Institute for Biological Sciences, National Research Council of Canada, Ottawa, ON, Canada (oral presentation by SAL Bennett).

### Research Advocacy and Outreach

2006 Appeared in "Alzheimer Disease: 2-part series" by Chris Day, CTV News Ottawa

2005 Appeared in and interviewed for "Seeing death in a new light" by Tim Lougheed, The University of Ottawa Research Perspectives Journal (Summer, 2005).

Appeared in "Breakthrough discoveries and research" as part of the University of Ottawa's "The future is now; leading the way in research and development" recruitment package (April, 2005).

2004 Invited speaker, Biochemistry undergraduate recruitment. Lecture title: "Honours in biochemistry: expectations and example research projects". University of Ottawa, Ottawa, ON, Canada.

2003 Appeared in "Berry Important Questions; Blueberries As Protector Of Brain Cells?" by Holly Lake, The Ottawa Sun (October 4, 2003).

Interviewed by CBCRadio regarding Alzheimer Disease research.

2002 Appeared in "Hope for the Hopeless" as part of "The Researchers" series by Sharon Kirkey, The Ottawa Citizen (June 3, 2002).

Invited speaker, BioX. Lecture title: "Molecular mechanisms of PAF signaling in Alzheimer's Disease-like neuropathology". University of Ottawa, Ottawa, ON, Canada.

## Conferences and Symposia Attended

2005 Canadian Student Health Research Forum. University of Manitoba, Winnipeg, Manitoba, Canada.

Department of Biochemistry, Microbiology, and Immunology Student Seminar Series. University of Ottawa, Ottawa, Canada.

Department of Biochemistry, Microbiology, and Immunology Research Day. University of Ottawa, Ottawa, Canada.

2004 International Congress on Platelet Activating Factor and Related Lipid Mediators. Best Western Hotel Steglitz International. Berlin, Germany.

The Partnership Group for Science and Engineering's Bacon and Eggheads Breakfast Series. "When cells choose the wrong time to die", oral presentation by Dr. Alex MacKenzie. Parliament Hill, Ottawa, ON, Canada.

Department of Biochemistry, Microbiology, and Immunology Student Seminar Series. University of Ottawa, Ottawa, Canada.

Department of Biochemistry, Microbiology, and Immunology Research Day. University of Ottawa, Ottawa, Canada.

2003 Society for Neuroscience 33rd Annual Meeting. New Orleans Convention Center. New Orleans, LA, USA.

Department of Biochemistry, Microbiology, and Immunology Student Seminar Series. University of Ottawa, Ottawa, Canada.

Department of Biochemistry, Microbiology, and Immunology Research Day. University of Ottawa, Ottawa, Canada.

2002 Society for Neuroscience 32nd Annual Meeting. Orange County Convention Center. Orlando, FL, USA.

Canadian Federation of Biological Societies 45th Meeting. Palais des Congres. Montreal, Canada.

Minisymposium on Cell Signaling and Neuronal Survival. Louisiana State University Neuroscience Center of Excellence. New Orleans, LA, USA.

Department of Biochemistry, Microbiology, and Immunology Student Seminar Series. University of Ottawa, Ottawa, Canada.

Department of Biochemistry, Microbiology, and Immunology Research Day. University of Ottawa, Ottawa, Canada.

2001 Society for Neuroscience 31st Annual Meeting. San Diego Convention Center. San Diego, CA, USA.

International Symposium on Mitochondrial Defects in Pathology and Aging. Institute for Biological Sciences, National Research Council of Canada. Ottawa, Canada.

Canadian Federation of Biological Societies 44th Meeting. Ottawa Congress Centre. Ottawa, Canada.

Department of Biochemistry, Microbiology, and Immunology Student Seminar Series. University of Ottawa, Ottawa, Canada.

Department of Biochemistry, Microbiology, and Immunology Research Day. University of Ottawa, Ottawa, Canada.

2000 Society for Neuroscience 30th Annual Meeting. New Orleans Convention Center. New Orleans, LA, USA.

## Membership in Professional Societies

Society of Neuroscience
International Brain Research Organization
Canadian Federation of Biological Societies
Canadian Association for Anatomy, Neurobiology and Cell Biology

## Membership in Academic Activities

Connexin Journal Club
Bioenergetics Journal Club
Neural Regeneration Journal Club

## TEACHING EXPERIENCE

2005 Senior Mentor, Neural Regeneration Laboratory, University of Ottawa
Co-supervised 4th year honours thesis project

2004-2005 Senior Mentor, Neural Regeneration Laboratory, University of Ottawa
Supervised 4th year honours thesis project

2003 Teaching Assistant, Dept. Biochemistry, University of Ottawa
BCH2336 Biochemistry Laboratory I (2nd year course)
Demonstrated biweekly laboratory sessions, conducted private tutorials, marked laboratory reports.

2002-2003 Senior Mentor, Neural Regeneration Laboratory, University of Ottawa
Supervised 4th year honours thesis project

2002 Guest Lecturer, Dept. Biochemistry, University of Ottawa
BCH4125 Cellular Regulation and Control (4th year course)
Lecture Title: "Techniques in Cellular Regulation: Detection of Caspase Activation"

1999 Teaching Assistant, Dept. Biochemistry, Carleton University
Practical Biochemistry (3rd year laboratory course)
Marked laboratory reports

Tutor, Dept. Biochemistry, Carleton University
3rd year biochemistry correspondence

Guest Teacher, Henry Munroe School
Taught fundamentals of science and demonstrated hands-on scientific applications

## PUBLICATIONS

### Refereed papers, published, submitted, or in preparation

1. Weaver JGR, Tarze A, **Moffat TC**, LeBras M, Deniaud A, Brenner C, Bren GD, Morin MY, Phenix BN, Dong L, Jiang SX, Sim VL, Zurakowski B, Lallier J, Hardin H, Wettstein P, van Heeswijk RPG, Douen A, Kroemer RT, Hou ST, Bennett SAL, Lynch DH, Kroemer G, Badley AD. 2005. Inhibition of adenine nucleotide translocator pore function and protection against apoptosis *in vivo* by an HIV protease inhibitor. *J.Clin.Invest.* **115**:1828-38.

2. Moffat TC, Wong S, Hozturk E, Migahed L, Paliga A, Bennett SAL (2006) Platelet activating factor elicits an endoplasmic reticulum-dependent caspase cascade in human neurons independently of its G-protein coupled receptor, in preparation

3. Moffat TC, Wong S, Hozturk E, Migahed L, Paliga A, Hill J, Bennett SAL (2006) Platelet activating factor elicits an endoplasmic reticulum-dependent caspase cascade in human neurons independently of its G-protein coupled receptor, in preparation.

4. Moffat TC, Whitehead S, Harper ME, Bennett SAL (2006) Role of uncoupling protein-2 in neuronal loss triggered by the bioactive phospholipid platelet activating factor, in preparation.

5. Harris CS, Moffat TC, Ryan SD, Migahed L, Mo F, Midzic, I, Bennett SAL (2006) Plant phenolic compounds protect against amyloid-$\beta_{1-42}$ neurotoxicity - a structure-activity analysis, in preparation

6. Moffat TC and Bennett SAL (2006) PAF inhibitors that prevent caspase-dependent apoptosis in human neurons triggered by PAF independently of its G-protein-coupled receptor, in preparation

## Abstracts

1. Ryan SD, **Moffat TC**, Bennett SAL. 2005. Neuroprotective properties of platelet activating factor acetylhydrolase I over the course of in vitro neuronal differentiation: rodent versus human comparison. Society for Neuroscience 35th Annual Meeting (Washington, DC, USA, poster presentation by SD Ryan).

2. **Moffat TC** and Bennett SAL. 2005. A novel platelet activating factor-induced apoptotic signaling pathway in human neurons that does not require activation of PAF receptor. Canadian Institutes of Health Research National Student Research Poster Competition, Canadian Student Health Research Forum (Winnipeg, MB, Canada, poster presentation).

3. **Moffat TC**, Ryan SD, Hill J, Bennett SAL. 2004. Platelet activating factor acts downstream of beta-amyloid and can be targeted to reduce neuronal loss – implications for Alzheimer Disease. 8th International Congress on Platelet-Activating Factor and Related Lipid Mediators (Berlin, Germany, oral presentation by SAL Bennett).

4. **Moffat TC** and Bennett SAL. 2004. A novel platelet activating factor-induced apoptotic signaling pathway in human neurons that does not require activation of PAF receptor. 8th International Congress on Platelet-Activating Factor and Related Lipid Mediators (Berlin, Germany, poster presentation).

5. **Moffat TC** and Bennett SAL. 2004. A novel platelet activating factor-induced apoptotic signaling pathway in human neurons that does not require activation of PAF receptor. Society for Neuroscience 34th Annual Meeting (San Diego, CA, USA, oral presentation, not able to attend).

6. **Moffat TC** and Bennett SAL. 2003. Platelet activating factor triggers apoptosis in terminally differentiated human neurons through a novel signaling pathway. Society for Neuroscience 33rd Annual Meeting (New Orleans, LA, USA, poster presentation).

7. Ryan SD, Bonin F, **Moffat TC**, Bennett SAL. 2003. Cytosolic platelet activating factor acetylhydrolases 1b and II protect PC12 cells from apoptotic loss. Society for Neuroscience 33rd Annual Meeting (New Orleans, LA, USA, poster presentation by SD Ryan).

8. **Moffat TC** and Bennett SAL. 2002. Contribution of mitochondrial pathways to platelet activating factor-mediated apoptosis of human neurons. Society for Neuroscience 32nd Annual Meeting (Orlando, FL, USA, poster presentation).

9. **Moffat TC** and Bennett SAL. 2002. Pathways of lipid mediator-induced neuronal apoptosis. Canadian Federation of Biological Societies 45th Meeting (Montreal, PQ, Canada, poster presentation).

10. **Moffat TC**, Harper M-E, Bennett SAL. 2001. Mitochondrial changes associated with platelet activating factor-induced apoptosis. Society for Neuroscience 31st Annual Meeting (San Diego, CA, USA, poster presentation).

11. **Moffat TC**, Harper M-E, Bennett SAL. 2001. Development of human neuronal apoptosis model to investigate the role of mitochondrial uncoupling protein-2 in platelet activating factor-induced death. Canadian Federation of Biological Societies 44th Meeting (Ottawa, ON, Canada, poster presentation).